



**A Study on the Effects of Combined Diesel-Hydrogen  
Combustion on Diesel Engines using Experimental and  
Simulation Techniques**

A Thesis submitted for the degree Doctor of Philosophy (PhD)

By

Ward Al-Asadi (1223857)

Supervisor: Professor Thanos Megaritis

School of Engineering and Design,

Brunel University

United Kingdom

September 2018

## Abstract

With the increasingly stringent regulations and laws being put in place worldwide with regards to a cleaner and a safer environment, the modern diesel engine has scope to be improved upon to help meet these new standards set for the betterment of our cities. There are many current modes of alternative transport, with diesel-hydrogen combustion being a transitional solution from fossil fuels to hydrogen powered vehicles.

The main objective of this research effort was to investigate the effects of intake air enrichment with hydrogen on the performance, combustion, and emissions of a diesel engine. The secondary aim was to design and optimise accurate engine models which can replicate real world experiments and conditions. This becomes increasingly useful in the modern era of engine testing and development as it allows for more manufacturers to test and optimise new combustion methods, without the need for a physical engine, to meet the ever-tightening emissions legislations. Therefore, the accuracy of the models produced could pave the way for more simulations to be carried out via manufacturers with more confidence.

The experimental tests were carried out on a 2.0 litre Ford High Speed Direct Injection (HSDI) diesel engine. The engine was tested at various conditions mimicking light- and medium-duty diesel engines. Hydrogen was used via a bottle with the composition of the gas replicating exhaust gas reformed intake air. The percentage of the hydrogen and the start of injection for diesel were altered for the tests. The simulations were carried out on a replicated four-cylinder 2.0 litre Ford HSDI diesel engine on Ricardo Wave® and a single-cylinder DI diesel engine modelled based on a small Yanmar L70N diesel engine. The experimental operating parameters were used in the simulations to measure the level of accuracy achieved with the models on the software.

The experimental results showed that with hydrogen enrichment of the intake air, the CO and smoke emissions were reduced significantly, however NO<sub>x</sub> emissions were found to have increased at certain conditions. The simulations for the multi-cylinder diesel engine showed great promise with an average of 95% accuracy across the operating conditions and emissions measured. The single-cylinder diesel engine displayed low levels of Total Hydrocarbons (THC), Carbon Monoxide (CO), with a slight increase in Oxides of Nitrogen (NO<sub>x</sub>) emissions but did show high levels of accuracy against literature and other experimental work based on similar operating conditions.

Although there is an abundance of literature currently investigating the effects of hydrogen enrichment of the intake air, the new contributions to knowledge of this research is the comparison between simulated and experimental work of transitional combustion methods such as this. This research is believed to help aid the industry in testing and optimising of simulated engine models for a more reliable manufacturing process.

## Acknowledgements

First and foremost, I would like to thank my principal supervisor Professor Thanos Megaritis and my second supervisor Dr Lionel Ganippa. Their immense expertise, understanding, and guidance has helped me greatly throughout my time at Brunel. A special mention to Professor Alasdair Cairns at University of Nottingham, who although was not part of my supervisory team, was still someone who I admired and learned a lot from during my time as a master's student at Brunel.

I would also like to thank the technical staff at Brunel, with special mention going to Andy, Eamon, Minal, and Tony for their unrelenting support in the lab and elsewhere. They were not just great technicians, but great friends as well.

Along the way, many people have come into my life to help me personally or professionally throughout my time here and I thank them all for all they have offered to me. I would like to acknowledge a few special individuals whom without, would have made my time at Brunel surely much harder. Thank you to Amin, Reza, Thompson, Vinícius, and Wei for making the good times better and the hard times easier.

I would also like to acknowledge the people who are dearest to me and who supported me throughout, not only my research but my life. Thank you to my parents Abbas and Nasreen and my sister Ayia for the unending love, friendship, and support of all my endeavours and I hope to one day make it up to you. No words are enough to portray what I feel so I just say thank you, forever and always thank you.

Last but certainly not least my thanks go to God whom without, none of this would have been possible.

## Nomenclature

AHRR	Apparent heat release rate
BITDC	Before injection top dead centre
BOC	British oxygen company
BSFC	Brake specific fuel consumption
BSN	Bosch smoke number
CAD ATDC	Crank angle degrees after top dead centre
CAD BTDC	Crank angle degrees before top dead centre
CDC	Conventional diesel combustion
CI	Compression ignition
CNG	Compressed natural gas
CO	Carbon monoxide
CO <sub>2</sub>	Carbon dioxide
COV	Coefficient of variation
CO <sub>x</sub>	Carbon oxide
CR	Compression ratio
DEF	Diesel exhaust fluid
deg. CA	Degrees crank angle
DI	Direct injection
DME	Dimethyl ether
DOC	Diesel oxidation catalyst
DPF	Diesel particulate filter
ECU	Engine control unit
EGR	Exhaust gas recirculation
EOC	End of combustion

EPA	Environmental protection agency
FID	Flame ionisation detector
FTIR	Fourier transform infrared spectroscopy
GC	Gas chromatography
GHG	Greenhouse gas
H <sub>2</sub>	Hydrogen
H <sub>2</sub> O	Water
HC	Hydrocarbons
HCCI	Homogenous charge compression ignition
HSDI	High speed direct injection
HV	Heating value
ICE	Internal combustion engine
ID	Ignition delay
IMEP	Indicated mean effective pressure
LFL	Lower flammability limit
LPG	Liquefied petroleum gas
LTC	Low temperature combustion
MFB	Mass fraction burned
N <sub>2</sub>	Nitrogen
NA	Naturally aspirated
NDIR	Non-dispersive infrared
NEDC	New European Driving Cycle
NH <sub>3</sub>	Ammonia
NMHC	Non-methane hydrocarbons
NO	Nitric oxide

NO <sub>2</sub>	Nitrogen dioxide
NO <sub>x</sub>	Nitrogen oxide
O <sub>2</sub>	Oxygen
O <sub>3</sub>	Ozone
OH	Hydroxyl
PAH	Polycyclic aromatic hydrocarbons
PCCI	Premixed charge compression ignition
PM	Particulate matter
RCCI	Reactivity controlled compression ignition
RDE	Real Driving Emissions
REGR	Reformed EGR
ROHR	Rate of heat release
RPM	Revolutions per minute
SCR	Selective catalytic reduction
SOC	Start of combustion
SOF	Soluble organic fraction
SOI	Start of injection
SOL	Solid fraction
STDV	Standard deviation
TCD	Thermal conductivity detector
TDC	Top dead centre
THC	Total hydrocarbons
UFL	Upper flammability limit
UHC	Unburned hydrocarbon
ULSD	Ultra-low sulphur diesel

## Contents

<b>Abstract</b> .....	- 2 -
<b>Acknowledgements</b> .....	- 4 -
<b>Nomenclature</b> .....	- 5 -
<b>Table of Figures</b> .....	- 13 -
<b>Table of Tables</b> .....	- 15 -
<b>Chapter 1</b> .....	- 17 -
<b>Introduction</b> .....	- 17 -
1.1 Introduction .....	- 17 -
1.2 Aims and Objectives.....	- 21 -
1.3 Outline of Thesis .....	- 23 -
<b>Chapter 2</b> .....	- 26 -
<b>Literature Review</b> .....	- 26 -
2.1 Compression Ignition Engines.....	- 26 -
2.1.1 Fuel Injection .....	- 27 -
2.1.2 Direct Fuel Injection in Diesel Engines.....	- 27 -
2.2 Air Management .....	- 29 -
2.3 Exhaust Gas Emissions.....	- 31 -
2.3.1 Oxides of Nitrogen .....	- 32 -
2.3.2 Particulate Emissions.....	- 33 -
2.3.3 Carbon Monoxide .....	- 35 -
2.3.4 Total Unburned Hydrocarbons .....	- 36 -
2.4 Legislation and Regulations .....	- 36 -
2.5 Exhaust Gas Aftertreatment.....	- 38 -
2.5.1 Exhaust Gas Recirculation.....	- 38 -
2.5.2 Diesel Particulate Filter .....	- 40 -
2.5.3 Selective Catalytic Reduction.....	- 40 -

2.5.4	NO <sub>x</sub> Adsorber.....	- 41 -
2.6	Diesel Combustion .....	- 42 -
2.7	Alternative Modes of Diesel Combustion .....	- 45 -
2.7.1	CAI/HCCI Combustion .....	- 46 -
2.7.2	Low Temperature Combustion.....	- 47 -
2.7.3	Premixed Charge Compression Ignition.....	- 48 -
2.7.4	Reactivity Controlled Compression Ignition.....	- 49 -
2.8	Alternative Fuels and Dual Fuelling.....	- 50 -
2.8.1	Hydrogen .....	- 51 -
2.8.2	Syngas.....	- 53 -
2.8.3	Liquefied Petroleum Gas .....	- 54 -
2.8.4	Compressed Natural Gas .....	- 55 -
2.8.5	Biodiesel .....	- 56 -
2.9	Exhaust Gas Assisted Fuel Reforming .....	- 57 -
2.10	Dilution of Intake Air .....	- 59 -
2.11	Motivation .....	- 59 -
<b>Chapter 3</b>	.....	- 62 -
<b>Methodology</b>	.....	- 62 -
3.1	Introduction .....	- 62 -
3.2	Research Engine .....	- 62 -
3.3	Dynamometer .....	- 65 -
3.4	Air Intake System .....	- 66 -
3.5	Diesel Fuel supply and Management.....	- 68 -
3.6	Exhaust Gas Analysis .....	- 69 -
3.6.1	Non-dispersive Infrared.....	- 71 -
3.6.2	Chemiluminescence.....	- 71 -
3.6.3	Flame Ionisation Detector .....	- 72 -

3.6.4	Gas Chromatography .....	- 73 -
3.6.5	Bosch Smoke Number .....	- 74 -
3.7	In-cylinder Pressure Data .....	- 74 -
3.8	Fuel Properties .....	- 76 -
3.9	Data Analysis.....	- 79 -
3.9.1	In-cylinder Volume.....	- 79 -
3.9.2	Apparent and Cumulative Rate of Heat Release .....	- 80 -
3.9.3	Mass Fraction Burned.....	- 82 -
3.9.4	Energy Supplied by Hydrogen .....	- 82 -
3.9.5	Combustion Efficiency of Hydrogen.....	- 82 -
3.9.6	Bottled Hydrogen Flow Rate .....	- 83 -
3.10	Engine Simulation Software and Test Procedure .....	- 83 -
3.10.1	Engine Simulation Software .....	- 83 -
3.10.2	Testing Procedure .....	- 85 -
<b>Chapter 4</b>	.....	- 87 -
<b>Effects of Combined Diesel-Hydrogen Combustion on Combustion Properties</b>	.....	- 87 -
4.1	Introduction .....	- 87 -
4.2	Methodology.....	- 88 -
4.3	Results and Discussion .....	- 90 -
4.3.1	Effects of Diesel-Hydrogen Combustion on NO <sub>x</sub> and Smoke Emissions .....	- 90 -
4.3.2	Effect of Diesel-Hydrogen Combustion on CO emissions.....	- 96 -
4.3.3	Effect of Diesel-Hydrogen Combustion on THC Emissions.....	- 98 -
4.3.4	Analysing Hydrogen Combustion Efficiency.....	- 100 -
4.4	Summary.....	- 103 -
<b>Chapter 5</b>	.....	- 106 -
<b>Comparison between Simulated and Experimental Diesel-Hydrogen Combustion.</b>		- 106 -
5.1	Introduction .....	- 106 -

5.2	Methodology.....	- 107 -
5.3	Results and Discussion .....	- 110 -
5.3.1	Comparison of Pressure and Heat Release Rate between Experimental and Simulated data .....	- 110 -
5.3.2	Comparison of NO <sub>x</sub> between Experimental and Simulated Data .....	- 112 -
5.3.3	Comparison of CO Emissions between Experimental and Simulated Data ...	- 115 -
5.3.4	Comparison of THC Emissions between Experimental and Simulated Data	- 117 -
5.4	Summary.....	- 120 -
<b>Chapter 6</b>	.....	- 123 -
<b>Studying the Effects of Hydrogen Addition on a Single-Cylinder Diesel Engine Using Ricardo Wave® Simulation Software</b>	.....	- 123 -
6.1	Introduction .....	- 123 -
6.2	Methodology.....	- 125 -
6.3	Results and Discussions.....	- 127 -
6.3.1	Effects of Diesel-Hydrogen Combustion on NO <sub>x</sub> .....	- 128 -
6.3.2	Effect of Diesel-Hydrogen combustion on CO emissions.....	- 131 -
6.3.3	Effect of Diesel-Hydrogen Combustion on THC Emissions.....	- 133 -
6.4	Summary.....	- 136 -
<b>Chapter 7</b>	.....	- 139 -
<b>Conclusions and Recommendations for Future Work</b>	.....	- 139 -
7.1	Conclusions .....	- 139 -
7.1.1	Effects of Combined Diesel-Hydrogen Combustion on Combustion Properties ....	- 139 -
7.1.2	Comparison between Simulated and Experimental Diesel-Hydrogen Combustion	- 140 -
7.1.3	Comparing Effects of Hydrogen Addition on a Single-Cylinder Diesel Engine between Simulated and Experimental Data.....	- 142 -
7.2	Recommendations for Future Work .....	- 143 -



## Table of Figures

Figure 1: Common types of direct injection in CI engines: (a) quiescent chamber with multihole nozzle; (b) bowl-in-piston chamber with swirl and multihole nozzle; (c) bowl-in-piston chamber with swirl and single-hole nozzle. [8] .....	- 28 -
Figure 2: Various bowl-in-piston designs for DI CI engines with swirl: (a) conventional straight-sided bowl; (b) reentrant bowl; square reentrant bowl [8] .....	- 29 -
Figure 3: Flow pattern set up in diametral plane by squish-swirl interaction in (a) conventional and (b) reentrant bowl-in-piston combustion chambers [8] .....	- 30 -
Figure 4: Schematic representation of diesel particulate matter [50] .....	- 34 -
Figure 5: Future testing plans and emission bands for major countries (Figure adapted from Mahle Powertrain, 2018) .....	- 37 -
Figure 6: Euro VI emission standards [24] .....	- 38 -
Figure 7 : Exhaust Gas Recirculation [6].....	- 39 -
Figure 8: Schematic showing function of diesel particulate filter [27] .....	- 40 -
Figure 9: Schematic showing a selective catalytic reduction system [27].....	- 41 -
Figure 10: Schematic of Dec's conceptual diesel combustion model during the quasi-steady period of diesel combustion [32] .....	- 43 -
Figure 11: Phases of Diesel Combustion [33] .....	- 44 -
Figure 12: Equivalence ratio-temperature diagram of different combustion concepts [50]-	46 -
Figure 13: Piston Bowl Design [50] .....	- 62 -
Figure 14: Schematic of Experimental Setup [50].....	- 63 -
Figure 15: Ford Puma 2.0L HSDI Engine .....	- 64 -
Figure 16: Cutaway of eddy current dynamometer [50].....	- 65 -
Figure 17: Encoder Technology ET758 heavy-duty Shaft Encoder .....	- 65 -
Figure 18: E+H Promass 83 Coriolis Flow Meter .....	- 69 -
Figure 19: Hamilton Gastight Syringe .....	- 70 -
Figure 20: Schematic representation of NDIR working Principle [79] .....	- 71 -
Figure 21: Schematic representation of flame ionisation [80].....	- 72 -
Figure 22: Schematic showing working cut-away and working principle of TCD [81] ....	- 73 -
Figure 23: Cylinder head cross-section [50].....	- 74 -
Figure 24: Kistler Pressure Transducer and Glow Plug Adapter.....	- 75 -
Figure 25: Kistler 2629C1 TDC Sensor w/Adapter.....	- 76 -
Figure 26: Schematic representation of piston and its connections.....	- 79 -

Figure 27: Schematic of Hydrogen Setup .....	- 88 -
Figure 28: Graph of energy supplied by hydrogen. (a) 1500 rpm, (b) 2500 rpm .....	- 89 -
Figure 29: Effect of diesel-hydrogen combustion on NO <sub>x</sub> and Smoke Emissions .....	- 91 -
Figure 30: Effect of Diesel-hydrogen combustion on NO <sub>x</sub> and Smoke emissions .....	- 93 -
Figure 31: Effect of Diesel-Hydrogen combustion on in-cylinder pressure and AHRR (a) 1500 rpm 2.5 bar BMEP, (b) 1500 rpm 5 bar BMEP, 4% Hydrogen concentration, SOI 9 CAD BTDC .....	- 94 -
Figure 32: Effect of Diesel-Hydrogen Combustion on CO Emissions.....	- 96 -
Figure 33: Effect of Diesel-Hydrogen combustion on CO Emissions.....	- 97 -
Figure 34: Effect of Diesel-Hydrogen combustion on THC Emissions .....	- 98 -
Figure 35: Effect of Diesel-Hydrogen combustion on THC emissions.....	- 99 -
Figure 36: Combustion Efficiency of Hydrogen .....	- 101 -
Figure 37: Combustion Efficiency of Hydrogen .....	- 102 -
Figure 38: 1D engine model of multi-cylinder HSDI engine .....	- 107 -
Figure 39: Properties of hydrogen fuel used for Ricardo WAVE [94][8] .....	- 109 -
Figure 40: Comparison of pressure and heat release rate between simulated and experimental data at 1500 rpm, load (a) 2.5 bar and (b) 5 bar BMEP, 4% hydrogen concentration, SOI 9 CAD BTDC .....	- 111 -
Figure 41: Comparison of NO <sub>x</sub> between experimental and simulated data .....	- 113 -
Figure 42: Comparison of NO <sub>x</sub> and Smoke emissions between experimental and simulated data.....	- 114 -
Figure 43: Comparison of CO emissions between experimental and Simulated Data .....	- 115 -
Figure 44: Comparison of CO emissions between experimental and simulated data.....	- 116 -
Figure 45: Comparison of THC emissions between experimental and simulated.....	- 118 -
Figure 46: Comparison of THC emissions between Experimental and Simulated data...	- 119 -
Figure 47: Screenshot of single-cylinder engine model .....	- 125 -
Figure 48: Effects of diesel-hydrogen Combustion on NO <sub>x</sub> emissions .....	- 128 -
Figure 49: Effects of diesel-hydrogen on NO <sub>x</sub> emissions .....	- 130 -
Figure 50: Effect of diesel-hydrogen combustion on CO emissions .....	- 131 -
Figure 51: Effects of diesel-hydrogen combustion on CO emissions.....	- 132 -
Figure 52: Effect of diesel-hydrogen combustion on THC emissions.....	- 134 -
Figure 53: Effects of Diesel-Hydrogen combustion on THC emissions .....	- 135 -

## Table of Tables

Table 1: Engine Specifications .....	- 64 -
Table 2: Measuring Equipment used along Engine Intake .....	- 66 -
Table 3: Intake charge as a function of hydrogen.....	- 68 -
Table 4: Measuring equipment for fuel .....	- 68 -
Table 5: Measurement Equipment for Exhaust Gas Emissions.....	- 70 -
Table 6: Measuring equipment used to measure in-cylinder data .....	- 75 -
Table 7: Properties of Hydrogen.....	- 77 -
Table 8: Diesel Fuel properties .....	- 79 -
Table 9: Testing matrix .....	- 85 -
Table 10: Energy Supplied by Hydrogen.....	- 89 -
Table 11: Yanmar L70N specifications .....	- 126 -

# Chapter 1

## Introduction

# Chapter 1

## Introduction

### 1.1 Introduction

The invention of the internal combustion engine has helped revolutionise the way society performs everyday tasks. Engine applications range from small engines running handheld power tools up to static installations for power generation or marine application. These technologies have advanced greatly in the last decade owing to the increased demand and funding in the markets. Society owes this advancement to the development of the modern Spark Ignition engine in 1876, by Nikolaus August Otto. Akroyd Stuart and Rudolf Diesel continued August's work by developing the Compression Ignition engine, which is now commonly known as the modern diesel engine. The original prototype that Stuart worked on was produced in 1892 and ran on a compression ratio of 3 and required an external heat source to ignite the fuel injected into the combustion chamber. The external heat source could then be removed once the fuel had been ignited. Diesel's work involved increasing the compression ratio thus allowing the fuel to spontaneously combust once the fuel had been injected into the cylinder. The concept was further developed in 1893 which meant that the engine could now run at a thermal efficiency of 26% which, at the time, was almost double the efficiency of a contemporary spark ignition engine available [1]. This increased efficiency has proved to be the backbone for success for the diesel engine. As a result of this, a wide range of applications have been implemented with the diesel engine used as the primary power source.

Current legislations that have evolved over the past 3 decades have meant that the diesel engine has had to be developed further in order to reduce the exhaust gas emissions which have a damaging effect on human health and to the environment. Manufacturers have now

implemented certain technologies in order to improve engine efficiency and to lower the emissions produced. With the diesel market growing to roughly 50% of the overall car sales market in Europe [2], it is important that these technologies are not only efficient in reducing these emissions but must be commercially implementable.

It is well documented that diesels produce harmful pollutants such as NO<sub>x</sub>, CO, and soot particulates. With the fact that in most developed countries, the transport sector is accountable for around 35% of all consumption of energy [3], the scrutiny placed on the production of diesel engines is increasing year on year. The various legislations and laws that have been implemented over the past three decades represent a more short-term solution, however if the current trends of fossil fuel usage continue, then we could face a deficit by the year 2038 [4] and that the number of vehicles increasing to up to 2.5 billion in the same time period [5], a more long-term solution would be to assess innovative technologies and ideologies that encourage the use of alternative and renewable fuels.

Various engine technologies exist that help improve engine performance, efficiency, and reduce fuel consumption. Such technologies are Exhaust Gas Re-Circulation (EGR), optimised fuel chambers, fuel injection improvements, and alternative combustion methods. These technologies help improve the engine performance at the start and during the combustion process which can ultimately lead to a reduction in exhaust gas particulates, and better fuel efficiency. There are also after exhaust treatment techniques that can retain much of the original engine components and features but will focus on the exhaust gasses. Such systems include: the diesel particulate filter (DPF), the selective catalytic reduction system (SCR), and the diesel oxidation catalyst (DOC). With the introduction of the common rail injection in diesels, the ability to atomize fuel at greater pressures allowed for a more improved combustion process and thus fuel efficiency.

Although the use of petrol and diesel fuel has become the standard in most modern combustion engines, alternative fuels have slowly been implemented over the last two decades or so in order to address the issues raised about climate change. One such fuel that has had a higher usage percentage than most is hydrogen. The use of hydrogen as a fuel has become increasingly popular since about 1998 and the reason behind using hydrogen over for other naturally occurring gasses e.g. methane is down to its chemical composition and wide availability. The ability to obtain hydrogen fuel by using a variety of different primary resources such as fossil fuels, solar power, and wind power has added to its increasing popularity.

The products of combustion when hydrogen is added to an Internal Combustion Engine (ICE) are what make it a more attractive approach. When hydrogen is burned in an ICE, the products are oxides of  $\text{NO}_x$  and water ( $\text{H}_2\text{O}$ ). There are also minimal levels of hydrocarbons (HC) and oxides of carbon ( $\text{CO}_x$ ) produced. The latter products are more as result of the combustion of the lubricating oils found in modern ICEs. Although  $\text{NO}_x$  are harmful to the environment, the quantity by which it is produced can be reduced by running the engine with a leaner air-hydrogen ratio. This helps maintain the engine combustion temperatures to a point low enough that is known for slower  $\text{NO}_x$  formation.

Due to its characteristics, hydrogen has the ability to be used as a fuel in modern IC engines. With regards to SI engines, the hydrogen-air mixture can be ignited with ease using the spark plug due to the minimum ignition energy being lower than that of gasoline. In CI engines, hydrogen is ignited using a small amount of pilot diesel fuel to aid in the combustion process as it has a lower ignition temperature when used in conventional CI engines. In both cases, the largest benefit of using hydrogen as opposed to other carbon based fuels is that the main by-product of its complete combustion is water. Now with increased technological

advancements, it is possible to use hydrogen as a standalone fuel in modified engines, however, there are some difficulties when it comes to this.

Despite the potential benefits of using hydrogen in modern IC engines, there are still challenges related to on-board storage and production solutions for hydrogen. One possible way of obtaining on board hydrogen production is by implementing a catalytic fuel reforming reactor in the EGR loop. The hydrogen enriched gas is then generated through direct catalytic interaction of a hydrocarbon fuel, such as diesel and petroleum. The high temperature exhaust gases are then ejected from the engine. The products of this catalytic interaction can then be re-directed back to the intake cylinder to be used as an addition to the engine's main fuel. The reformed gases that are generated from this process are a mixture of hydrogen and carbon monoxide. The process can however be tuned to focus on the increased production of hydrogen as opposed to other compounds.

With the way that engines are being manufactured in the current climate, much of the pre-testing stage is carried out using engine simulation software. With this software, OEMs can fine tune and specify the conditions and parameters that are required before manufacturing the engine so to avoid needless testing and preparation. Current engine simulation software, such as AVL and Ricardo WAVE, are allowing companies to reach accuracy levels high enough for them to base confident hypotheses on. In doing so, the parameters that are selected to base the experimental tests on can be finalised and thus used for comparison.

Other benefits of using engine simulation software include the ability to re-create conditions for engine simulation that may be difficult to replicate in the real world or in experimental test cells. Parameters such as fuel compositions, altitude, temperature amongst others can all be easily altered within the simulation software to prepare engines for experimental testing. Other parameters which are easily implemented in engine simulation software include driver

behaviours and tendencies. Modern engine simulation software can allow for detailed algorithms that help adjust testing to mimic true driver behaviours to broaden the range of data that can be obtained. This may be more difficult to reproduce in experimental conditions as the way the engine is tested is limited to the conditions of the apparatus used.

With the future of diesel and fossil fuels being the subject of many debates in the last decade, alternative fuels and combustion means have always been touted as replacements for fossil fuel energy in the next three decades or so. Hybrid and full electric powertrain options are what governments and emissions legislators focusing primarily on, however not all combustion and energy applications can be derived from these methods. Large scale commercial vehicles and power generators are still reliant on fossil fuel energy and for the foreseeable future, do not have a readymade replacement. Small single-cylinder diesel engines and large heavy-duty diesel engines are still commonly used and are as practical as needs be within their own field. Therefore, to investigate the possibilities of reducing the harmful emissions emitted from these engines is a requirement to help improve the efficiency and the public image of diesel and fossil fuels until suitable replacements are implemented.

## **1.2 Aims and Objectives**

The primary aims of this thesis is to investigate the effects of the enrichment of the intake air with hydrogen on the performance, combustion and emissions of an HSDI diesel engine using an experimental test engine and comparing the data to that obtained from Ricardo WAVE engine simulation software. This was to analyse the difference in accuracy between experimental and simulated data to help improve the simulation landscape for increased future use. The hydrogen that was used in this research was tested via bottle storage close to the engine and was also simulated in this fashion. The comparisons will be carried out on two types of engine, a small single-cylinder diesel engine and a larger four-cylinder diesel engine. This will give a range of data for varying uses of the research used for this thesis.

Initially, tests were carried out using hydrogen gas to investigate the way the hydrogen introduction affects parameters such as emissions, combustion and performance of a diesel engine. These results were then compared to an engine re-created using simulation software for a comparison to analyse the difference in accuracy between experimental and simulated data. The second set of tests included replicating the conditions using a single cylinder diesel engine and subsequently repeating these tests on the simulated model for comparison again. Finally, the last tests included the comparison between single and multi-cylinder operation and the possibility of using smaller diesel engines for light-duty applications. The main objectives of this research are outlined below:

- Look at how the introduction of hydrogen affects the performance, combustion and the emissions using different engine operating conditions. The conditions selected for the tests represent light- and medium-duty diesel engines. Injection parameters and hydrogen concentration was also altered for each case.
- Observe whether hydrogen can reduce the NO<sub>x</sub> and CO emissions.
- Analyse the combustion efficiency of the hydrogen introduced in the engine under the different operating conditions and hydrogen concentrations.
- Investigate the use of Ricardo WAVE to obtain comparison of the experimental data as close as possible to the simulated data by generating a replica model of the two different engines.
- Compare the data obtained from the multi- and single-cylinder test engines and simulated data to investigate the use of smaller diesel engines in the aggressive downsized market.

### **1.3 Outline of Thesis**

The outline of the thesis for the following chapters after this introductory one are as follows:

#### **Chapter 2 – Literature Review**

This chapter will look at the how emissions are formed in diesel engines. It will also look at the current European Emission Standards and the future standards. Alongside this, the future and present of exhaust after treatment will be presented. Alternatives to diesel combustion modes and injection parameters will also be presented. Alternative fuels, intake charge dilutions for diesel and dual fuel methods are reviewed in this chapter. Lastly, the impact of downsizing and engine simulation software will be discussed.

#### **Chapter 3 – Experimental equipment, procedures and data analysis**

This chapter details the specifics of how the experimental data was collected by outlining the facilities used, the measuring equipment, the procedure and the method by which data was analysed. It will also outline the technique used for the engine simulation software, the parameters set and the conditions that have been replicated via the software with full justification as to why certain parameters were chosen.

#### **Chapter 4 – Effects of Combined Diesel-Hydrogen Combustion on Combustion Properties**

This chapter will present the findings of the effects of combined diesel-hydrogen combustion on a HSDI diesel engine with regards to the operating conditions, the combustion properties and the emissions produced. Here the NO<sub>x</sub>, Bosch Smoke Number (BSN), Carbon Monoxide (CO), and the Total Hydrocarbons (THC) emissions will be measured and compared. The hydrogen combustion efficiency will also be examined.

## **Chapter 5 – Comparison between Simulated and Experimental Diesel-Hydrogen Combustion**

In chapter 5, the data collected during chapter 4 will be compared and analysed using an engine model built and optimised to replicate the same experimental engine using Ricardo Wave®. Here, the goal is to achieve a high level of accuracy between the simulation and the experimental data to analyse the use of software for engine testing and development. The emissions that are primarily looked at here are the NO<sub>x</sub>, BSN, CO, and the THC emissions.

## **Chapter 6 –Studying the Effects of Hydrogen Addition on a Single-Cylinder Diesel Engine Using Ricardo Wave® Simulation Software**

In this chapter, a single-cylinder diesel engine based on a Yanmar L70N diesel engine is built and optimised in Ricardo Wave® running with diesel-hydrogen dual-fuel combustion, with the results of the simulations compared with similar data found in other experimental work and literature with the objective of utilising diesel engines in light-duty capacities. The accuracy of the simulations will also be looked at along with the NO<sub>x</sub>, BSN, CO, and THC emissions produced as a result of the hydrogen addition.

## **Chapter 7 – Conclusions and Future Work**

This chapter will summarise the findings outlined in the previous chapters along with the future work that could be created as a result of this research.

# Chapter 2

## Literature Review

## Chapter 2

### Literature Review

#### 2.1 Compression Ignition Engines

The mechanics of a compression ignition (CI) engine and how it operates differs slightly to that of a spark ignition (SI) engine. In a SI engine, the combustion process is ignited via the spark plugs generating the required temperature increase. For CI engines, the combustion process begins during the compression stroke, whereby the increased pressure raises in-cylinder temperature adequately enough to ignite the air-fuel mixture. Some CI engines use the input of glow plugs to aid in this process. Glow plugs are used in a similar fashion to spark plugs, however their effect is witnessed before ignition and they are used as a pre-warmer of the cylinder head. Although CI engines exist as 2 or 4 stroke engines, the majority of modern CI engines are 4 stroke engines. Obtaining an efficient running condition for modern CI engines depends on the air-fuel mixing ratio. The way on which the fuel mixes is primarily governed by the air motion and the fuel injection, which are both discussed in further detail later during this chapter. Ideally, an engine will have high efficiency, rapid combustion, high output, clean exhaust fumes and silent operation. These characteristics are immensely sought after with current manufacturers however it is almost impossible to produce an engine that can meet all of these criteria [1].

There are certain traits of the CI engine which place it at a disadvantage next to the SI engine. A slower combustion rate has meant that the CI engine has a limit to the maximum speed it can achieve. Another issue is the problem of cold starting where the need for extra components such as glow plugs to heat the combustion chamber, has meant that the engine will not start until reaching an optimum temperature using these components. In addition to

this, the combustion chamber itself has been designed to reduce heat transfer in which doing so will reduce the ignition delay and in turn, increase the exhaust gas temperatures. These types of engines are known as adiabatic and they are primarily designed to simply reduce the heat losses rather than eliminate them all together. These higher exhaust gas temperatures can be used to operate turbochargers, which will be discussed in further detail later in the chapter [1].

### **2.1.1 Fuel Injection**

The way fuel is injected into the engine is a catalyst for much of the engines characteristics such as power output, torque and fuel economy therefore this relationship must be carefully managed. Once managed correctly, the air/fuel ratio and the air movement will lead to complete combustion, which is arguably one of the most desirable characteristics a diesel engine can have. Due to the fact that the load is controlled by varying the amount of fuel injected and not throttling the air intake, it is important that complete control is available for the fuel injectors [1, 6]. With the purpose of understanding this further, both main types of fuel injection for diesel engines shall be studied. The first being indirect injection and the second being direct injection. This has a bearing on the question at hand due to the importance of the air flow into the cylinder via the inlet valves. The air flow, as mentioned earlier, needs to be managed efficiently in order to obtain an effective fuel/air mixture.

### **2.1.2 Direct Fuel Injection in Diesel Engines**

The direct fuel injection system injects fuel at high pressure directly into the combustion chamber. Due to the lack of spark ignition available in a diesel engine, the fuel atomisation, heating, evaporating and the mixing must happen quickly in order to condense with the compression stroke. This technique is possible only when high turbulence is available in the

combustion chamber, which is brought about by the design of the chamber encouraging different air movements such as swirl and swish [1, 6].

Direct fuel injection can distribute the fuel in two distinct manners. The first being the air-distribution method and the second being wall-distribution. The former involves the use of multiple nozzles at high pressure to inject the fuel directly into the compressed air above the piston in the combustion chamber whereby the fuel mixes with the air due to the air movement and its interaction with the atomised fuel [1, 6].

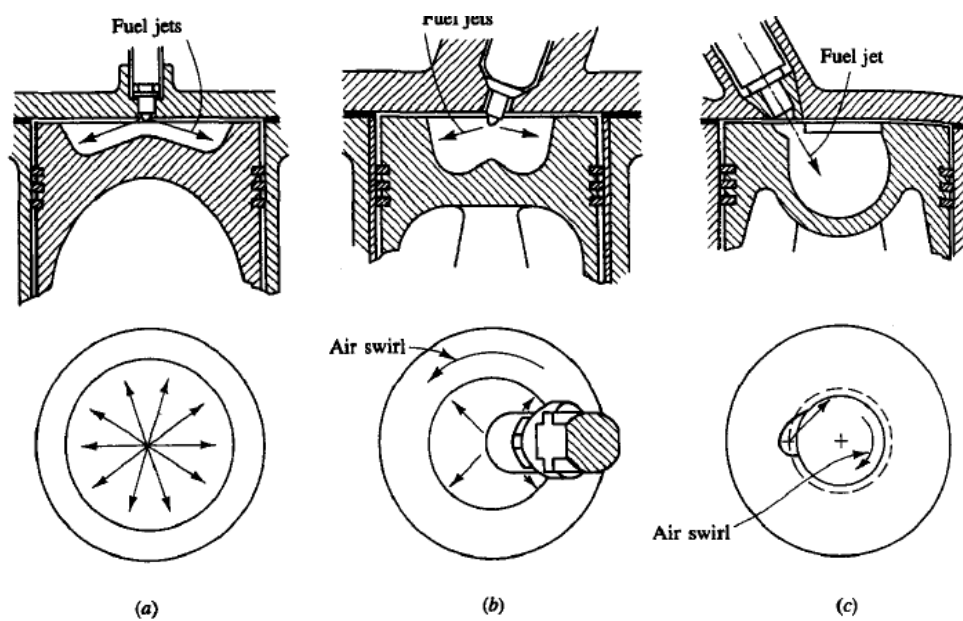


**Figure 1: Common types of direct injection in CI engines: (a) quiescent chamber with multihole nozzle; (b) bowl-in-piston chamber with swirl and multihole nozzle; (c) bowl-in-piston chamber with swirl and single-hole nozzle. [8]**

The second technique, mentioned above, is the wall-distribution method. This involves a single low-pressure fuel nozzle, injecting the fuel at relatively low pressures directly onto the cylinders walls. The high temperatures of the cylinder walls allow for the fuel to instantly evaporate into chamber. This method, however, does increase fuel consumption in comparison to air-distribution [1, 6]. The most common type of high pressure fuel injection for diesel engines is the common rail fuel injection system. In this system, the high-pressure fuel is accumulated in an overhead rail consisting of injectors over every cylinder head. The

injectors are controlled via the ECU and are reliant on various sensors dictating when and how much fuel is to be injected into the system. The main advantage of this system is that the fuel injection pressure remains relatively stable during injection and that there is no need for high pressure fuel lines [6].

Recent technologies have been introduced which now allow improvements in the design and the level of control available for the common rail injection system. These improvements have the ability to effectively reduce the amount of emissions produced. Along with the addition of sophisticated and modern ECUs, up to 5 split injections per cycle per cylinder is also now a form of increasing the amount of control in the combustion process making it more efficient in the long run [7].

## 2.2 Air Management

The intake of air is of the highest importance in an engine, making controlling its input into the engine very critical. Due to the fact that the air volume does not fluctuate in an engine, it is important to keep a constant intake temperature and density in order to ensure that the engine is running efficiently. The use of valve technology can govern how air enters the combustion chamber and the existing lift technologies are vital in controlling this [8].

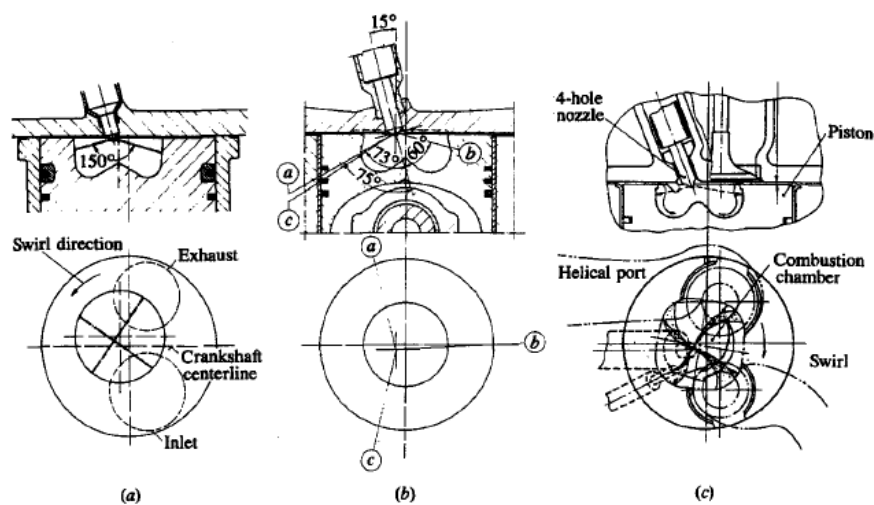
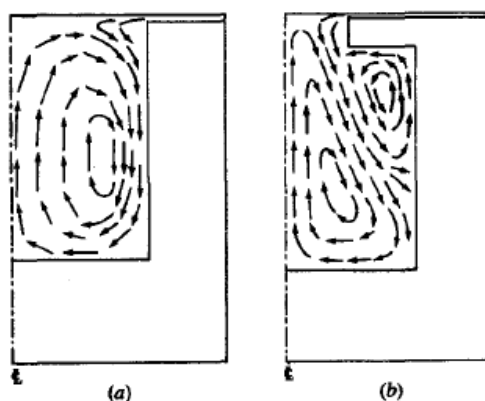


Figure 2: Various bowl-in-piston designs for DI CI engines with swirl: (a) conventional straight-sided bowl; (b) reentrant bowl; square reentrant bowl [8]

Dense air is always preferred when used in combustion as it provides a leaner fuel mixture and more efficient burning of the fuel. In order to achieve this density level, the air must be free from any particles, clean and as cool as possible. There are two known methods with which intake air can be filtered in an engine. The first being wet filtered, which involves air being passed through an oil basin removing any impurities in the process. The intake air is then subsequently passed through a fine screen in order to remove any remaining oil. This system is usually found in stationary engine cases. The second method of filtering is the use of a dry filter. A dry filter is usually made of cloth, paper or metal screens where any particles in the intake air are trapped. As mentioned earlier, the cooler the air the denser it will become and thus the more efficient the engine will run. Keeping this in mind, the air filter, in automotive cases especially, is usually located outside of the engine bay or as far away from the engine as possible. This ensures that the intake air is not contaminated with how engine air and any particulates surrounding the immediate area. Once the air is filtered, modern diesel engines have various technologies to make the air cooler or denser or even in some cases, both. This is done by passing the air through a cooler or a compressor before entering



**Figure 3: Flow pattern set up in diametral plane by squish-swirl interaction in (a) conventional and (b) reentrant bowl-in-piston combustion chambers [8]**

the inlet manifold itself [8].

The diesel engine can run in various formats such as supercharged, turbocharged or naturally aspirated. These methods will be discussed in further detail later in this chapter. For now, the focus will be on the methods used to cool the intake air. Turbo and supercharging involves forcing the air at a much higher rate into the intake manifold. Increasing the rate of flow of air raises its temperature and a result of this is reducing its density, something that is undesirable in the combustion process. When cooling the intake air after compression there are two methods that can be applied. The first being water-cooled intercoolers. This is usually found in larger, slower vehicles where the intake air passes through the compressor into the intercooler and is then cooled via the radiator in the car. The second method is by using a fast flow of ambient air over the intercooler. Many different techniques exist for this; however, the most common would be deploying a bonnet scoop which allows the air to flow directly over the intercooler. This is usually aimed at faster vehicles as it allows for a faster flow rate of ambient air over the cooler [8].

### **2.3 Exhaust Gas Emissions**

The world's leading engineers and manufacturers are forever verging towards a cleaner world with less pollution. Most have achieved that in the creation of hybrid and full electric vehicles. In an ideal world, the only emissions to be released from a diesel engine would be from complete combustion resulting in carbon dioxide and water. This combustion process begins with the chemical process of oxidising hydrocarbon fuels resulting in the output of energy in the form of heat, movement, and light. Ideal combustion is primarily achieved under stoichiometric conditions, which indicate that the air-fuel ratio is 1:1. In reality, however, the engine does not run under ideal conditions due to the vast complexities involved in engine combustion. These complexities include, the variance in the local equivalence ratios in diesel engines, the difference in components and structures within the engine, and

environmental impacts all lead to the production of unwanted chemical substances such as NO<sub>x</sub>, CO, unburned hydrocarbons (UHCs), and particulate matters (PMs). The adverse effect on human health has been observed and published on a constant basis [10-12]. Recent technological advancements have allowed for the diesel engine to control the amount of unwanted exhaust emissions through the use of catalytic converters, thermal reactors and particulate traps [8]. These have helped reduce the amount of carbon monoxide, nitrogen oxide and other harmful gasses affecting the environment and human health and will be discussed further in the coming sections.

### **2.3.1 Oxides of Nitrogen**

Oxides of nitrogen consist of two particular pollutants: nitrogen dioxides (NO<sub>2</sub>) and nitric oxides (NO). During typical combustion, NO constitutes to over 90% of the NO<sub>x</sub> emissions produced from a diesel engine. One of the primary causes of NO<sub>x</sub> formation is elevated in-cylinder temperatures during combustion. NO<sub>x</sub> formation tends to occur when in-cylinder temperatures rise to between 1527-1727 °C and when running close to stoichiometric. This particular operating region is known as the ‘thermal’ NO formation mechanism. This mechanism is more likely to occur after the onset of heat release and the amount produced increases two-fold every 90 °C increase above 1827 °C [13].

In order to truly attempt to reduce the NO<sub>x</sub> emissions, it is crucial to gain a deep understanding of the mechanisms that produce the harmful emissions, which can ultimately aid in the improvement of human health and the environment. Environmentally, NO<sub>x</sub> is culpable to being a key contributor to smog and acid rain, which all speed up the global warming process. With regards to the effect on human health, NO<sub>x</sub> emissions are potentially poisonous and can lead to respiratory problems and premature deaths if left untreated.

### 2.3.2 Particulate Emissions

The issue of diesel particulate matter has become of increasing concern within the last decade or so due to the increase in awareness of the possible threat to the environment and the human health. Due to the complexity involved in the chemical and physical characteristics of PMs, the classification of them is becoming increasingly difficult. Simply put, PM comprises of solid carbon particles and various chemical species which agglomerate forming the complex PM. The agglomerated particles are formed via the carbon formation from reactive intermediates. These intermediates are found primarily in the fuel rich zone of combustion where fuel has not been burned to completion when in a region of excess oxygen. The result of this process is that fine carbon particles agglomerate onto the remaining combustion products, such as nitrogen oxides, sulphur oxides, and heavy hydrocarbons, all formed due to the higher combustion temperatures [14].

Particulates are usually found to be divided into three separate fractions, being Solid Fractions (SOL), Soluble Organic Fraction (SOF), and Sulphate Particles [15].

SOL particulates occur when the unburned carbon particles agglomerate whilst in transition from cylinder to ambient air. The rate of oxidisation of the particles is known to decrease once they move from the cylinder as a result of the drop in temperature around them. Other sources of SOL are the metallic ash compounds which originate from lubricating oil additives, and engine wear.

SOF particulates are engine load dependant and the quantity produced varies on the technology and the test cycle used. It is possible for SOF particulates to comprise of over 50% from the total amount of PM.

The third and final fraction is the sulphate particulates, which are formed as a result of the reaction between the molecules of  $H_2O$  and  $H_2SO_4$ . Sulphur particulates formulation levels are dependent on the sulphur levels in the fuel; therefore, controlling this particular aspect of the fuel is a major prevention mechanism for forming sulphur particulates. Combining these sulphur particulates with SOF and SOL, the final PM is formed.

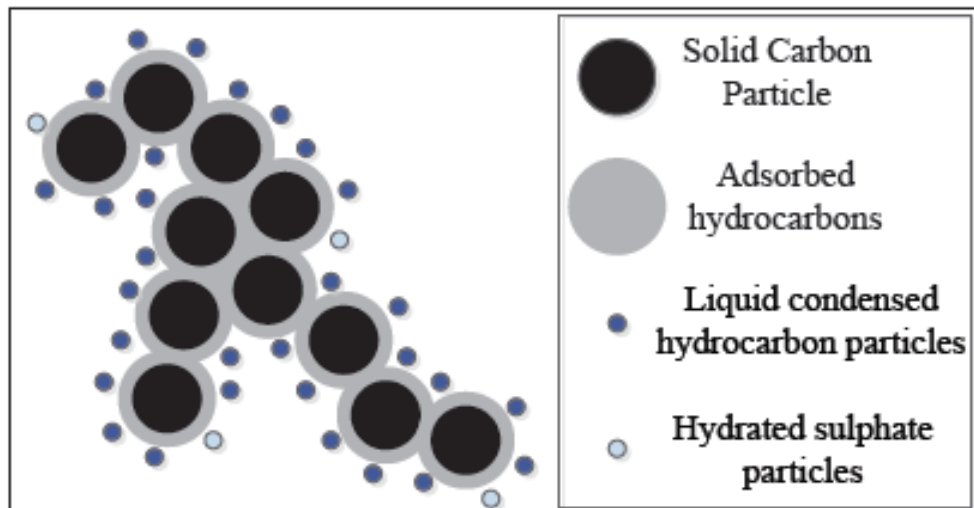


Figure 4: Schematic representation of diesel particulate matter [50]

The effects of PM on human health has been documented extensively [16] and it is shown that contact with PM could lead to developing asthma, or in more extreme cases lung cancer also. The size of the PM is what determines how much damage could be potentially done to the human health, where larger particles of around  $10\mu m$  and above can be filtered out via the nose and throat. Smaller particles of less than  $2.5\mu m$  are able to infiltrate deeper into the lungs. For this reason, it is dangerous to assume that the reduction in the quantity of the PM has resulted in a cleaner combustion.

To better understand the formation of the particulates during combustion in-cylinder, various methods have been used to analyse how and when they are formed. Examples of the techniques are cylinder dumping [17], rapid acting valves [18], and optical absorption techniques [19]. These methods all are involved in analysing the formation of PM in the

cylinder however due to the complexity of both their physical and chemical characteristics, the analysis and subsequent treatment becomes increasingly challenging. In addition to the complex structures of the PM, there are other factors that influence the formation of PM within the cylinder such as the temperature, pressure, and the fuel composition. The more damaging PM is those that are allowed to leave the exhaust, where electrical mobility analysers are used.

Although there are many publications outlining the possibility of analysing PM emissions in-cylinder, currently the most feasible technique of reducing them is via exhaust after treatment. Some examples of this which have been widely implemented by manufacturers include the use of diesel particulate filters. For treating PM emissions in-cylinder, more research is needed to tackle this issue.

### **2.3.3 Carbon Monoxide**

CO is one of the more harmful substances that are generated as a result of incomplete combustion with fuels that contain carbon. A primary reason for the production of CO is the reduced levels of oxygen in the combustion chamber, which leads to incomplete fuel oxidation. There are other factors that are responsible for the formation of CO such as, non-homogenous air-fuel mixing and lower combustion temperature. By understanding how CO is produced in the engine, it is possible to take preventative methods to help reduce the effects of CO poisoning on human health and the environment.

Inhaling CO leads to the CO particles being absorbed into the blood stream, which ultimately leads to the CO poisoning by decreasing the oxygen carrying capacity of the haemoglobin in the blood and subsequently, rotting of the tissue [20]. With regards to the environment, CO is not widely thought to be a large direct contributor to pollution however its indirect effects on the environment are still important to discuss. CO<sub>2</sub>, which is one of the more damaging

greenhouse gases to the ozone layer and the environment, is produced via the reaction between hydroxyl (OH) radicals and CO. The usage of OH results in larger methane concentrations which are also harmful to the ozone layer [21].

#### **2.3.4 Total Unburned Hydrocarbons**

Hydrocarbon pollution usually occurs when fuel that has been unburned or partially burned exits the exhaust pipes of a vehicle. There are various methods which contribute to the formation of UHCs within a diesel engine such as, the possibility of crevices in the combustion chamber, flame quenching and formation of liquid films on the combustion chamber surfaces, improper or under-mixing of fuel and air leading to overly rich fuel zones which cannot be burned due to the lack of oxygen, and the over-mixing of fuel and air beyond the lean flammability limits during ignition delay periods [8, 22, 23].

#### **2.4 Legislation and Regulations**

The current initiative to reduce greenhouse gasses has led to governments introducing various legislative standards by which car manufacturers under their jurisdiction must comply with. These legislations and regulations are constantly being adjusted to reflect the current environmental and consumer market for the automotive field. The parameters that are usually included as part of the legislations are based on harmful exhaust emissions, specifically substances such as UHCs, PM, NO<sub>x</sub>, and CO emissions. The UK is currently part of the European Euro VI emissions standards where all cars manufactured must comply by October 2014. There are sub sections of 6b, c, and d which is expected to stretch to 2020 and beyond whereby vehicles must comply by ever stricter emissions values as it gets closer to 2020.

Figure 1 indicates the method of testing that is currently being carried out to measure these emissions and the future methods that will take place. Currently, the NEDC testing method is being used. This is based on a typical speed-time pattern of driving; however, it has been found to be slightly inaccurate as it does not take into account the differences in terrain, conditions, and most importantly driver behaviour. For this reason, the RDE (Real Driving Emissions) and the WLTP (Worldwide Harmonized Light-Duty Vehicles Test Procedure) test have been implemented so to better represent a more real-to-life driving cycle, thus providing more accurate data for the emissions.

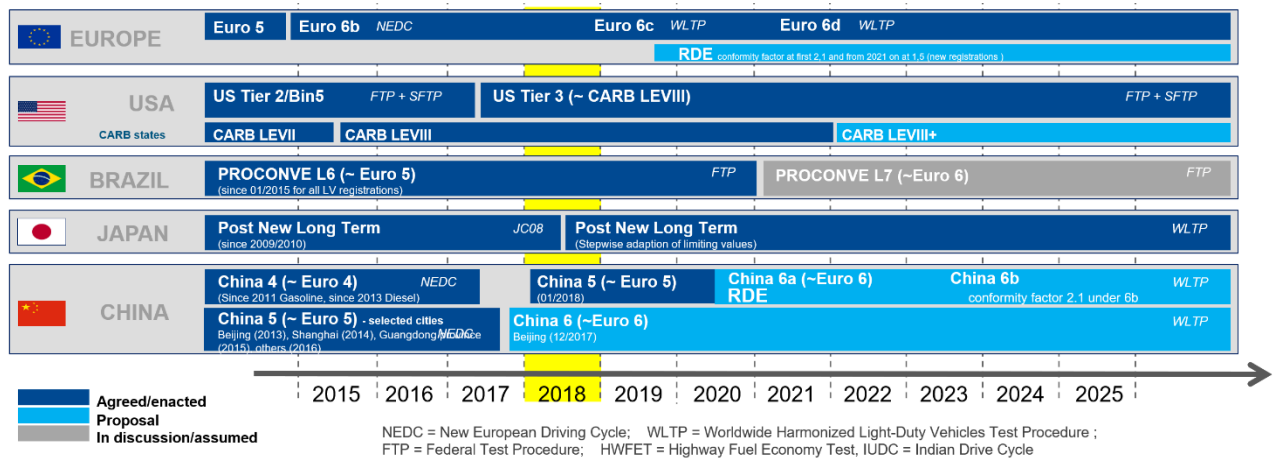


Figure 5: Future testing plans and emission bands for major countries (Figure adapted from Mahle Powertrain, 2018)

As mentioned, vehicles up until this point had to comply with the Euro VI emissions standards, which were implemented in September 2014 and vehicles had to be fully compliant by September 2015, The Euro VI standard required a 67% reduction of NOx emissions compared to the outgoing Euro V standards. Various exhaust after treatments were available to use on vehicles to help reduce certain emissions and thus aid in the compliance of vehicles. These treatments will be discussed in the coming chapters.

Figure 2 displays the current maximum level of harmful emissions allowed as part of the Euro VI standard.

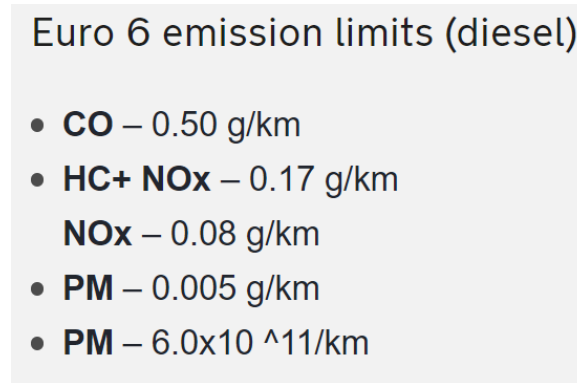


Figure 6: Euro VI emission standards [24]

## 2.5 Exhaust Gas Aftertreatment

Despite the possibility of reducing the harmful emissions produced during combustion by using in-cylinder emission control methods, the employment of exhaust aftertreatment is often a necessity in order to meet the required legislative emission standards. There are a variety of different methods that manufacturers use for their own particular aftertreatment needs and in most cases, use a combination of them to further reduce the emissions to meet legislations.

### 2.5.1 Exhaust Gas Recirculation

Exhaust gas recirculation (EGR) is a recently developed technology implemented to reduce the amount of NO<sub>x</sub> emissions generated by diesel engines. Two reasons which cause NO<sub>x</sub> emissions to occur in engines are the speed of the flame and the temperature of the flame. When implemented, EGR reduces both of these so in turn reduces the NO<sub>x</sub> emissions. The hot exhaust gasses are extracted and then cooled in an EGR cooler, lowering the temperature to below 150°C. This exhaust gas is then mixed with fresh air and then fed into the combustion chamber. The inclusion of H<sub>2</sub>O and CO<sub>2</sub> components occurs due to the reduction

in the amount of oxygen in the fresh mixture. This leads to combustion zone being cooled by a few hundred degrees Celsius, depending on the exhaust gas recirculation rate. Additional effects of this system, along with reduced NO<sub>x</sub> emissions, are the reduced wall heat losses and reduced cylinder components temperatures [6].

Typically, EGR is used in turbocharged engines with two different approaches. Low pressure exhaust gas recirculation occurs when the exhaust gas is extracted after the turbine, where it

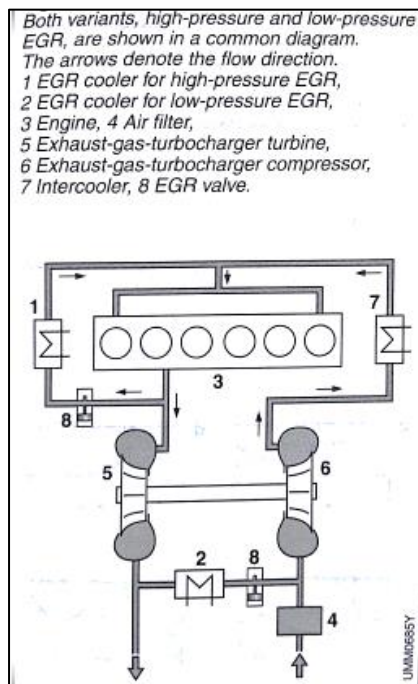


Figure 7 : Exhaust Gas Recirculation [6]

is then cooled and then re-introduced before the compressor. In terms of high pressure exhaust gas recirculation, which prevents increased thermal loads and contamination on the compressor, it is affected on the high-pressure side (Figure 3). A suitable scavenging drop must be maintained between the exhaust and the intake sides, leading to a deterioration of the charge cycle loop. Flutter valves between the exhaust gas and the fresh air tracts are sometimes used in conjunction with this system. The flutter valves allow control over the pressure pulsations, where they open and close in response to overpressure on the exhaust side [6].

Currently, low pressure exhaust gas recirculation is already in commission with commercial and passenger vehicles and is still undergoing further development. Particularly, EGR uniform distribution and the less disadvantageous pressure differential, which applies to the pressure after the turbine rather than the pressure before the compressor, are highly desirable features. However, in order to avoid contamination to the compressor, the exhaust gas must be extracted after the particulate filter in diesel engines. In addition to this, the higher thermal loads with which the compressor is subjected to must also be noted [6].

### 2.5.2 Diesel Particulate Filter

A diesel particulate filter is used to catch particulate matter that is emitted during combustion via a filter that can achieve up to 90 % filtration efficiency [25]. The method in which the DPF works is by separating the particles in the exhaust gasses that are harmful through filtration walls within the cylinder. The physical characteristics of the DPF is shown in figure 4, where there are a series of dead-end channels which run parallel to one another in the axial direction. The exhaust gasses are forced through the porous walls of the tubes to an exit, resulting in the particles being deposited on the filter walls. Build of these particles on the filter walls could lead to increased exhaust back pressure, which may lead to damaging effects on the fuel consumption and the engine torque, making the vehicle appear to feel less powerful [26]. For this reason, a regeneration process is often needed to clean out the DPF. This can be done automatically via the engine programming to run slightly higher exhaust temperatures to burn the particles away, or it can be done manually by driving the vehicle consistently and a steady speed and load for a period of time, usually on motor or highway driving conditions.

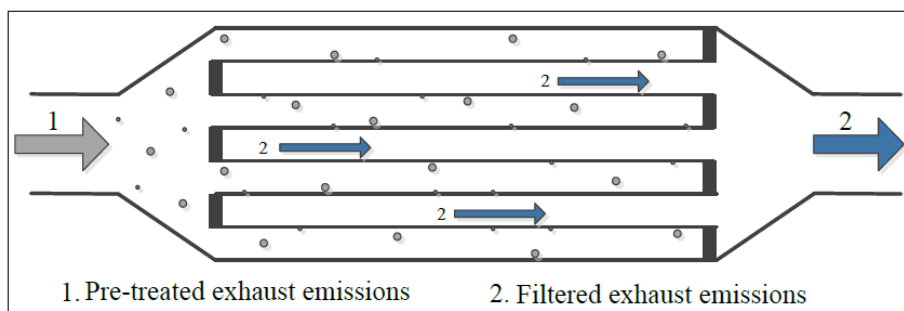


Figure 8: Schematic showing function of diesel particulate filter [27]

### 2.5.3 Selective Catalytic Reduction

The method of SCR is well established in the stationary and marine diesel applications for reducing NO<sub>x</sub> emissions. For automobiles, EGR is the more common technique that is used

to achieve the same type and amount of reductions. Despite the successes of EGR, the ever-increasing strictness of the legislations and regulations on diesel powered vehicles means that EGR is no longer sufficient enough to keep NO<sub>x</sub> emissions to an acceptable limit. Thus, the use of SCR technology in the exhaust pipe of diesel powered vehicles is key in maintaining the adequate NO<sub>x</sub> levels. Traditional systems used ammonia (NH<sub>3</sub>) as the additive in SCR systems that would mix with the exhaust fumes in the exhaust pipe and thus break-down the NO<sub>x</sub> emissions. However, the toxicity of NH<sub>3</sub> meant that production and storage of the substance proved impractical and dangerous for use in vehicles. Currently, the replacement for NH<sub>3</sub> is Urea, which fulfils the same requirements that NH<sub>3</sub> filled without the apparent drawbacks. Figure 5 displays a typical SCR system whereby diesel exhaust fluid (DEF) or commonly known as Ad-Blue, is used to achieve the reductions in NO<sub>x</sub> emissions. Ad-Blue is an aqueous solution which consists of 67.5% deionised water and 32.5% urea [27]. Once the exhaust gas temperature reaches 160 °C, NH<sub>3</sub> forms through particular reactions in the decomposition reactor.

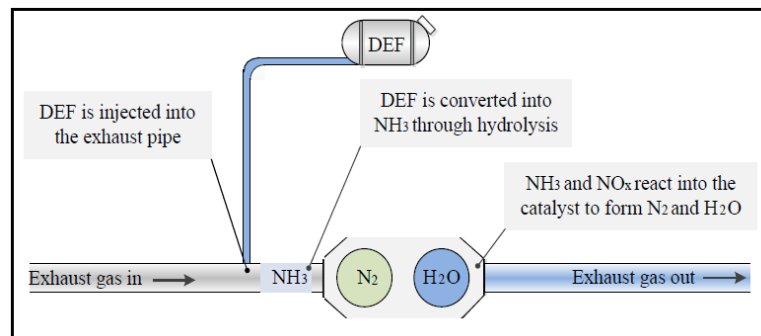


Figure 9: Schematic showing a selective catalytic reduction system [27]

#### 2.5.4 NO<sub>x</sub> Adsorber

Although SCR is a viable method and is widely employed in modern diesel-powered vehicles, a potential alternative is using a NO<sub>x</sub> adsorber. NO<sub>x</sub> adsorbers use storage

components such as Potassium (K), Sodium (Na), Calcium (Ca), Barium (Ba) trapping any NO<sub>x</sub> emissions emitted from the exhaust during a lean combustion process. During the combustion process, if oxygen is present, NO<sub>x</sub> is stored as part of the oxidation of NO to NO<sub>2</sub>, where the process is shown below [27]:



Which is then stored in the trap as a nitrate species:



At this point, the stored nitrate species is decomposed as the engine operates at higher temperatures or in fuel-rich conditions:



At this point, the NO is then reduced over the trap. This is shown in the final equation below:



In order for equation 4 to be completed correctly without NO<sub>x</sub> spikes, the temperature needs to be high enough [28]. There has been reports of efficiency ratings ranging between 80-90%, where the highest efficiency occurring usually in the range of 350-380 °C [29].

## 2.6 Diesel Combustion

For the improvement of diesel combustion and increasing its efficiency, a deeper understanding is needed of how the science and mechanics of diesel combustion takes place is needed. There is a vast amount of research revolving around the combustion concept of diesel where various models have been researched involving the spray formation, vaporisation, ignition, mixing, pollutant formation, and the destruction mechanisms [30, 31, 32]. Figure 6 is a depiction of a conceptual model for diesel combustion during the quasi-steady phase [32].

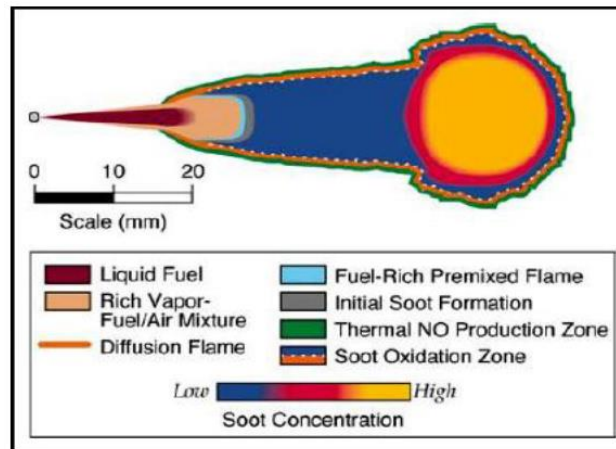


Figure 10: Schematic of Dec's conceptual diesel combustion model during the quasi-steady period of diesel combustion [32]

The process involves the liquid fuel vaporising as it moves from the nozzle down the jet due to it entraining the hot in-cylinder air quickly. The result of this process is the formation of fuel-vapour/air mixture layer surrounding the sides of the jet in a sheath-like fashion. As the fuel-vapour/air mixture flows into the jet, oxidation occurs whilst being exposed to high temperatures. The final phase of the oxidation will then take place at the border of the jet stream. As the amount of fuel-vapour/air and hot combustion products enter the penetrating jet increase, the rate of combustion increases. This specific part of the process is what is being represented in figure 6 [32].

Understanding the basics of the combustion process is also needed acquire a wider appreciation of the process in general and how to increase its efficiency. The following paragraph will look at exploring the combustion process as it goes through the start of ignition (SOI) and the end of combustion (EOC) with various aspects of the combustion process looked at in more detail. One of the more important aspects of the combustion process is the apparent heat release rate (AHRR), which can be analysed using the in-cylinder

data. Using the data obtained from figure 8, which was collected using a heavy-duty diesel

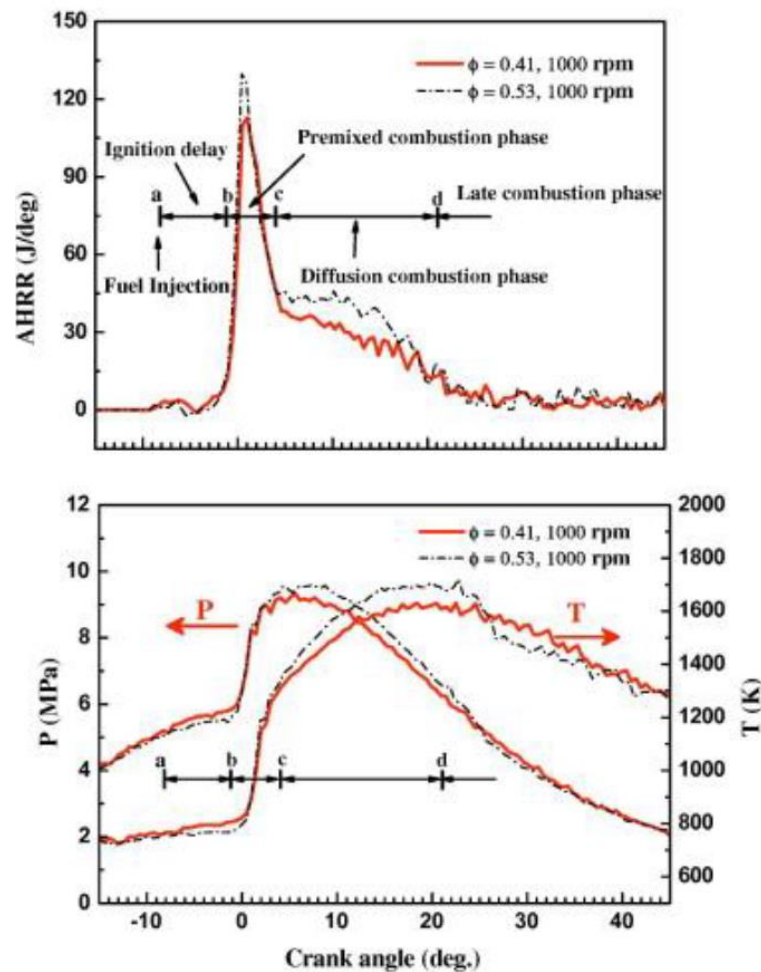


Figure 11: Phases of Diesel Combustion [33]

engine, the AHRR can be analysed visually [33].

Observing the figure, the different combustion phases are displayed and will be explained in further detail. Point *a* represents the SOI where this point is taken at either the time when the injector needle lifts off its, assuming there is a needle lift indicator, or when the engine control unit (ECU) relays a signal to the injector if no needle lift indicator is present.

Phase *a-b* represents the ignition delay (ID) phase which is the interval between the SOI and the start of combustion (SOC). As a result of the absorbed heat from the evaporated liquid fuel, the AHRR during ID is more usually negative. The operating conditions of the engine,

the injection timing, the level of diluted intake air, and the amount of fuel being injected are all parameters that can alter the duration of the ignition delay.

Phase *b-c* represents the premixed combustion phase which takes place after the ID phase. During the ID phase, a fuel-air mixture, which is pre-mixed ready for ignition, is formed where combustion soon follows once the temperature of auto-ignition for diesel combustion is achieved. As can be observed in figure 7, there is an undesirable effect of a swift increase and rise in pressure, temperature and AHRR. This specific point of combustion is what produces the characteristic noise in diesel engines. Moreover, the increase in oxygen and temperatures directly contribute to an increase in the NO<sub>x</sub> formation within the cylinder.

Phase *c-d* is known as the diffusion combustion phase or is also known as the mixing-controlled phase. This phase starts directly after the pre-mixed combustion phase and ends at the completion of the fuel injection period. The injection rate and the fuel-air mixing process determines the rate at which fuel is consumed by the engine. Should the mixing be inadequate and a richer fuel mixture is created, these conditions coupled with high in-cylinder temperatures could increase the chances of soot formation.

The final phase, *d*, is the EOC phase. Here, late combustion allows any residual fuel or partially-burned species to burn at a lower than usual rate. This is reliant on the fact that there is adequate movement within the cylinder.

## **2.7 Alternative Modes of Diesel Combustion**

Although the fundamentals of diesel combustion remain the most common method of combustion that most manufacturers employ, there are other methods with which diesel combustion can occur that other researchers have examined and documented. These alternative diesel combustion techniques have shown potential in reducing the formation of harmful emissions [34-37]. The research that is currently being undertaken is looking at

allowing for the usage of these alternative combustion modes in a larger scale, consumer setting. One of the more challenging aspects of changing the combustion control are the fuel consumption penalties, the emission trade-off effects and the need for smarter fuel control units. Low Temperature Combustion (LTC), Homogenous Charge Compression Ignition (HCCI), Pre-mixed Charge Compression Ignition (PCCI), and Reactivity Controlled Compression Ignition (RCCI) are all going to be examined and discussed in the following section, so to appreciate the efforts of research made to understand them.

### 2.7.1 CAI/HCCI Combustion

Controlled Auto-Ignition (CAI) and Homogenous Charge Compression Ignition (HCCI) are two forms of internal combustion occurring in the engine in which the air and fuel are mixed fully prior to auto-ignition. The differences between the two are small but relevant. HCCI is defined as controlled auto-ignition of pre-mixed air and fuel when diesel is the fuel source whereas CAI occurs when used petroleum type fuels. Understanding these forms of combustion is important for the project as it has major bearings on the way the air and fuel is delivered into the cylinder via the valves.

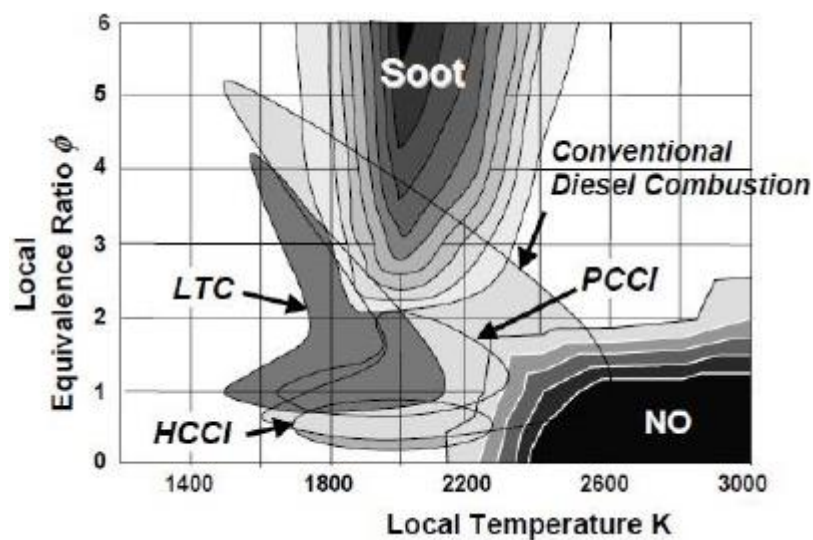


Figure 12: Equivalence ratio-temperature diagram of different combustion concepts [50]

In order to obtain ideal HCCI combustion, a low temperature and lean combustion is required which is initiated at various points throughout the cylinder. The result of this is no flame propagation and which means vast reduction in nitrogen oxide emissions. A traditional problem amongst common CI engines is the amount of unburned hydro-carbons and nitrogen oxide emissions. HCCI combustion appears to be the perfect solution to this problem due to its leaner mixture and lack of flame propagation which also allows it to be more efficient than normal CI ignition. The only apparent problem of HCCI combustion is the lack of control of the ignition point. Where SI engines uses a spark to ignite the fuel/air mixture in the cylinder, the CI engine must rely on the injection of the fuel at high compression to reach this. The ignition can only occur using the charge mixture and the temperature history. This factor was the substance behind many of the current technologies available such as high-level exhaust gas re-circulation, and variable compression ratio [9].

### **2.7.2 Low Temperature Combustion**

With LTC, the primary goal of adopting this technique is to change the combustion chemistry of a conventional diesel engine to reduce the production of harmful emissions. There are a large number of benefits involved in reducing the harmful emissions that exit from the exhaust of a diesel engine, chief among which is the aid it could provide aftertreatment apparatus and techniques as there is much less pollutant to treat. Moreover, the benefits on the environment are as important and are an added possible benefit of this technique.

One of the more difficult challenges in employing LTC occurs when looking to control the combustion process due to the operating range of the engine being drastically limited when employing such combustion techniques. Also, the use of LTC creates the issue of a trade-off between emission formation and fuel consumption. For this reason, researchers such as Feng

et al. [38] have looked at the effects on diesel combustion whilst employing the LTC combustion technique. They studied the effects of EGR on the combustion and emission formation of the engine using five different diesel blends. During the testing, it was observed that by using EGR, the thermal efficiency was reduced, the ignition delay had been extended, and the levels of HC and CO were increased. Additionally, these three parameter changes were increased as the initial boiling point of the fuel is lowered. Han et al. [39] had also targeted LTC combustion during EGR to reduce harmful emissions and had found that the diesel combustion had shown low NO<sub>x</sub> and soot emissions at 0.8-1.0 MPa IMEP load operations. However, their research was not without its own issues. It was found that this combustion process had created load related problems which limited their usage at higher loads. Also, when they used premature auto-ignition for the fuel, there was a damaging effect on the emissions production. Ultimately, they concluded that by using a ethanol/diesel mixture, it was possible to run higher loads whilst operating during LTC in order to benefit both the combustion control and the emission production.

### **2.7.3 Premixed Charge Compression Ignition**

PCCI is a variant of the LTC strategy which also allows for lower emissions. Alternatively, to HCCI, with PCCI the air-fuel mixture is not completely homogenous. In reality, it is difficult to obtain a fully homogenous diesel-air mixture as a result of the low volatility and the low auto-ignition temperature of diesel. When using PCCI in a diesel engine, there is a spontaneous ignition of the fuel-air mixture, which results in no flame propagation. This subsequently results in a high pressure rise rates, which can have a detrimental effect on the engine's life span.

When using early fuel injection, the premixed charge is usually achieved at this stage. There are however side-effects that may arise as a result of employing this strategy, namely wall-wetting, which is having excess fuel on the cylinder walls before combustion occurs. This

tends to increase the CO and HC emissions. Boot et al. [40] experimented in reducing the level of wall-wetting by using uncooled EGR methods. They raised the intake temperature by roughly 60 °C which was found to aid in the evaporation of the diesel on the cylinder wall. They also found that smoke number was reduced significantly whilst improving the IMEP.

Beatrice et al. [41] displayed research that showed that by altering the compression ratio (CR), they were able to maintain more control over the ignition delay in a PCCI engine. The CR should be balanced, as too high or too low could be detrimental to the combustion process where the former could increase the fuel consumption and cold engine stability issues, and the latter could hinder the benefits of PCCI. The authors found that by employing low CR conditions, the smoke production was reduced with minimal to no effect on the fuel consumption at the expense of HC and CO emissions. The NO<sub>x</sub> emissions were found to be relatively unaltered during the research and was primarily controlled using EGR. The authors concluded that the optimal CR was around 15.5 to offer the best compromise in results.

#### **2.7.4 Reactivity Controlled Compression Ignition**

To achieve RCCI, two specific fuels with differing reactivity levels are delivered into the combustion chamber. The fuel with the lower reactivity is supplied first, some time before the injection of the higher reactivity fuel. Doing this certifies that the low reactivity fuel is sufficiently mixed with the air and spontaneously ignites once the combustion of the high reactivity fuel begins. Adopting this combustion mode, fuel efficiency is increased, heat transfer losses are reduced, and NO<sub>x</sub> and PM emissions are greatly reduced.

Splitter et al. [42] experimented on a single-cylinder heavy-duty engine using RCCI. In this research, port fuelled E85 fuel was port injected as the low reactivity fuel and cetane enhanced direct gasoline injected fuel was the high reactivity fuel. The authors concluded that

by using this combustion mode, thermal efficiency was improved by almost 60% as well as negligible NO<sub>x</sub> and PM emissions.

Hanson et al. [43] used a heavy-duty Caterpillar single-cylinder engine running in RCCI mode. Their research was based on two types of fuelling: dual and single fuelling strategies. With the dual-fuel strategy, they used port gasoline and direct diesel injection and the latter, gasoline was used in both streams where the cetane number of the direct injection stream was increased by adding 2-Ethylhexyl Nitrate. The conclusion of their research found that using either of their fuelling strategies, the NO<sub>x</sub> and PM emissions were reduced without installing any exhaust aftertreatment apparatus whilst increasing thermal efficiency.

Curran et al. [44] attempted to investigate the efficiency and the emissions mapping of an RCCI light-duty diesel engine. the two fuels used were gasoline and ultra-low sulphur diesel. With regards to the operating conditions, the diesel fuel was delivered using single or split injection and the results obtained were comparable to that of conventional diesel operation. The authors concluded that the RCCI engine showed efficiency levels similar to that of standard diesel operation at when tested at lower speeds and loads. However, a 5% increase in the thermal efficiency was achieved when operating at higher speeds and loads. Additionally, RCCI operation led to lower NO<sub>x</sub> emissions but higher CO and HC emissions, when compared to standard diesel combustion.

## **2.8 Alternative Fuels and Dual Fuelling**

As mentioned in previous sections, current trends, resources, and government legislations are becoming more and more stringent on fossil-fuel powered vehicles. For this reason, the study and understanding of alternative fuels and fuelling strategies becomes vital in improving the efficiency and dependability of fossil fuels. Despite the recent promise shown towards the wide-spread use of alternative fuels, there are still some hindrances which prevent the heavy

use of alternate fuels on a more commercial level. These hindrances could include the storage, the transportation, refuelling infrastructure, safety, and combustion and engine related issues. There is already a great deal of research that has taken place that shows in some cases that dual-fuelling is a viable option where diesel-hydrogen or diesel-syngas is able to provide a transition from fossil fuels to alternate fuelling strategies.

### **2.8.1 Hydrogen**

Due to the vast availability of hydrogen and hydrogen-based compounds occurring naturally, the increase in trends of using this gas as a fuel appears almost inevitable. In terms of research, there have been a large number of researchers that have looked to discover the use of hydrogen as a fuel where a collection of the findings has been detailed in the coming section.

The introduction of hydrogen into the combustion chamber can be achieved either via port or direct injection in a diesel engine. with port injection, hydrogen is usually injected into the intake manifold at a pressure slightly higher than atmospheric. For direct injection, the hydrogen is directly injected into the cylinder during the compression stroke [45]. With both scenarios the combustion process is initiated using a small amount of diesel fuel due to the autoignition temperature of hydrogen being 585 °C which is much higher than that of diesel.

Saravanan et al. [46] examined the effects of diesel-hydrogen combustion on a single-cylinder direct injection (DI) diesel engine, which was modified to allow for the hydrogen to be injected into intake port during the suction stroke. The diesel injection was fixed at 23 crank angle degrees (CAD) before top dead centre (BTDC). The hydrogen was injection duration varied from 5 CAD BTDC to 5 CAD after top dead centre (ATDC) and from 30 to 90 CAD respectively. The researcher had found that there was a 5.8% increase in thermal

efficiency as a result of the improved combustion. They also reported a reduction in NO<sub>x</sub> and smoke emissions which was due to the leaner equivalence ratios.

Shirk et al. [47] had found that the diesel-hydrogen combustion had not affected drivability of the vehicle. They did however display that diesel-hydrogen combustion resulted in slightly lower thermal efficiency and NO<sub>x</sub> emissions. Other studies [48-51] have found however that part substitution of diesel with hydrogen has led a damaging effect on the NO<sub>x</sub> emissions. This is primarily due to the higher adiabatic flame temperatures achieved when combustion occurs with hydrogen. The use of EGR has been found to reduce this effect by lowering the temperature of combustion.

As mentioned in previous sections, the primary cause for increased NO<sub>x</sub> formation is higher combustion temperatures. The introduction of hydrogen into the combustion chamber is known to increase combustion temperatures thus drastically increasing the NO<sub>x</sub> emissions. Researchers have presented a reduction in NO<sub>x</sub> emissions when the main fuel has been partially replaced with hydrogen [46, 52]. Ultimately there are many factors that can affect the combustion temperatures, which could lead to changes in on the high temperature zones, under certain conditions. Some of these factors include the equivalence ratio, the operating conditions, and the high heat capacity of hydrogen can all attribute to the combustion temperature changes. With regards to carbon based emissions produced as a result of hydrogen-enriched combustion, many researchers conclude that increase hydrogen results in lower carbon-based emissions [46, 48, 53]. The primary cause of this is that during diesel-hydrogen combustion, the quantity of carbon is greatly reduced when compared to diesel combustion.

Wichterlova et al. [54] demonstrated that hydrogen enriched combustion is able to improve the functionality of aftertreatment apparatus. They achieved this by showing that hydrogen addition over a SCR catalyst drastically improved NO<sub>x</sub> conversion. Similarly, Bromberg et

al. [55] demonstrated that the introduction of hydrogen into the exhaust stream is able to assist in the regeneration process of the DPF. This is useful when in some cases the exhaust temperature is not high enough to undergo the regeneration process itself, so the oxidation of hydrogen can raise the temperature to the desired level for proper regeneration.

### 2.8.2 Syngas

Syngas is also known as synthesis gas due to the mixture being made synthetically on-board in diesel engines. The mixture usually comprises of hydrogen and CO mixed in different quantities. For on-board diesel production, syngas can be formed by injecting diesel into a catalytic fuel reformer, found inside the exhaust pipe. The product formed is usually a mixture of syngas and EGR where it is then delivered back to the engine via the intake manifold [56].

The specific composition of the producer gas has been reported to affect the performance of the engine and the emissions formation where the composition itself is dependent on reactions that occur during the reforming process as well as the input gases used. It was found that the gaseous fuel with 100% hydrogen content displayed an improvement of engine performance at the expense of NO<sub>x</sub> emissions when comparing to the syngas that contained CO. Additionally, the CO and HC emissions increased as the amount of CO in the mixture was increased [57].

Bika et al. [58] presented that when partially substituting diesel fuel with syngas in any H<sub>2</sub>/CO proportion, a reduction in engine efficiency was observed. They found that the main reason behind this reduction in efficiency is the unburned syngas that was escaping through the exhaust pipe. Moreover, due to the increased amount of HO<sub>2</sub> radicals formed as part of the combustion, the NO<sub>2</sub>/NO levels were almost twice the amount when using syngas as opposed to standard diesel combustion.

Dong et al [59] examined the effects of different H<sub>2</sub>/CO ratios on the flame speed, where they concluded that the laminar flame speed had increased as the concentration of the hydrogen increased. They also reported that the laminar flame speed of the hydrogen-air mixture and the CO/air mixture reached its maximum value when using equivalence ratios of 1.7 and 1.6 respectively.

Ultimately the benefits of syngas in a CI engine, which has been produced on-board via fuel reforming, are that the exhaust emissions can be reduced, the thermal efficiency can be improved, the combustion stability can be improved and the exhaust aftertreatment can be made easier [60].

### **2.8.3 Liquefied Petroleum Gas**

Liquefied Petroleum Gas (LPG) is a fossil fuel derived mixture of propane and butane and is rated in the top three most used fuels worldwide [61]. It displays a higher specific energy than most diesel or gasoline; however, both diesel and gasoline display better energy density by volume figures than LPG. Due to the density of LPG being greater than that of air, it carries higher risks in terms of suffocation and explosion in the event of leakages. The higher octane numbers and autoignition temperatures of LPG make it a suitable fuel for use in Otto cycle engines [62]. Similarly, to hydrogen-diesel combustion, when used in CI engines, LPG requires a small amount of diesel pilot fuel to meet the ignition temperatures for diesel combustion. In the coming paragraphs, the findings of some of the studies that have combined LPG and diesel will be presented.

There have been some performance improvements and emissions reductions along with fuel cost savings when using LPG-diesel combustion [63]. In this study the gaseous fuel was injected into the intake manifold where it was reported that the combination of the fuels had negligible effects on NO<sub>x</sub> and CO<sub>2</sub> emissions and reduced PM emissions.

Lata et al [64] studied the effects on the combustion parameters when injecting hydrogen or LPG in a dual-fuel diesel engine. They reported that the peak cylinder pressure during LPG-diesel combustion, with a supply of 50% LPG, was higher than that of the base operation. They also reported that the heat release rate was lower at the same LPG concentrations, when compared to standard diesel operation.

Other studies have reported that when adding propane of up to a 40% gaseous fuel mass fraction, into the intake manifold of a diesel engine, the fuel conversion efficiency improved [65]. The author had also compared the fuel conversion efficiency levels when fuelling with stand-alone propane and a propane-butane mixture. Here, when butane was added, it was found that the fuel conversion efficiency dropped but did lead to a reduction in NOx emissions.

#### **2.8.4 Compressed Natural Gas**

By breaking down organic matter in anaerobic environments compressed natural gas (CNG) can be produced. It can also be found naturally on top of oil deposits. When using the organic matter to form CNG, it can be considered a renewable energy source. The lower density in comparison to air makes it safer than, for example LPG, in the case of a leakage. When used in CI engines, combustion is achieved through the injection of diesel or having a diesel-like fuel.

Hegab et al. [66] experimented on a natural gas fuelled diesel engine and reported that NOx emissions were reduced significantly. The CO and HC emissions however, were increased considerably when compared to stand-alone diesel operation. Therefore, the authors concluded that by using CNG in either a SI or CI engine, the effect on the NOx, CO, and HC emissions are the same.

Namasivayam et al. [67] experimented with three different pilot fuels: dimethyl ether (DME) and two water-based biodiesel emulsions with 5% and 10% water by volume. They looked at the effects on the performance and the emissions of a CI engine when fuelled with the CNG. They presented that both pilot emulsion fuels displayed higher CO and HC emissions than the DME pilot. DME produced lower NO<sub>x</sub> emissions when running under low and medium loads, and higher NO<sub>x</sub> when running at higher loads. DME also had a detrimental effect on the thermal efficiency.

### **2.8.5 Biodiesel**

Biodiesel is, as the name suggests, a fuel based on organic substances such as vegetable oils and animal fats. The production of biodiesel occurs when a chemical reaction called transesterification occurs. This produces methyl esters (biodiesel), and glycerine as a by-product [68]. Biodiesel shares some of its properties with petrodiesel and can be used in most standard CI engines with minimal modifications needed to implement. Usually, biodiesel is mixed with petrodiesel where the properties of the fuel mixture can differ significantly depending on the original biodiesel and the concentration of biodiesel used. To classify the blends of biodiesel, the B factor is used where a B100 fuel would contain 100% biodiesel and a subsequently a B50 would be 50% bio and petrodiesel.

Ultimately one of the main benefits of biodiesel is that it loosens the strain on the dependency fossil fuels as it is produced from renewable sources. It is also known to reduce the net CO<sub>2</sub> emissions as it uses a closed loop carbon cycle, where the CO<sub>2</sub> produced in the combustion process is re-used via plant absorption where the plants themselves are used as biodiesel [69].

Lapuerta et al [70] studied the effect of biodiesel in diesel engines where they reported that there were discrepancies in relevant literature which could be due to reasons that include the types of biodiesel, different engine technologies, operating conditions and driving cycles.

Regardless of the discrepancies found, they reported that the introduction of biodiesel in the engine does not drastically affect the thermal efficiency as the increased BSFC is in keeping to the reduction of the heating value. It was found that biodiesel does allow for an increase in NO<sub>x</sub> emissions, albeit minor ones. PM was also found to be reduced in majority of studies which used biodiesel fuelled engines. Other researchers have also presented a reduction in CO and THC emissions when using biodiesel, when compared to standard diesel operation.

Atadashi et al [71] presented a study which looked at the general characteristics of biodiesel such as the lubricity, the biodegradability and the physiochemical properties. The use of biodiesel is not limited to land use as it has non-toxic capabilities allowing it to be used in marine applications where it can degrade in soil and water. Also due to its improved lubricity in comparison to petrodiesel, the wear on the fuel injectors and pump is reduced when using high quality biodiesel.

## **2.9 Exhaust Gas Assisted Fuel Reforming**

Due to the complexity of storing hydrogen, hydrogen fuelling infrastructure and distribution researchers are attempting to produce and store hydrogen on-board. This procedure is still considered to be in its infancy as there is still a great deal of logistics involved in realising this procedure. The procedure involves the fuel to be injected into a catalytic reformer, integrated into the EGR loop. At this point, the hydrogen-rich fuel is then delivered back into the cylinders, where the benefits include lower emissions and increased combustion efficiency. Along with the hydrogen produced as part of the reforming process, CO is also able to be produced where unlike fuel cells; combustion of CO in a diesel engine does not contaminate the components of the engine.

When producing hydrogen-rich and syngas-rich gas streams, there are various reactions. These reactions include water-gas shift reaction, steam reforming, auto-thermal reforming,

partial oxidation, endothermic dry reforming reaction, and thermal decomposition of the fuel. There are cases when a combination of these techniques is employed.

Tsolakis et al [72] used a reforming miniature reactor in the exhaust of a single-cylinder diesel engine to produce a hydrogen-rich gas. The study found that the products of the reformer contained almost 16% hydrogen. They also presented that complete oxidation was the main reaction in the reformer. Additionally, when simulating REGR with 14% hydrogen, the trade-off between NO<sub>x</sub> and smoke emissions has been improved.

In other research, Tsolakis et al [73] experimented with the effects of simulated reformer product gas in a diesel engine. The research concluded that a low level of REGR can allow for reductions in both NO<sub>x</sub> and smoke emissions. Also, when increasing the REGR levels, the smoke emissions can be reduced further. This does however come at the expense of NO<sub>x</sub> emissions. Adjusting fuel injection timing can also reduce NO<sub>x</sub> emissions without a negative effect on smoke emissions.

Other studies studied how simulated REGR can affect the engine performance and SCR system [74]. The study concluded that REGR can aid both the SCR system and the engine performance. The NO<sub>x</sub> emissions were reduced due to the unburned hydrogen present in the exhaust gas.

As mentioned in earlier sections, the use of syngas is limited and can produce poor performances when used in low-load conditions. The primary reason is the inefficient flame propagation in the gaseous fuel when the concentration is less than the lower flammability limit (LFL). Moreover, under low-load conditions, due to the small amount of diesel injected into the cylinder, the resulting flame cannot burn the gaseous fuel completely. This has a disadvantageous effect on the thermal efficiency.

## **2.10 Dilution of Intake Air**

Reducing the NO<sub>x</sub> emissions produced during combustion can be achieved using various techniques, most of which have been explored in previous sections. Dilution of the intake air is another technique which can be employed. Commonly, EGR is the favoured method of recirculating the exhaust gas back into the intake pipe, where the details of its operation were explained in section 2.5. EGR can be introduced relatively simply to most conventional diesel engine and is used commonly to meet legislative standards. Despite the documented successes of EGR, there are some negativities surrounding it, which may allow for other dilution methods to be used.

There have been some researchers that have proposed to use nitrogen as an enrichment with intake air [75, 76, 77]. In both scenarios where nitrogen or EGR is used, the main reason for the NO<sub>x</sub> emission reduction is the reduction in the oxygen concentration in the intake air, which results in a reduction in peak combustion temperature. The study of nitrogen enrichment could aid in the development of the on-board reforming technologies due to the producer gas allowing for an increase in the nitrogen/oxygen ratio in the intake air. It has been reported that the implementation of dilution techniques can negatively affect the CO, THC and the smoke emissions [78], however substituting part of the diesel fuel with hydrogen can lower the emissions levels.

## **2.11 Motivation**

Based on the information presented in this chapter, the gaps in knowledge that can be determined from the literature explored is that there is a clear opportunity to look at the possibility of combining the use of simulation and experimentation to analyse the effects of a dual-fuel diesel-hydrogen CI engine. For this reason a decision was made on investigating the effect of dual-fuelling with diesel-hydrogen combustion whilst using simulations to compare

the results. Both tests were carried out on a high speed direct injection (HSDI). Specifically, a prototype diesel engine that was modified to inject hydrogen via the intake port. Due to the importance of improving the efficiency of the diesel engine and the impact it has on the environment it is necessary to analyse and investigate the effects on the emissions, along with the engine performance and how it can maintain its stature in the automotive market.

# Chapter 3

## Methodology

## Chapter 3

### Methodology

#### 3.1 Introduction

In this section, the research engine, the analysers, the data collection, the calibration and measurement equipment, and the data processing methods are intricately described. This section also includes detailed descriptions and justifications for the operation parameters and conditions selected to conduct the experiments. A safety analysis has also been included to ensure safe practice for future researchers.

#### 3.2 Research Engine

The experiments were carried out on a pre-production prototype Ford diesel engine. The engine block was based on the 2.0L Ford Duratorq engine; however, the cylinder head was identical to a production Ford Zetec engine. The cylinder head was equipped with two camshafts and four valves per cylinder. Table 1 shows the full specifications for the engine. The engine had two key modifications made to it that made it slightly different from production specification.

The first modification was the piston bowl design. The pistons fitted on the test engine had larger bowl volumes which led to a reduction in the compression ratio. The compression ratio of the test engine was at 18.2:1 in comparison to 19:1 compression ratio found in the

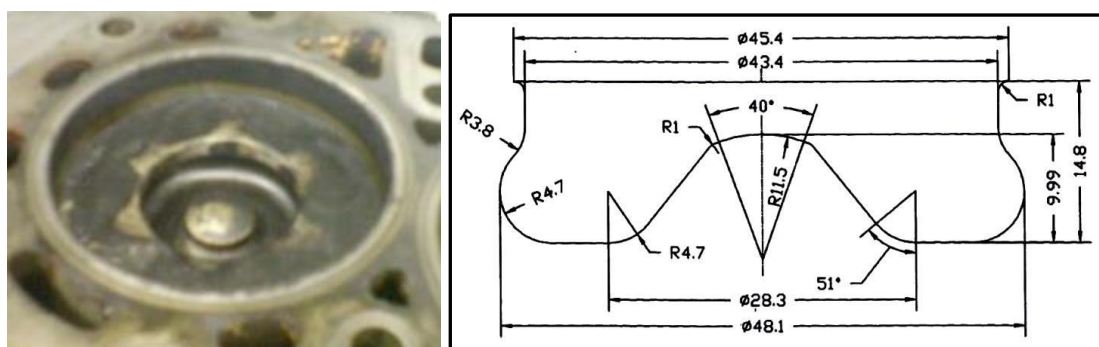


Figure 13: Piston Bowl Design [50]

production engines. An illustration and photograph [50] of the piston bowl design can be found in figure 8.

The second modification was the air intake manifold. With the production versions of the engine, the intake manifold was designed to encourage swirl, where in some models, they had a variable swirl port fitted. The test engine did not have this feature and instead had straight cylinder feeds.

Figure 9 represents a schematic of the engine test cell set up and where various readers and equipment are placed.

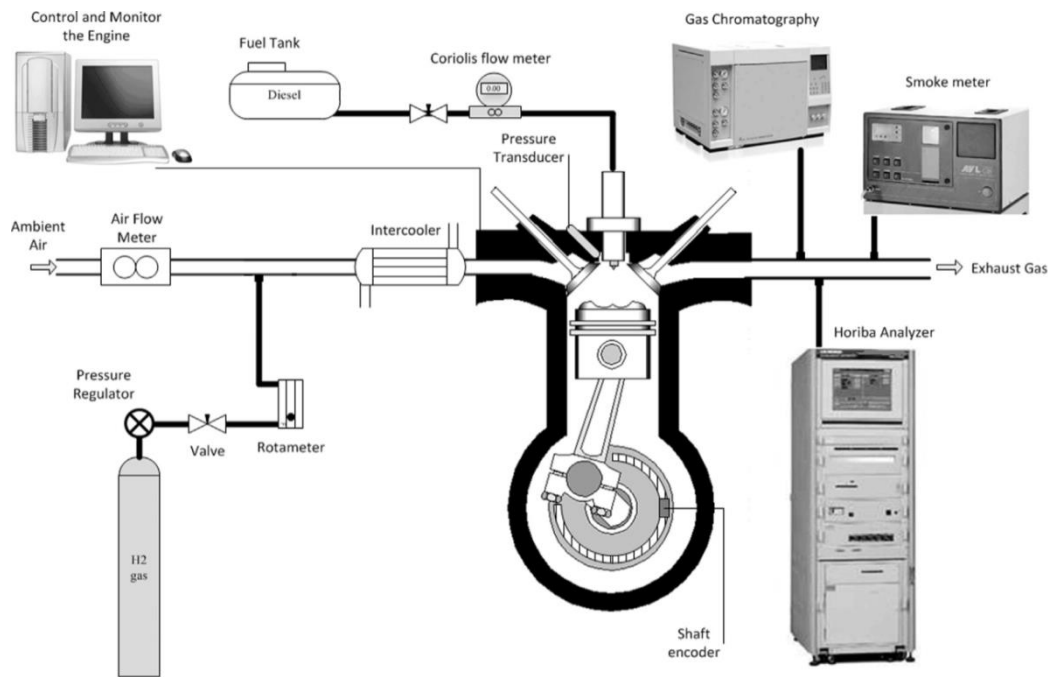


Figure 14: Schematic of Experimental Setup [50]

The engine was also installed with a Garrett turbocharger with a Variable Geometry Turbine. The VGT has been designed to allow for a balance between the need for a small turbine housing for lower engine speeds and the turbo – lag experienced from a turbocharger designed to run at higher speeds.

Engine model and type	Ford Puma, 2.0l, 4 cylinder, 16 valve, HSDI, turbocharged (but runs in NA mode), EGR, water cooled, fuelled by ULSD
Bore/Stroke [mm]	86/86
Compression Ratio [-]	18.2:1
Swept Volume [cc]	1998.23
Con-Rod Length [mm]	155

**Table 1: Engine Specifications**



**Figure 15: Ford Puma 2.0L HSDI Engine**

The fuel injection system was a common rail Delphi system where each injector had six holes of nominal 0.154 mm diameter and a 154-degree spray hole angle, with an injection pressure of 800 bar, although the engine was capable of achieving up to 1600 bar at higher speeds. The test engine cooling was achieved using two separate cooling circuits. The first circuit picked up the heat from the lubricating oil and the second circuit removed the heat from the engine block and head, by sending water through the passages of the block and head. The coolant inlet and outlet temperature were set to  $77 \pm 3$  °C, which was controlled by sending a signal to a thermostat that controlled the coolant flow. To ensure that the temperature of the engine did not exceed critical levels, a safety cut off feature was implemented to switch off the engine if the coolant temperature reached 100 °C.

### 3.3 Dynamometer

To control the engine load and speed, the engine was connected to a W130 Schenck eddy current dynamometer. Figure 10 [50] shows an illustration of the dynamometer.

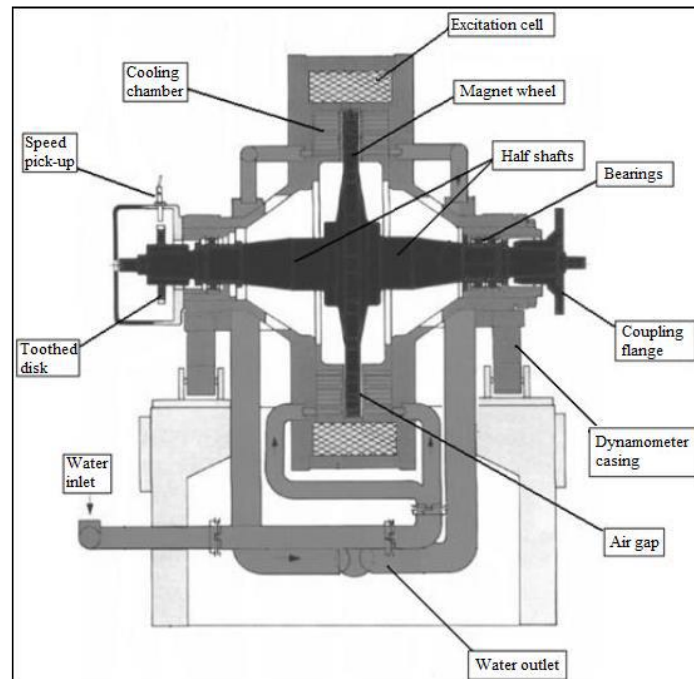


Figure 16: Cutaway of eddy current dynamometer [50]

The dynamometer is operated by having an electrical current passing through the excitation coil, which in turn generates a magnetic field. As the engine is in operation, its output shaft spins the dynamometer's rotor, which causes a consistent change in flux density on all stator points.

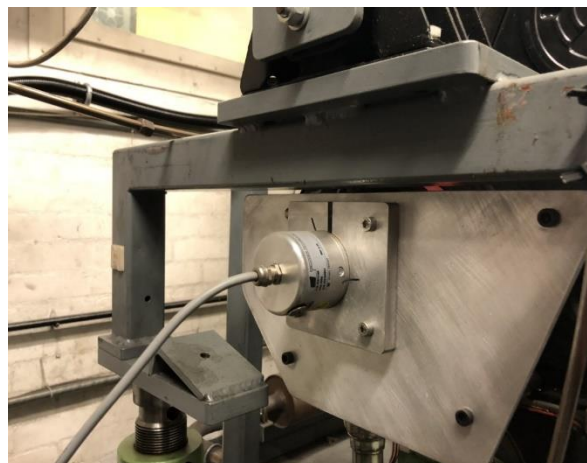


Figure 17: Encoder Technology ET758 heavy-duty Shaft Encoder

The result of this is that the eddy currents created cause a braking action on the rotor [112]. In order to calculate the shaft and torque power, the current force and the length of the arm is required. A feature of the dynamometer is that it allows the user to fix either the speed or the torque of the engine. When the speed is kept constant, the torque can be adjusted by controlling the fuel supply to the engine and vice versa. The heat generated whilst under operation is withdrawn by the water cooling system. The dynamometer also features a safety emergency shutdown system.

### 3.4 Air Intake System

Initially, the engine was running with a variable geometry turbocharge, however in the case of this study, the turbocharger was disconnected resulting in naturally aspirated operating mode. Additionally, the EGR valve fitted to the engine was kept hermetically shut during the experiments. Table 2 shows the measuring equipment used alongside the engine intake.

Measuring Equipment	Manufacturer	Type	Range	Error
<b>Glass tube rotameter (H<sub>2</sub> measurement)</b>	RM&C	NG	10-180 l/min	±2.0% (On the actual flow rate)
<b>Intake air flow meter</b>	Romet	RM	260-5191 l/min	+0.25%
<b>Pressure regulator</b>	BOC	HP	0-17 bar	-
<b>Thermocouple</b>	NG	K	0-1100 °C	≤ ± 0.3%

Table 2: Measuring Equipment used along Engine Intake

Initially, the intake air was passed through a positive displacement flow meter and subsequently through a paper filter. The flow meter was used to measure the volumetric flow rate of the air, which was actually found by the rate of rotor revolution, while the paper filter filtered larger airborne particles. The hydrogen was admitted into the intake pipe via the probes that were fitted perpendicular to the main air flow, which was placed downstream of

the paper filter. The introduction of the hydrogen into the engine resulted in the equivalent volume of air intake air replaced by the gas mixture. The line used to transport the hydrogen to the intake manifold was fitted with a backfire arrestor and a relief valve due to the flammable properties of hydrogen. The line was placed in between the pressure regulator and the glass tube rotameter. Additionally, there was a control valve present as well as hydrogen and CO leak detectors in both the engine and control cell. The control valve would close automatically after 5 minutes of inactivity to avoid prolong use and pressure build up.

The hydrogen was purchased from the British Oxygen Company (BOC) and was stored in 15l bottles. The bottles had pressure regulators allowing control of the line pressure and to monitor the remaining gas. The flow rate of the gas was measured using the glass tube rotameters. The temperature of the gas downstream of the rotameter was measured and a correction for the temperature was applied to reduce the gas flow uncertainties. Additionally, the inlet manifold was modified to allow a uniform distribution of the gas-air mixture in the cylinders. The pressure for the gas lines was fixed at 3 bar due to it being the pressure needed to reach the maximum flow rate of the gasses. Lastly, the mixing quality of the hydrogen in the intake air was certified using the gas chromatograph.

As mentioned previously, the equivalent volume of air was replaced with a percentage of bottled hydrogen when injected into the engine, which resulted in a reduction in the oxygen concentration in the intake. Table 3 shows the composition of the intake charge after the hydrogen had been injected.

Hydrogen (% vol. of intake air)	Intake charge concentration (% vol.)		
	O <sub>2</sub>	N <sub>2</sub>	H <sub>2</sub>
-			
0	21	79	0
2	20.58	77.42	2
4	20.16	75.84	4
6	19.74	74.26	6
8	19.32	72.68	8

Table 3: Intake charge as a function of hydrogen

### 3.5 Diesel Fuel supply and Management

The diesel fuel was stored externally in a central reservoir where the fuel was sent to the engine test cell via an electric fuel pump. The pump was able to increase the pressure up to 1600 bar, which meant fuel delivery was very quick. There were two ways with which the fuel flow rate could be measured. The first was by using a glass burette and the second was by using a Coriolis flow meter. Both methods were installed upstream of the high-pressure pump. The engine had a common rail system installed which would allow for multiple injections per cycle. Below, table 4 displays the specifications of the fuel measurement apparatus.

Measuring Equipment	Manufacturer	Type
Glass Burette	Plint & Partners Ltd	50-100-200
Coriolis Flow Meter	E + H	Promass 83

Table 4: Measuring equipment for fuel

When using the glass burette to measure the flow rate of the fuel, a stopwatch was used to count the time taken for the engine to consume a specific volume of fuel. The mass flow of

diesel was calculated by multiplying the volume flow by the fuel density. In comparison to using the Coriolis flow meter, this produced slightly higher errors due to there being a large amount of human input to calculate the values.



**Figure 18: E+H Promass 83 Coriolis Flow Meter**

The accuracy of the Coriolis flow meter is enhanced due to its ability to measure not only the fuel flow rate, but also the density, the temperature and the viscosity of the fluid. Coriolis forces occur when liquid or gas flows through an oscillating tube. The tube is usually symmetrical and can be either straight or curved. The oscillations in the tube are generated by a driver giving uniform oscillations. Once a fluid moves into the tube, extra twisting occurs on the oscillation. There are sensors which are placed at the inlet and outlet ends of the tube which pick up the distortion of the tube, where the information gathered is processed giving the mass flow rate.

### **3.6 Exhaust Gas Analysis**

The analysis for the exhaust gas was carried out using a range of equipment. A Horiba Mexa 7170DEGR was used for analysing the CO and CO<sub>2</sub> emissions using Non-Dispersive Infrared

(NDIR). The amount of NO emissions found in the exhaust was found using the chemiluminescence of their reaction with the ozone, whilst the THC emissions were determined using a flame ionisation detector (FID) An MKS multigas 2030 FTIR gas analyser was used to measure the nitrogen-based emissions. The regulated and unregulated emissions can also be measured using the FTIR analyser. For this research it was primarily used to measure the nitrogen-based emissions. A AVL 415S smoke meter was used to measure the smoke number, which will be explained in further detail in the coming paragraphs. A Chrompack gas chromatograph (GC) CP 9001 coupled with a thermal conductivity detector (TCD) was also used. Table 5, below displays the range of equipment used to measure the exhaust gas emissions.

Measuring Equipment	Manufacturer	Type
<b>Exhaust gas analyser</b>	Horiba	Mexa 7170
<b>Exhaust gas analyser</b>	MKS	2030
<b>Smoke meter</b>	AVL	415S
<b>Gas chromatography</b>	Chrompack	CP 9001

**Table 5: Measurement Equipment for Exhaust Gas Emissions**

For the Horiba, the smoke meter, and the FTIR, samples were supplied directly from the exhaust gas pipe via the sample lines, whereas the GC needed a small exhaust gas sample that was collected from the exhaust pipe using a gastight syringe.



**Figure 19: Hamilton Gastight Syringe**

### 3.6.1 Non-dispersive Infrared

NDIR is a type of infrared spectroscopy, where it measures the specific gas molecules contained in a sample. This is done by the gas molecules absorbing the infrared light at a specific wavelength. The quantity of each gas is determined by how much light has been absorbed and how much light is remaining at a specific wavelength. To measure carbon-

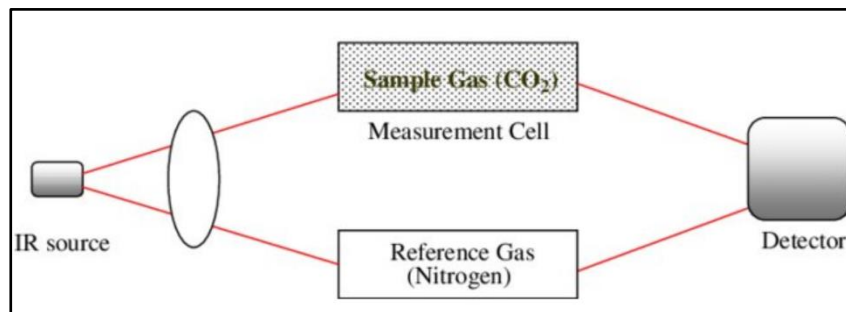


Figure 20: Schematic representation of NDIR working Principle [79]

based gasses, a sample cell and a reference cell are used. The reference cell is filled with an inert gas such as nitrogen and an infrared beam is directed through the sampling and reference cells along with the band pass filter until it ultimately reaches the detector. Figure 11 displays how the NDIR works in theory.

### 3.6.2 Chemiluminescence

The chemiluminescence method is used primarily to detect the nitrogen-based compounds in the exhaust gas and undergoes a reaction between NO and ozone (O<sub>3</sub>). Below is an equation representing this reaction:



The NO originates from the exhaust gasses and the ozone is generated by the device itself. When the excited NO<sub>2</sub> molecules revert to their ground state, they emit red light. This is measured by a photo multiplier once it passes through a filter to eradicate interference from other unwanted gasses. Using this technique, the quantity of NO<sub>x</sub> and NO<sub>2</sub> emissions can be

established. This is done where the  $\text{NO}_2$  is converted to  $\text{NO}$ , where the converted molecules react with the ozone, along with the original  $\text{NO}$  molecules. This provides a signal which will display the amount of  $\text{NO}_x$  emissions generated, which is the summation of the  $\text{NO}$  and  $\text{NO}_2$  emissions. The final concentration of  $\text{NO}_2$  is calculated by subtracting the original  $\text{NO}$  from the  $\text{NO}_x$ .

An  $\text{O}_3$  detector was placed close to the source of  $\text{O}_3$  in case of leakage. This is due to the harmfulness of long term  $\text{O}_3$  exposure on the lungs and respiratory system.

### 3.6.3 Flame Ionisation Detector

The THC emissions were measured using a FID. Figure 12 shows a representation of the device:

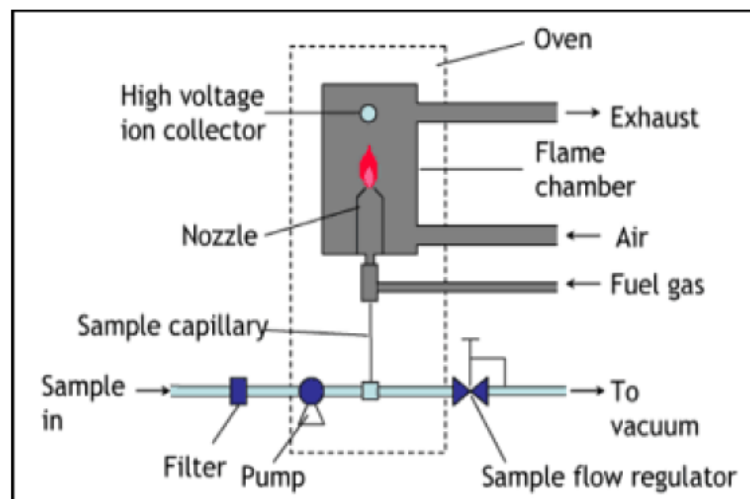


Figure 21: Schematic representation of flame ionisation [80]

The principles of operation are based on the detection of ions during the combustion of HC in a hydrogen flame. Instead of pure hydrogen, a balance gas mixture of 40% hydrogen-helium was used. A current that is proportional to the number of carbon atoms burned in the flame is generated between the burner and the electrode. The signal is then subsequently processed to provide the quantity of THC emissions. The final value depicts the number of carbon atoms in the sample gas, as opposed to the amount of HC.

### 3.6.4 Gas Chromatography

The GC was fitted with a TCD which was used for the measurement of the unburned hydrogen in the exhaust gas. The thermal conductivity of the carrier gas is compared with the sample gas using the TCD. In this research, the sample gas was the exhaust gas and it was collected using a Hamilton gastight syringe. The carrier gas in this case was bottled argon. Similar to the NDIR, the GC consists of a reference cell and a sample cell. The argon was passed through both the reference cell and the sample cell, where the gas that passed through the reference cell had a higher thermal conductivity. This results in a difference in the resistance of the electrically heated wires found inside the cells. A voltage signal proportional to the amount of gas present is produced, which depends on the difference of the resistance.

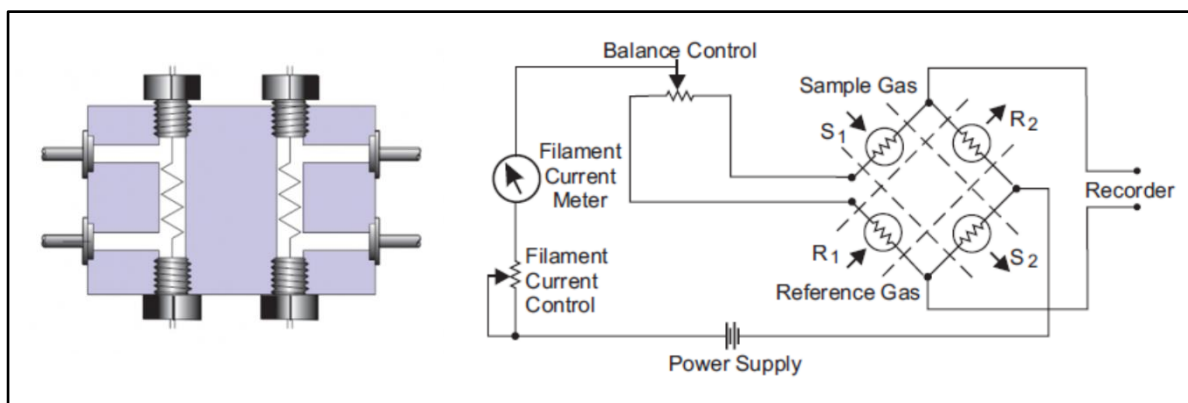


Figure 22: Schematic showing working cut-away and working principle of TCD [81]

Figure 12 displays the working principle of the TCD along with a cross sectional view of the device itself. Other than measuring the hydrogen content in the exhaust gasses, the GC is also capable of determining whether the hydrogen being injected into the intake pipe has been sufficiently mixed. For this reason, a rubber-sealed access point was placed at the point where the intake charge enters the intake manifold and one was placed in the middle of the manifold. This allowed the collection of the hydrogen-enriched intake air, which was subsequently supplied to the GC.

### 3.6.5 Bosch Smoke Number

The smoke concentration of the exhaust gasses can be found by using the filter paper method. A probe is mounted in the exhaust line which draws the exhaust gas through a clean filter paper. Depending on how black the filter paper becomes after the exhaust gas passes through it, determines the BSN. A reflectometer was used to quantify the blackness of the paper with zero being a white paper and 10 being completely black paper [82].

### 3.7 In-cylinder Pressure Data

The pressure data was measured from the first cylinder using a Kistler 6125A piezoelectric pressure transducer retro-fitted into the glow plug hole. Figure 14 presents the cross-section of the cylinder head with the pressure transducer installed and the sensor that was used to dynamically determine the TDC.

The changes in the cylinder pressure were converted to an electrical charge where the sensitivity of the transducer was set to 16 pC/bar. This was amplified using a Kistler 5001 charge amplifier and the data was recorded using LabVIEW together with the shaft encoder signal. A heavy-duty model ET758 shaft encoder was used, setting the resolution to 1440 pressure data per crank shaft revolution. This equates to 4 samples per CAD. Table 6 shows the measuring equipment used to record the in-cylinder data.

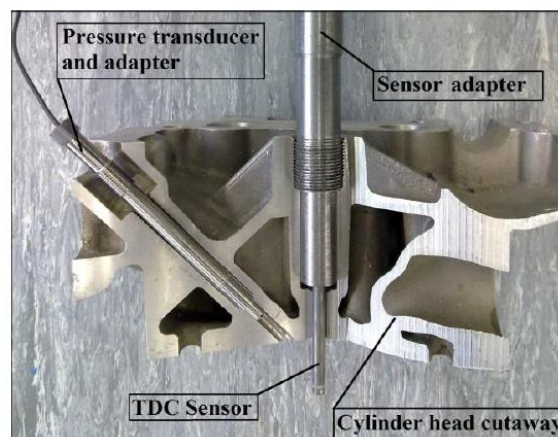


Figure 23: Cylinder head cross-section [50]



Figure 24: Kistler Pressure Transducer and Glow Plug Adapter

Measuring Equipment	Manufacturer	Type	Range	Sensitivity
Pressure transducer	Kistler	6125A	0-250 bar	-16.8 pC/bar
Shaft encoder	Encoder Technology	ET758	0-8000 rpm	0.017°

Table 6: Measuring equipment used to measure in-cylinder data

A Kistler 2629C1 TDC sensor was used to dynamically determine the TDC position. During the calibration process, the injector of the primary cylinder was removed, and this sensor was installed in its place. The engine was subsequently run for a few minutes on the motored mode by de-activating the diesel injectors. The output signal of the sensor, coupled with the shaft encoder signal, was recorded with LabVIEW where depending on the position of the maximum in-cylinder pressure, a correction factor was applied. The TDC sensor (figure 25) works by generating a signal when the top of the piston approaches the sensor tip. The magnitude of the signal is inversely proportional to the distance between the piston and the sensor. The maximum value relates to the TDC position. The biggest advantage of using this sensor is the lack of correction for the degree of the thermodynamic loss angle.



Figure 25: Kistler 2629C1 TDC Sensor w/Adapter

### 3.8 Fuel Properties

The engine was fuelled using ultra-low sulphur diesel (ULSD), through the entirety of the experiment. When admitting the hydrogen, the engine ran in a dual-fuel combustion mode where the flow rate of the ULSD was brought down to stabilise the speed and load. When running the engine in dual-fuel combustion mode, diesel was used to initiate the combustion due to the higher auto-ignition temperature of hydrogen. Table 7 displays the properties of the bottled hydrogen used for the engine. These properties were also used when using hydrogen in the simulation tests.

<b>Property</b>	<b>Value</b>
<b>Adiabatic flame temperature (<math>\phi=1</math>) (K)</b>	2480
<b>Autoignition temperature in air (K)</b>	858
<b>Density (kg/m<sup>3</sup>)</b>	0.0824
<b>Flame velocity (<math>\phi=1</math>) (ms<sup>-1</sup>)</b>	1.85
<b>Flammability limits (%vol. in air)</b>	4-75
<b>Lower heating value (MJ/kg)</b>	119.7
<b>Minimum ignition energy (<math>\phi=1</math>) (mJ)</b>	0.02

**Table 7: Properties of Hydrogen**

The wide flammability limit of hydrogen can be advantageous for the combustion of dual-fuel operation. This is due to the ability that it allows the engine to operate with more stability under lean-burn conditions. Lean-burn operation characteristically produces lower NO<sub>x</sub> emissions as a result of the lower combustion temperatures. Another advantage of hydrogen dual-fuelling is the accelerated reaction rate as opposed to the slower rates when using standard diesel combustion [83].

As stated in previous sections, the formation of NO<sub>x</sub> emissions is very flame temperature dependant, where a higher flame temperature during combustion will increase chances of NO<sub>x</sub> emissions. Combustion with hydrogen is known to produce higher flame temperatures. Another issue that occurs is that when injecting the hydrogen gas via the intake pipe, the volumetric efficiency is reduced, which leads to a loss in power density.

With standard CI combustion, the maximum temperature at the end of the compression stroke does not reach the autoignition temperature of hydrogen. For this reason, there is a small amount of diesel injected into the cylinder to aid the combustion process. Subsequently, the combustion of diesel-hydrogen dual-fuel operation is reliant on the diesel injection timing.

Despite the possible benefit of increasing the thermal efficiency of the engine when using hydrogen, the increased explosive burn could exert greater forces on the engine and its components as a result of the increased pressure.

Hydrogen requires 0.02 mJ of energy to ignite, which is roughly ten times less than that of gasoline for example. Despite the benefit of quicker ignition timing, the lower energy could result in premature ignition where hot spots and hot deposits serve as potential ignition surfaces [84]. The heating value of hydrogen per unit mass is roughly three times greater than diesel. Despite this, diesel still has a better volumetric efficiency. This may become a disadvantage if the hydrogen is not produced on-board due to the importance of volume occupation in particular vehicle applications [85].

Table 8 presents the properties of the diesel use for this research. The diesel was supplied by Shell.

<b>Property</b>	<b>Value</b>
<b>Ash content [%]</b>	<0.005
<b>Autoignition temp. in air [K]</b>	483
<b>Calorific value [kJ/kg]</b>	44800
<b>Carbon [%]</b>	86.2
<b>Carbon residue [%]</b>	0.2
<b>Cetane number</b>	52.1
<b>Cloud point [K]</b>	263
<b>Density at 288 Kelvin [kg/m<sup>3</sup>]</b>	583.8
<b>Flash point [K]</b>	341
<b>Hydrogen [%]</b>	13.4
<b>Oxidation stability [g/m<sup>3</sup>]</b>	14

Oxygen [%]	0
Sulphur content [mg/kg]	10
Total aromatics [%]	10.5
Viscosity at 313 Kelvin [cSt]	2.5
Water content [mg/kg]	61

Table 8: Diesel Fuel properties

### 3.9 Data Analysis

The majority of the data recorded via the test engine was processed externally using various calculations and equations. The data recorded from the simulation software was processed where possible via the software itself, and in some cases externally. The results that will be displayed in the coming chapters are based on testing points that have good combustion stability and repeatability.

#### 3.9.1 In-cylinder Volume

Measuring the in-cylinder volume is important to understand in more detail the combustion process allowing room for improvement in terms of engine performance and efficiency.

Figure 15 displays the parameters of the piston, connecting rod, and the crankshaft.

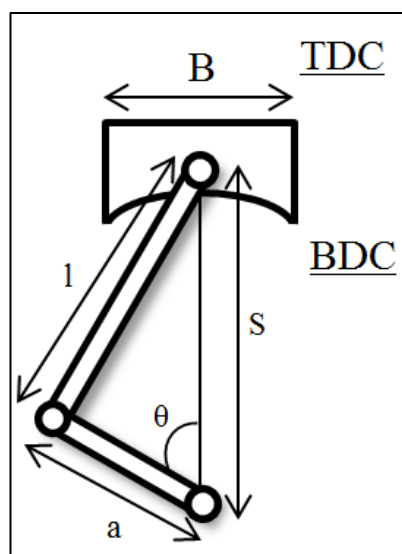


Figure 26: Schematic representation of piston and its connections

To begin calculating the in-cylinder volume, the following equation must be used to obtain the in-cylinder volume at any given crank position:

$$V = V_c + \frac{\pi B^2}{4}(l + a - s) \quad \text{Equation 6 [8]}$$

Where  $V_c$  is the clearance volume,  $B$  is the cylinder bore in mm,  $l$  is the connecting rod length mm,  $a$  is the crank radius in °, and  $s$  is the distance between the crank axis and the piston pin axis in mm.

The distance  $s$  can be found using the following equation:

$$s = a \cos \theta + (l^2 - a^2 \sin^2 \theta)^{1/2} \quad \text{Equation 7 [8]}$$

Equation 7 can be re-arranged to find the in-cylinder volume at any crank angle  $\theta$ :

$$\frac{V}{V_v} = 1 + \frac{1}{2}(r_c - 1) \left[ R + 1 - \cos \theta - (R^2 - \sin^2 \theta)^{1/2} \right] \quad \text{Equation 8 [8]}$$

Where  $r_c$  is the compression ratio (which is the maximum cylinder volume over the minimum cylinder volume) and  $R$  is the ratio of the connecting rod length to crank radius  $l/a$ .

### 3.9.2 Apparent and Cumulative Rate of Heat Release

The heat release rate analysis can be classified as either gross or net apparent rate of heat release. The gross heat release rate can be determined using exhaust gas data whereas the net apparent can be obtained using in-cylinder pressure data. For the purpose of this research, the net apparent heat release rate will be used. The formula to calculate this is given below:

$$\delta Q_{ch} = dU_s + \delta Q_{ht} + \delta W + \sum h_i dm_i \quad \text{Equation 9 [8]}$$

This equation is based on the first law of thermodynamics where  $U_s$  is the internal energy,  $Q_{ht}$  is the convective heat transfer to the cylinder walls,  $W$  is the work output, and  $h_i dm_i$  are the losses by the crevices.

Equation 9 can be re-arranged into the following to prepare for the final equation which can calculate the AHRR:

$$\frac{dQ_{ch}}{d\theta} = \frac{\gamma}{\gamma-1} p \frac{dV}{d\theta} + \frac{1}{\gamma-1} V \frac{dp}{d\theta} + V_{cr} \frac{dp}{d\theta} + \frac{dQ_{ht}}{d\theta} \quad \text{Equation 10 [8]}$$

The final form of the equation, which does not take into account the correction for heat loss to the cylinder walls, is:

$$\frac{dQ_n}{d\theta} = \frac{\gamma}{\gamma-1} p \frac{dV}{d\theta} + \frac{1}{\gamma-1} V \frac{dp}{d\theta} \quad \text{Equation 11 [8][50]}$$

Where  $Q_n$  is the net heat release,  $\gamma$  is the ratio of specific heats,  $P$  is the pressure, and  $V$  is the volume.

Assuming the pressure and volume data was given, the only other variable in this formula would be  $\gamma$ . There have been various publications stating methods of calculating  $\gamma$ , however for the purpose of this research, a value of  $\gamma = 1.3$  [8] was used and was maintained throughout the experiments.

The cumulative heat release rate can also be calculated, which is the summation of the heat release rates at each crank angle, using the formula below:

$$CHRR = \sum_{IXA}^{EOC} \frac{dQ_{ch}(i)}{d\theta(i)} \times k(i) \quad \text{Equation 12 [8][50]}$$

Where,  $EOC$  is the end of combustion,  $IXA$  is the point the heat release curve intersects the x axis, and  $k$  is the resolution of the heat release rate.

### 3.9.3 Mass Fraction Burned

Another common method to define cumulative combustion is by calculating the mass fraction burned, which is expressed as a ratio of the cumulative heat release to the total heat release:

$$MFB(\theta) = \frac{\int_{\theta_{soc}}^{\theta} \frac{dQ_{ch}}{d\theta} d\theta}{m_f \times n_{comb} \times LHV} \quad \text{Equation 13 [50]}$$

Where  $m_f$  is the mass of fuel,  $n_{comb}$  is the combustion efficiency, and  $LHV$  is the lower heating value of the fuel. For the purpose of this research, the start of combustion was taken as the point at which the heat release curve intersected the x axis.

### 3.9.4 Energy Supplied by Hydrogen

The energy supplied by hydrogen was calculated using the equation below. The final value of the energy supplied from the diesel was obtained by subtracting the value calculated from equation 14 from the total value:

$$E_{H_2} = \frac{CV_{H_2} \times (\dot{V}_{H_2i} - \dot{V}_{H_2e}) \times \rho_{H_2}}{CV_{diesel} \times \dot{V}_{diesel} \times \rho_{diesel} + CV_{H_2} \times (\dot{V}_{H_2i} - \dot{V}_{H_2e}) \times \rho_{H_2}} \quad \text{Equation 14 [50]}$$

Where  $CV_{H_2}$  represents the calorific value of hydrogen measured in kJ/kg,  $\dot{V}_{H_2i}$  is the volume flow rate of hydrogen in the inlet measured in m<sup>3</sup>/s,  $\dot{V}_{H_2e}$  is the volume flow rate of hydrogen in the exhaust measured in m<sup>3</sup>/s,  $\dot{V}_{diesel}$  is the volume flow rate of diesel measured in m<sup>3</sup>/s, and  $\rho_{diesel}$  is the density of diesel measured in m<sup>3</sup>/s. to ensure stable load and speed conditions during a specific operation, the quantity of diesel fuel was gradually lowered as the quantity of hydrogen was increased.

### 3.9.5 Combustion Efficiency of Hydrogen

To calculate the combustion efficiency of hydrogen, the following equation was used:

$$\eta_{H_2,ce} = \left(1 - \frac{\dot{V}_{H_2e}}{\dot{V}_{H_2i}}\right) \times 100 \quad \text{Equation 15 [50]}$$

Where  $\eta_{H_2,ce}$  denotes the combustion efficiency of hydrogen as a %,  $\dot{V}_{H_2e}$  is the volumetric flow rate of hydrogen in the exhaust measured in  $m^3/s$ , and  $\dot{V}_{H_2i}$  is the volume flow rate of hydrogen in the inlet measured in  $m^3/s$ .

### 3.9.6 Bottled Hydrogen Flow Rate

Calculating the flow rate for the bottled hydrogen was done by using the following equation:

$$BG_{flow} = VAF \times (BG_{pc} \times 10^{-2}) \quad \text{Equation 16 [50]}$$

Where  $BG_{flow}$  represents the hydrogen flow rate measured in  $m^3/s$ ,  $VAF$  is the volumetric air flow when the engine is operating without hydrogen measured in  $m^3/s$ , and  $BG_{pc}$  is the % of the bottled hydrogen.

## 3.10 Engine Simulation Software and Test Procedure

In this section, the engine simulation software that was used will be explained, pointing out the key features of the software and why it was chosen to carry out the tests. Additionally, the testing procedure for both the experimental and simulated tests will be explained stating the parameters varied and how the experimental engine was prepared for testing.

### 3.10.1 Engine Simulation Software

The engine simulation software that was used to carry out the simulations was Ricardo WaveBuild® Ver. 2016.1 Build 82525 which was supplied via the Centre of Advanced Powertrain and Fuels Research (CAPFR) at Brunel University London. Ricardo Software allows for various testing techniques with a range of possibilities in terms of the components

available to implement and subsequently replicate. The software allows for the creation of engine types ranging from SI single-cylinder down-sized engines to CI multi-cylinder heavy-duty engines. It also has the capability to simulate running conditions to produce data which can be used to analyse the engine characteristics and emissions.

The simulations were carried out using 1-D simulation which allowed for analysis of the engine power outputs, torque, fuel efficiency, exhaust emissions, and other key parameters that were able to be compared with experimental data. The models created were a single cylinder and a multi-cylinder dual-fuel CI engine which replicated the specifications of the experimental engine used. The properties of the fuels were taken from the data presented in the earlier sections of this chapter.

One limitation that exist within the software is that it is unable to simulate the effect of weather onto the fuels and engine operation. The software does allow for the basic manipulation of air temperatures and pressures, but not to the same level of accuracy based on real world storage and usage of fuels. This means that the fuels and gasses used to simulate the combustion will not be under the same external weather effects as their real-world counterparts.

Another limitation is the parameters that are able to be tested using 1-D simulation. The basics such as in-cylinder pressure, power, torque, BMEP etc are possible however, a more detailed analysis of the for example the flow and spray characteristics is only possible using 3-D simulations.

In terms of the emissions, the basic emissions that are able to be tested using the 1-D simulation such as the NO<sub>x</sub>, THC, and CO emissions. This is down to the multi-Wiebe two zone combustion model that exists in Ricardo WAVE, which will be explained in more detail in chapters 5 and 6.

### 3.10.2 Testing Procedure

The testing procedure for the experimental engine followed the same testing matrix as the simulations in order to maintain continuity to ensure reliable results. The reasons behind these selections for the parameters is that they are selected to mimic the operating conditions of light-duty and medium-duty diesel engines, which is where the majority of the running time occurs in standard passenger vehicles.

Prior to taking any readings from the experimental engine, the engine would run until the water temperature reached its optimum of  $80\text{ }^{\circ}\text{C} \pm 3\text{ }^{\circ}\text{C}$  and the emissions readings stabilise to an acceptable rate.

	Name	Units	Case 1	Case 2	Case 3	Case 4	Case 5
Status			Run	Run	Run	Run	Run
Title			1500-2500 rpm				
1	SPEED	rpm	1500-2500	1500-2500	1500-2500	1500-2500	1500-2500
2	A_F		14.7	14.7	14.7	14.7	14.7
3	Diesel_Fuel	kg/hr	0.2	0.2	0.2	0.2	0.2
4	Diesel_Injdur	deg	35	35	35	35	35
5	Diesel_SOI	deg	3-12	3-12	3-12	3-12	3-12
6	HYD_comp	§	0	0.02	0.04	0.06	0.08
7	intake_air	§	1.0	0.98	0.96	0.94	0.92
8	Load	bar	2.5-5	2.5-5	2.5-5	2.5-5	2.5-5

Table 9: Testing matrix

## Chapter 4

# Effects of Combined Diesel-Hydrogen Combustion on Combustion Properties

## Chapter 4

### Effects of Combined Diesel-Hydrogen Combustion on Combustion Properties

#### 4.1 Introduction

In recent years, diesel has grown in popularity and the market share of diesel ownership has improved since the late 1990's. However, for the last half a decade, the relationship between diesel vehicles and government legislations has become increasingly strained due to the ever-growing concern for the environment and the potential damage that diesel emission may be causing. This has led to an increased effort by researchers to develop cleaner and more efficient diesel engines, in the hope that their popularity can increase again. There has been an increase in the development of alternative powertrains such as electrical power and hybrid technologies [86]. Research on alternative fuels has also increased which have renewable capabilities or that can be produced on-board such as hydrogen, LPG, CNG, and biodiesel [87, 88, and 89]. The concept of hydrogen combustion appears to be gaining more popularity due to its cleaner emissions production, as discussed in earlier chapters. It can be both stored or produced on-board vehicles, which allows for the flexibility of using the fuel in a more wide-spread capacity. On-board hydrogen production is seen more as a transitional technique until the difficulties surrounding the infrastructure, distribution, and the on-board storage of hydrogen are overcome. Researchers have attempted to produce hydrogen on-board by using a fuel reforming reactor located inside the EGR loop, allowing the hydrogen to be produced from diesel fuel [72].

This chapter looks to investigate the effects of combined diesel-hydrogen combustion on the hydrogen combustion and brake thermal efficiency, and the smoke, CO, THC, and NO<sub>x</sub> emissions produced. The hydrogen was admitted into the engine via the intake port replacing an equal volume of air. In doing this, the oxygen concentration is reduced as opposed to using

direct injection, however, this method was deemed to be the most cost effective and closely related technique to the on-board storage and production techniques explored previously.

## 4.2 Methodology

Figure 16 presents a detailed representation of the hydrogen gas supply setup illustrating where various controllers and valves were placed to ensure safe operation. A more in-depth schematic of the entire engine set-up can be found in chapter 3.

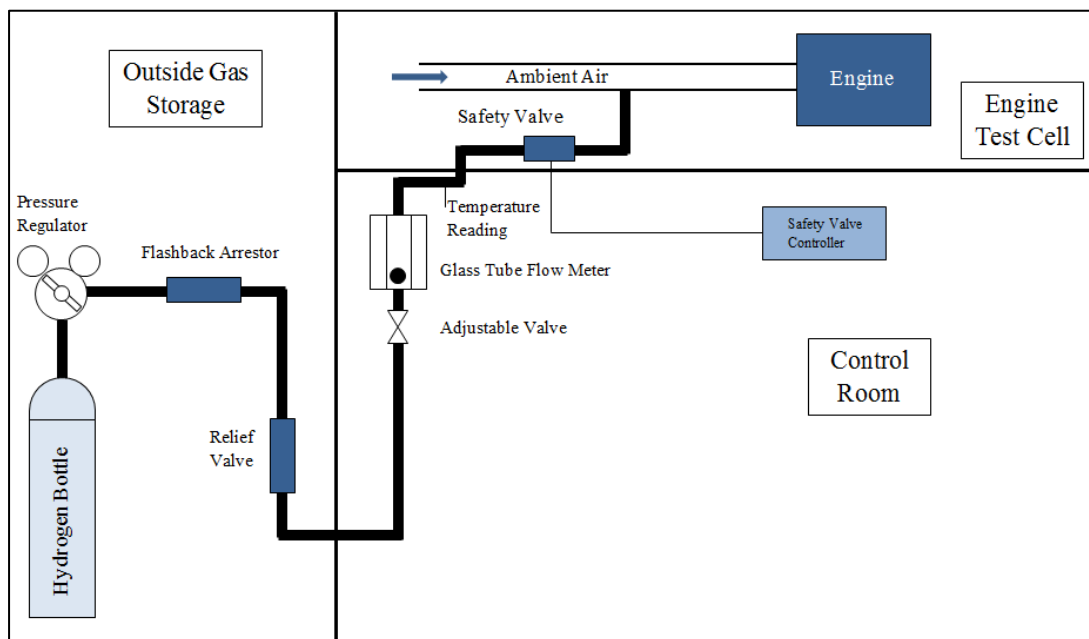


Figure 27: Schematic of Hydrogen Setup

The hydrogen was transported via the pressure regulator to the intake pipe. The pressure regulator allowed the control of the line pressure and it displayed the pressure of the remaining gas in the bottle. The flash back arrestor was critical in preventing any potential flame bodies from travelling back through the hydrogen line and back into the bottle. The line pressure was maintained at a safe operating level by using the relief valve, which exerted excess pressure when necessary. The hydrogen gas flow rate was measured using a glass tube rotameter which had an adjustable valve. The line temperature was measured using a K-type

thermocouple, where whenever the temperature did not meet the calibration temperature of the flow meter (25 °C), a correction was applied to the reading on the flow meter. To increase the level of safety when using the hydrogen gas, an additional control valve was installed which was fitted downstream of the thermocouple. This valve was programmed to shut after 5 minutes once opened.

The concentration of hydrogen admitted into the intake pipe was varied from 2% to 8 % in 2% increments. To ensure the speed and load remained stable, the quantity of diesel was gradually reduced as the quantity of hydrogen was injected. This subsequently meant that as the concentration of hydrogen was increased in the intake air, the energy provided by hydrogen was increased as well. Table 10 displays the energy gained at different concentrations of hydrogen during the combustion process.

H <sub>2</sub> Addition (%vol.)	Intake air (%vol.)	Energy from H <sub>2</sub> (%) at 1500 rpm		Energy from H <sub>2</sub> (%) at 2500 rpm	
		2.5 bar BMEP	5 bar BMEP	2.5 bar BMEP	5 bar BMEP
0	100	0	0	0	0
2	98	13.15	8.79	12.67	7.43
4	96	26.74	18.53	23.81	14.22
6	94	45.56	29.21	-	23.54
8	92	-	41.23	-	-

Table 10: Energy Supplied by Hydrogen

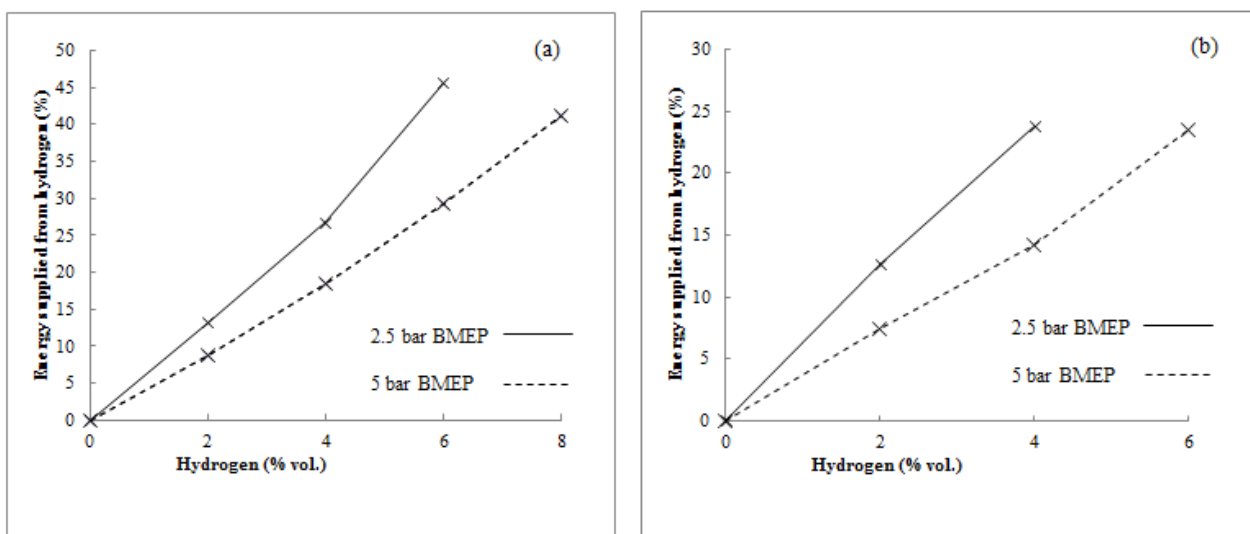


Figure 28: Graph of energy supplied by hydrogen. (a) 1500 rpm, (b) 2500 rpm

To change the load, the engine speed was fixed, and the flow rate of the diesel fuel was adjusted. Therefore, the medium-load operating condition was obtained by increasing the amount of diesel fuel whilst keeping the hydrogen flow rate constant.

### **4.3 Results and Discussion**

In the following sections the performance, emissions, and the combustion properties are displayed and analysed. Some of the parameters investigated were the NO<sub>x</sub>, CO, and THC emissions, as well as the combustion efficiency of hydrogen. The heat release rate was analysed as well as the brake thermal efficiency. The tests were carried out at 1500 and 2500 rpm and at 2.5 and 5 bar which is to replicate medium- and low-load conditions. The SOI was altered from 3 to 12 CAD BTDC in 3-degree steps.

#### **4.3.1 Effects of Diesel-Hydrogen Combustion on NO<sub>x</sub> and Smoke Emissions**

As stated in earlier chapters, when combining hydrogen with diesel combustion, a trade-off occurs between the NO<sub>x</sub> and smoke emissions where by increasing the hydrogen concentration can result in potentially higher NO<sub>x</sub> emissions but lower smoke emissions depending on the load and speed.

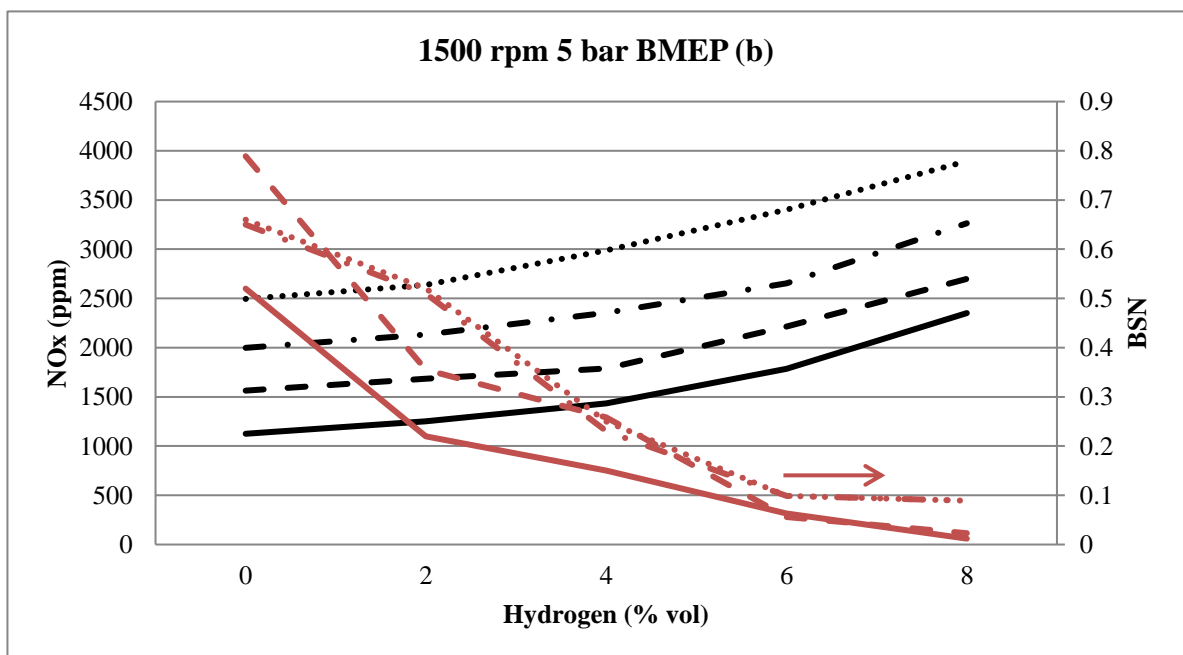
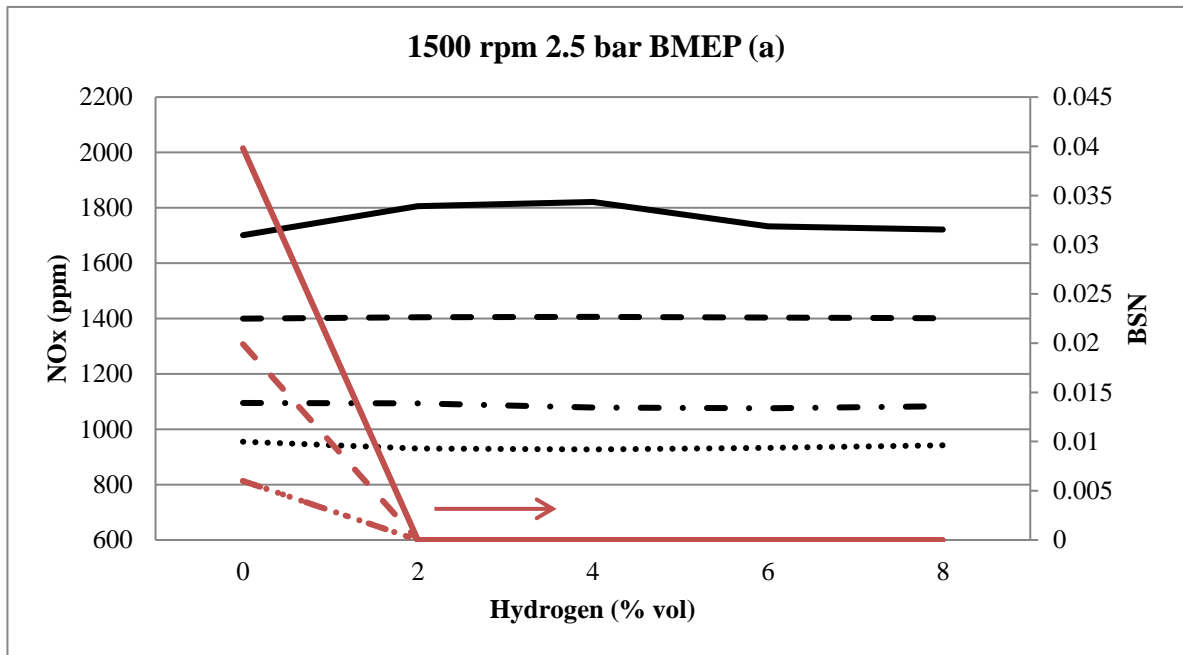


Figure 29: Effect of diesel-hydrogen combustion on NOx and Smoke Emissions

Looking at figure 29(a), with the introduction of hydrogen, the NOx emissions remained relatively unchanged. The smoke emissions prior to the introduction of hydrogen were already low and so with hydrogen became lower still. It was observed that the smoke

emissions for SOI 3 and 6 CAD BTDC were almost identical and so appears as one single entry. The overall reduction of the fuel carbon to hydrogen ratio could be linked to the temperature changes within the combustion chamber, which is as a result of the smoke reduction mechanism.

In figure 29(b), the NO<sub>x</sub> emissions increased as the concentration of hydrogen was increased. This was as expected according to literature due to the increased adiabatic combustion temperatures of hydrogen when compared to standard diesel combustion. The smoke emissions reduced incrementally as the hydrogen concentration increased, which was in keeping with the literature. One specific point to mention was at 8% hydrogen concentration where the NO<sub>x</sub> emissions were relatively higher without a large reduction in smoke emissions. For this reason, when operating under low-speed medium-load conditions, 6% hydrogen concentration should be the limit.

When observing the data obtained from the high-speed runs in figure 19, it is seen that when operating under high-speed conditions the NO<sub>x</sub> emissions were generally lower when compared to low-speed operation. This is despite the possibility of achieving higher combustion temperatures when operating under higher speeds. This could be as a result of the decreased time for the charge flame to remain in the combustion chamber, which is vital in NO<sub>x</sub> formation. As stated earlier, the higher speed was achieved by increasing the flow rate of diesel, which ultimately led to an increase in smoke production. Additionally, the energy supplied from diesel is greater at higher speeds than at lower speeds under the same loads.

Looking at figure 30(b), the BSN decreased substantially after increasing the concentration of hydrogen above 2%. Also, the pattern displayed in figure 30(b) is in keeping with that of figure 29(b).

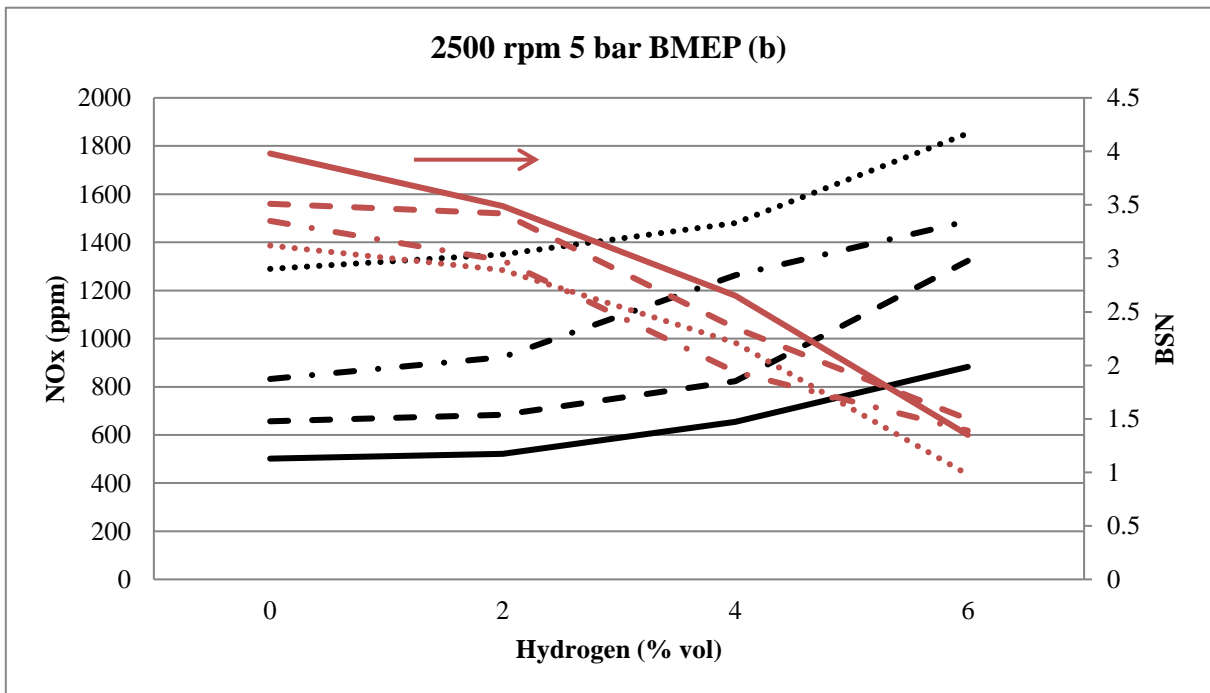
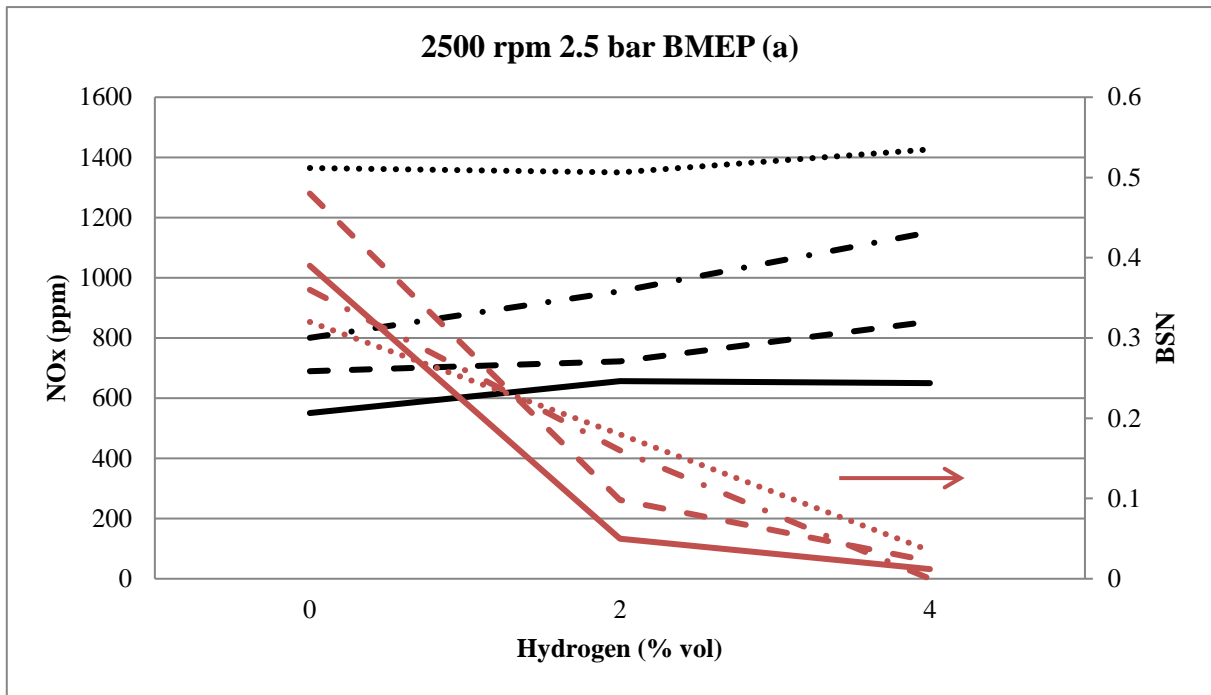


Figure 30: Effect of Diesel-hydrogen combustion on NOx and Smoke emissions

One main way that diesel-hydrogen combustion can affect the smoke production is primarily due to the inherent reduction in carbon within the diesel-hydrogen mixture. Another way is that the higher in-cylinder temperatures achieved as a result of diesel-hydrogen combustion promotes soot oxidation. Lastly, diesel-hydrogen combustion has not had a significant effect on the particle size and mass distribution according to reports [90].

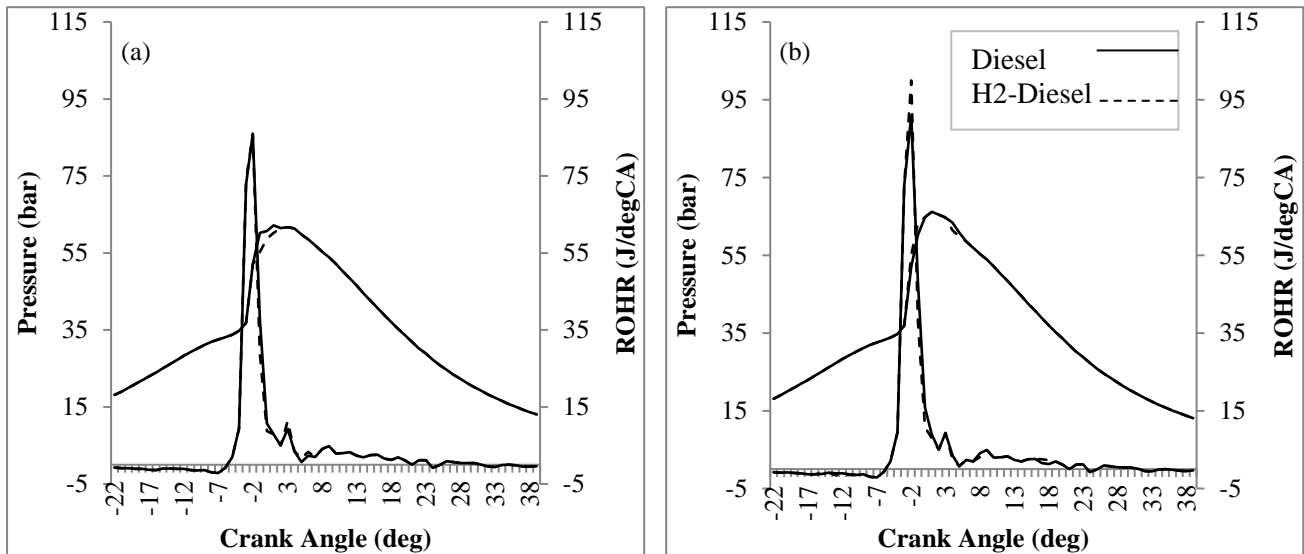


Figure 31: Effect of Diesel-Hydrogen combustion on in-cylinder pressure and AHRR (a) 1500 rpm 2.5 bar BMEP, (b) 1500 rpm 5 bar BMEP, 4% Hydrogen concentration, SOI 9 CAD BTDC

When examining figure 29(a), the admission of hydrogen at any concentration led to minimal changes to the NO<sub>x</sub> formation, therefore a deeper understanding could be gained if other information is looked at during this operating condition. Specifically, looking at the in-cylinder pressures and rate of heat release at low speeds and at medium- to low-loads, which is displayed in figure 31. Looking at figure 31(a), it appears that there is a slight drop in the in-cylinder pressure under diesel-hydrogen combustion. Based on this, it can be assumed that there was no increase in in-cylinder temperature at this operating condition, which would lead to an increase in NO<sub>x</sub> formation. Figure 31(b) shows that when operating at medium load, the in-cylinder pressure is increased when operating under diesel-hydrogen combustion. It can therefore be concluded that the primary factor for the increase in NO<sub>x</sub> formation was this increase in the in-cylinder pressure, which ultimately raised the in-cylinder temperature. The

reason for this large increase in the in-cylinder pressure could be as a result of the unstable conditions that can be observed when operating at varying loads due to the conditions not always favouring efficient oxidation of hydrogen, leading to a reduction in stability of the engine combustion [48]. The lack of any EGR could also be a factor, as McWilliam et al states, EGR is capable of lowering the maximum in-cylinder pressure [48].

### 4.3.2 Effect of Diesel-Hydrogen Combustion on CO emissions

It is widely known that CI engines are relatively low CO emissions producers due to the lean operating conditions. When admitting hydrogen, the quantity of CO is reduced even further as the carbon content in the mixture is reduced when in comparison to standard diesel combustion.

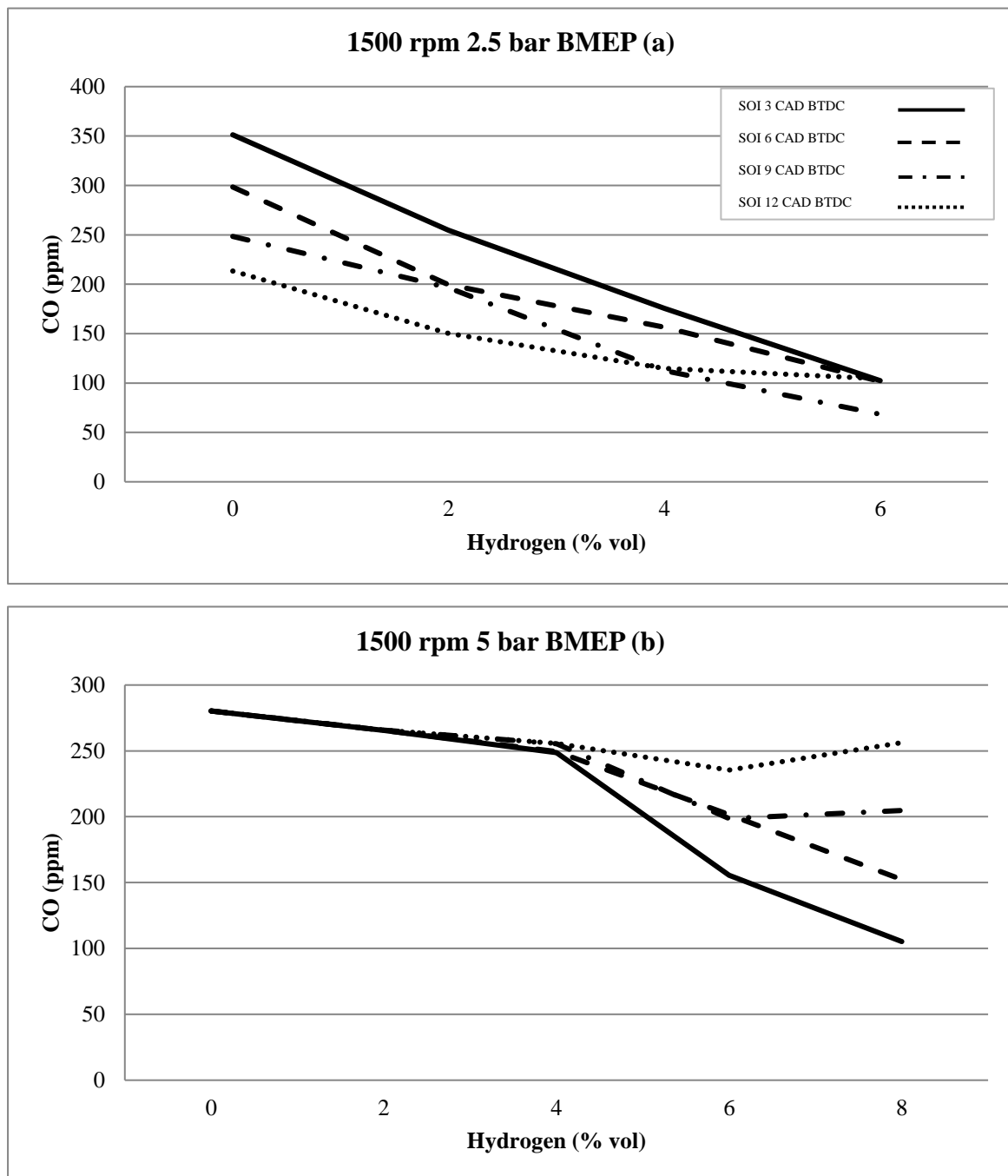


Figure 32: Effect of Diesel-Hydrogen Combustion on CO Emissions

There were some points during the sweep that produced slightly higher CO emission values, where it is thought that diesel misfire could have been the reason for this due to the reduction in oxygen concentration and diesel fuel when introducing hydrogen. Looking at figure 32(b), at SOI 9 and 12 CAD BTDC at 6-8% hydrogen concentration, an increase in the CO can be seen. Therefore, in order to reduce the CO emissions, these running conditions could be avoided.

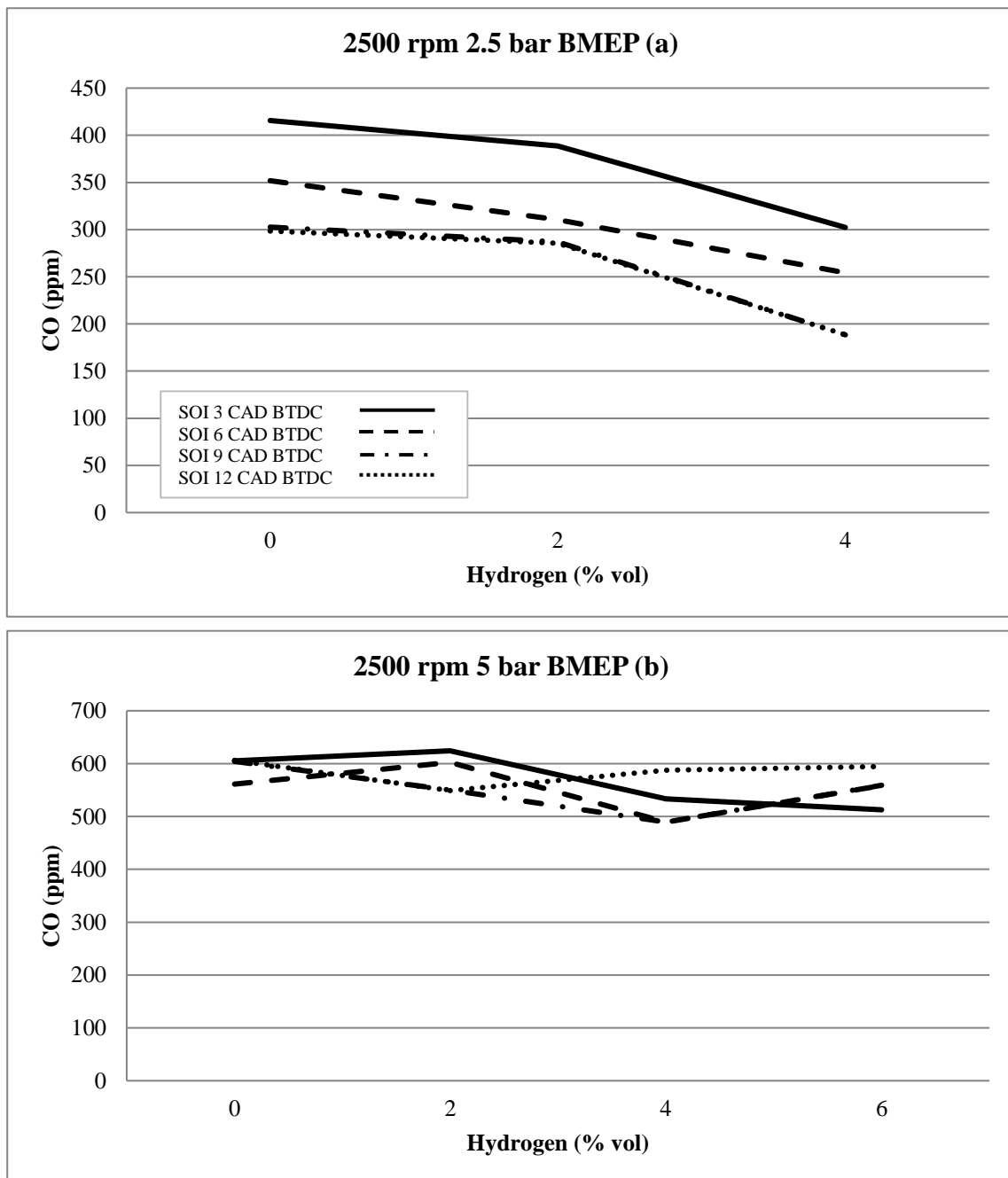


Figure 33: Effect of Diesel-Hydrogen combustion on CO Emissions

### 4.3.3 Effect of Diesel-Hydrogen Combustion on THC Emissions

THC emissions are the result of a combination of diesel fuel and lubricating oils combusting in the cylinder. The THC emissions consist of different carbon-based emissions such as the un-burned hydrocarbons (UHC) and non-methane hydro-carbon (NMHC) emissions. The figures below show that the THC emissions are commonly found to be in the range of 20-300 ppm, which is as expected based on research [27].

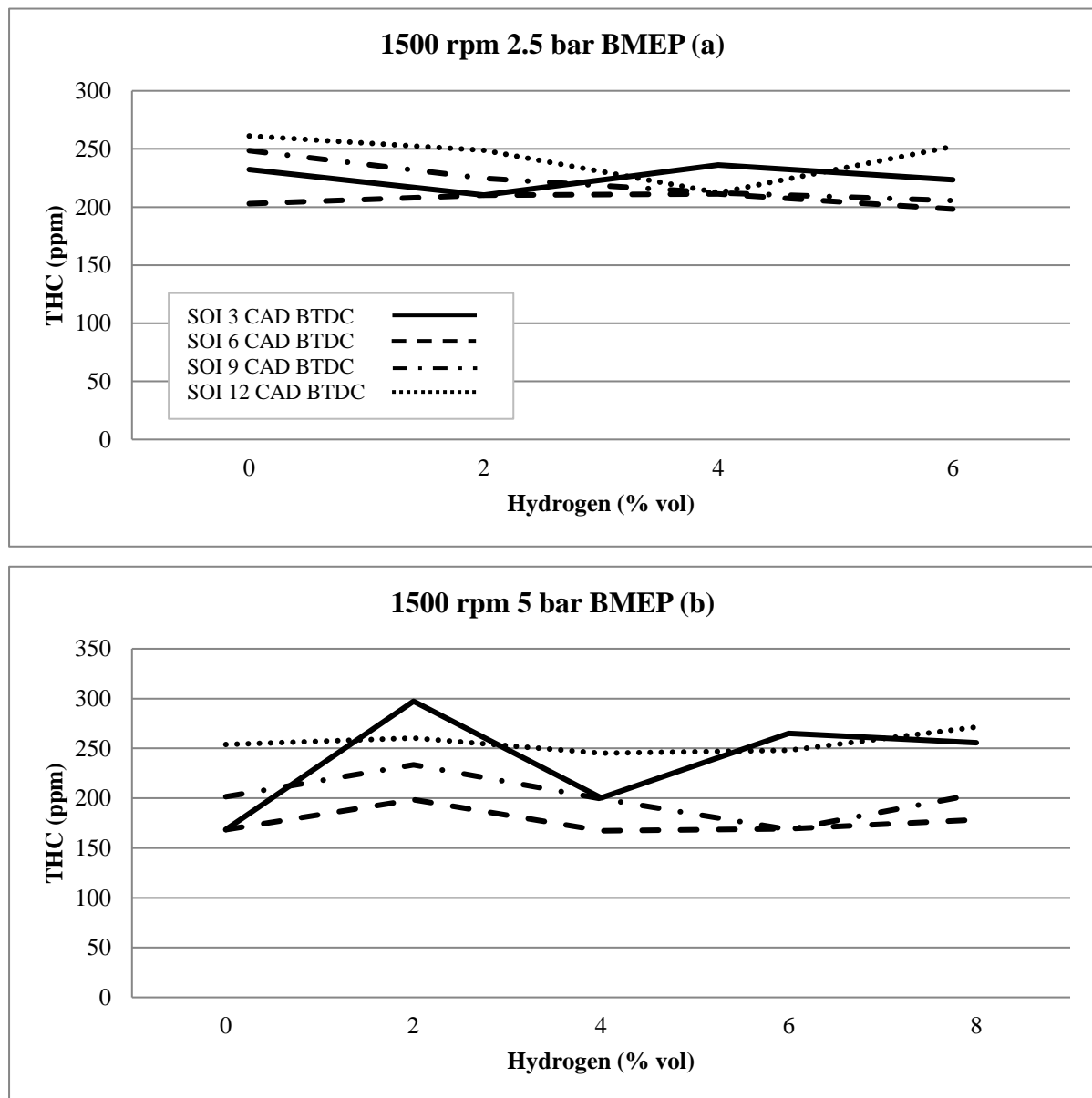


Figure 34: Effect of Diesel-Hydrogen combustion on THC Emissions

When under diesel-hydrogen operation, it is seen that the THC emissions fluctuated in comparison to standard diesel combustion. For example, looking at figure 35(b), the THC emissions increased as the concentration of hydrogen increased. A reason for this could be spray on the cylinder wall as a result of the lower density of hydrogen and the high levels of diesel fuel injected into the cylinder needed to operate at this condition. Conversely, in figure 34(a) it is seen that the THC levels have reduced, which could have been the result of the smaller levels of diesel needed, coupled with the excess, air leading to a reduction in the intake charge density.

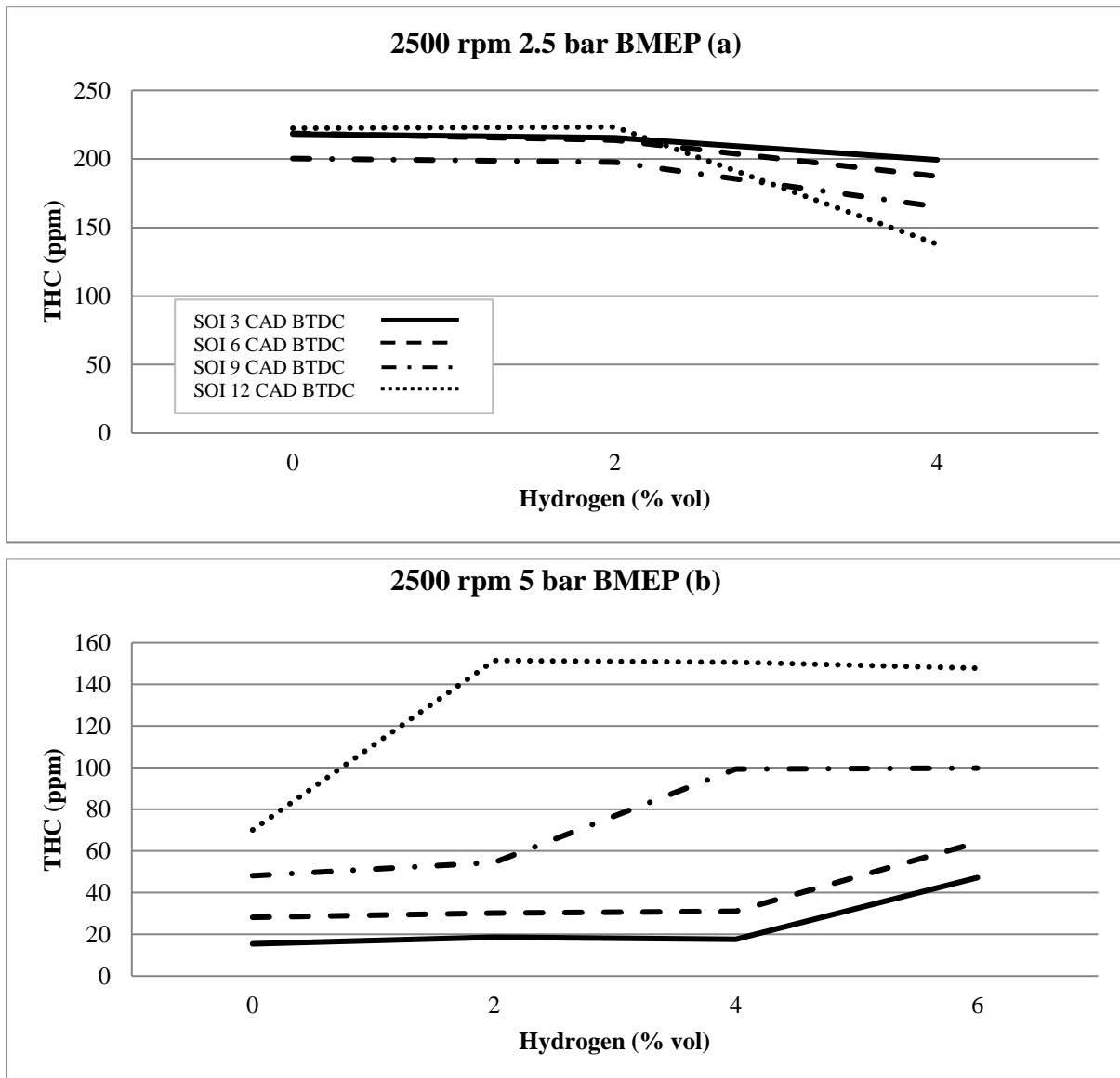


Figure 35: Effect of Diesel-Hydrogen combustion on THC emissions

The optimum conditions for producing low THC emissions appear to be at high-speed medium-load conditions, which can be seen in figure 35(b). Based on this, the assumption can be made that the in-cylinder temperatures have a significant impact on the production of THC emissions by producing much lower levels. Additionally, the injection timing of diesel seems to affect the THC emission production where by advancing the timing led to an increase in THC emissions, due the tip of the spray point penetrating the charge much deeper, leading to residue on the spray wall.

#### **4.3.4 Analysing Hydrogen Combustion Efficiency**

There is a possibility of increasing the strain on the environment when using hydrogen as a fuel in a modern combustion engine by releasing more through the exhaust into the environment [91]. For this reason, the optimisation of the combustion of hydrogen is vital in ensuring that minimal hydrogen is allowed to escape unburned in the atmosphere. Unburned hydrogen in the exhaust is an implication that there is inefficient or incomplete hydrogen combustion. It could also be due to the charge passing through the exhaust valve during the valve overlap period, which ultimately could lead to a drop in the thermal efficiency of the engine.

The hydrogen in the exhaust was measured using a gas chromatograph (TCD) which was described in detail in chapter 3. The equipment was calibrated with pure bottled hydrogen ranging from 2-4% where the values were calculated using equation 15.

It must be mentioned that before using data from the dual-fuel mode, it was important to ensure the hydrogen content found in the exhaust was produced specifically from the bottle as opposed to be the by-product of diesel combustion, which has been reported [92]. This process was carried out by injecting exhaust samples from the standard diesel combustion mode into the GC, where there was no data given. Therefore, it was assumed that standard

diesel operation was not producing hydrogen, or the quantity produced was too low for the equipment to detect.

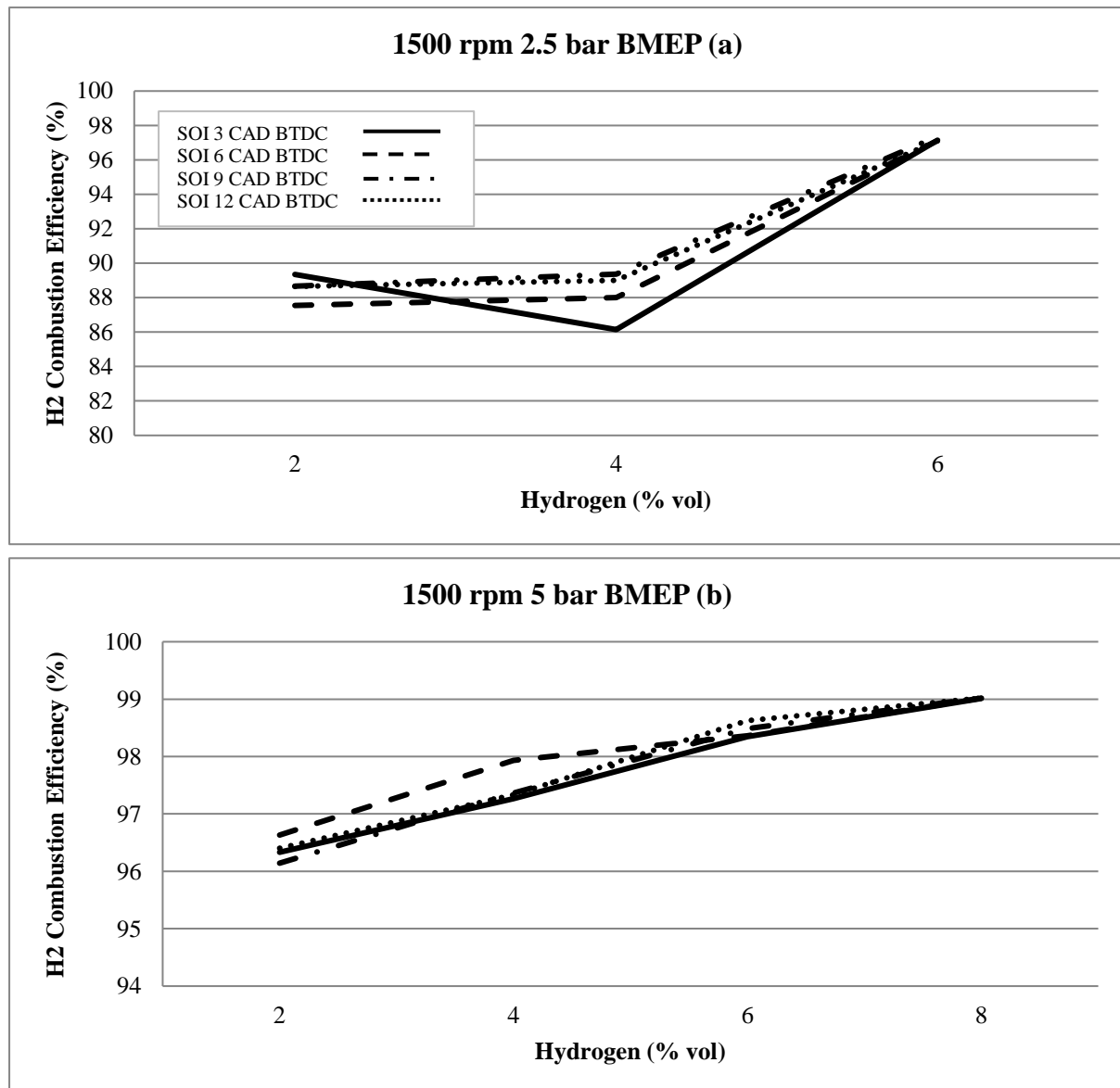


Figure 36: Combustion Efficiency of Hydrogen

To analyse these results, the lower flammability limit (LFL) of hydrogen will be used. This gives an indication as to how much hydrogen is being used as part of the combustion process when under dual-fuel operation. In chapter 3, it was presented that the LFL of hydrogen is 4% at 25 °C and 1 bar whereas during diesel combustion, these temperatures and pressures are much higher in the combustion chamber giving differing LFL values. It has been reported

that the LFL of hydrogen is known to increase under higher pressures but can decrease in higher temperatures [93].

Looking at figure 36(a), specifically at where the hydrogen concentration is over 4%, the combustion efficiency was higher than 90%. At this point, the hydrogen concentration was higher than LFL, whereas when the concentration drops below the LFL, the flame is unable to propagate into the hydrogen-air mixture due to it being too lean. It can also be seen in the same figure that when the hydrogen concentration was increased from 2-4% and at SOI 9 CAD BTDC, the combustion efficiency dropped.

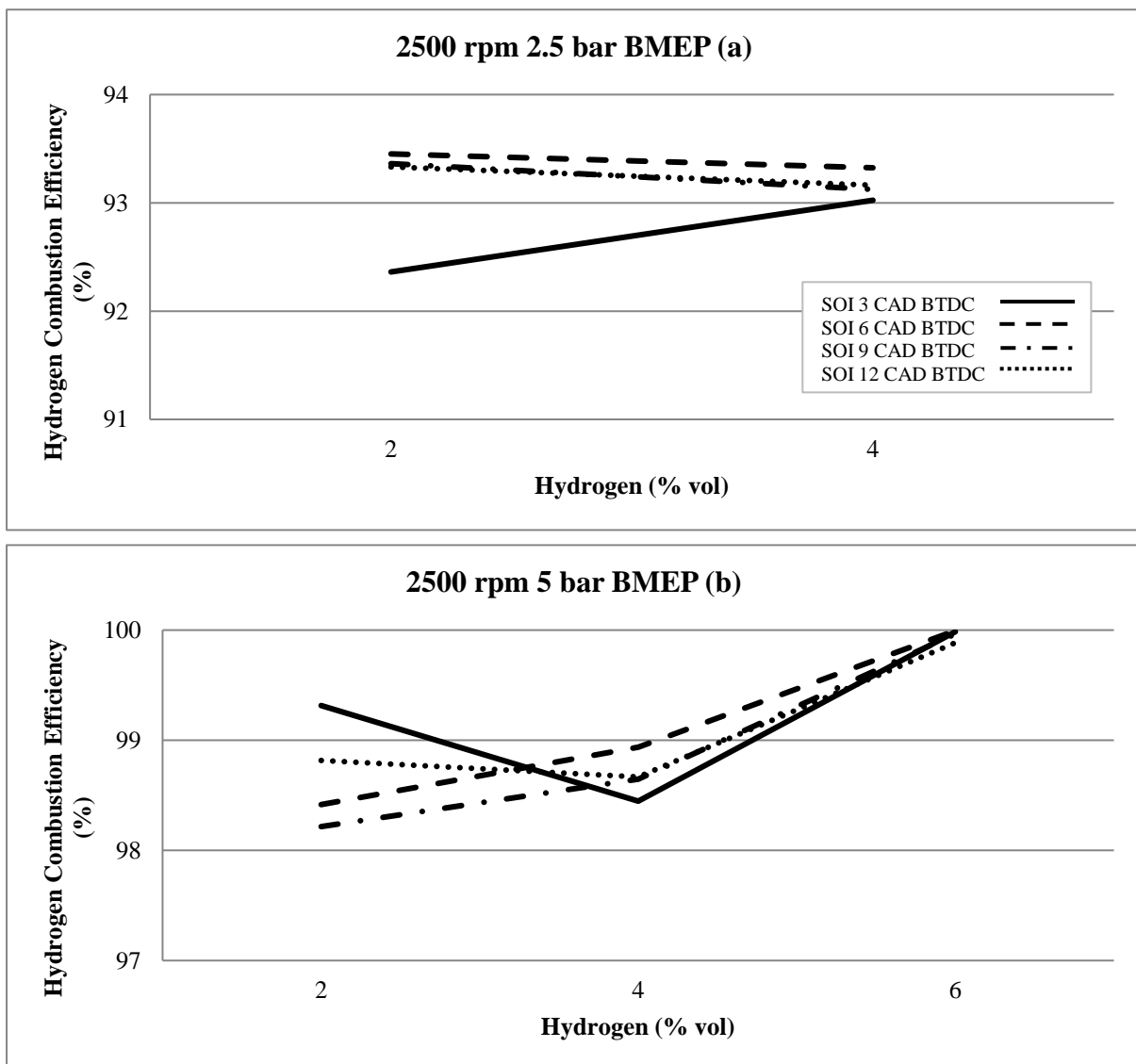


Figure 37: Combustion Efficiency of Hydrogen

When increasing the concentration of hydrogen under medium loads, the combustion efficiency is increased, as seen in figure 36(b). The primary reasons behind this are the higher in-cylinder temperatures and the larger quantity of diesel both of which lead to a reduction in the LFL.

When operating under higher speeds, the hydrogen combustion efficiency was increased still further. Looking at figure 37(a) the combustion efficiency ranged from 92-93.5% and under a medium-load condition, the combustion efficiency rose to almost 100%.

#### **4.4 Summary**

In the previous sections, the effects of diesel-hydrogen combustion on the performance and combustion characteristics of a HSDI CI engine were investigated and analysed. The hydrogen was admitted in 2% increments from 2-8% concentration levels where the hydrogen would replace the intake charge at those concentration levels. The key findings obtained during these experiments are concluded below:

- The smoke emissions were reduced, and the NO<sub>x</sub> emissions increased when hydrogen was part substituted for diesel, during much of the operating conditions tested. During low-load low-speed conditions, the admission of hydrogen was found to have minimal effect on the NO<sub>x</sub> production.
- When using 8% hydrogen concentration and operating under low-speed medium-load conditions, the NO<sub>x</sub> emissions increased significantly without a substantial drop in BSN. In order to balance the NO<sub>x</sub>-BSN trade-off, the optimal hydrogen concentration can be assumed to be 6% at this operating condition.
- When operating at higher speeds, the NO<sub>x</sub> emissions were reduced relative to the lower speeds whilst keeping the load and SOI of diesel constant. At these conditions,

it was assumed that the low NO<sub>x</sub> emissions were attributed to the reduction of the time for the charge to remain in the combustion chamber before ignition.

- The CO emissions were found to be reduced as the concentration of hydrogen was increased due to the reduction in the carbon content of the charge.
- The THC emissions were lowered when the injection timing was advanced due to the spray tip entering deeper in the cylinder, as a result of the low charge density, which ultimately led to interference to the spray wall.
- When admitting hydrogen into the intake, it was seen that the THC can either increase, reduce, or remain stagnant relative to standard diesel operation. For example, when operating under high-speed medium-load conditions, the THC emissions increased as the hydrogen concentration increased. This is due to the hydrogen-air mixture having a lower density relative to air alone, which due to the higher amounts of diesel fuel needed for the operating conditions, could have resulted in interference in the spray wall. Under opposite conditions of low-speed and -load, the hydrogen admission did not increase the THC emissions. This could be due to the smaller quantity of diesel needed relative to higher speeds and loads, along with the excess air in the combustion chamber, which ultimately led to no real impact from the lower charge density.
- The combustion efficiency of hydrogen was increased as speed, load, hydrogen concentration increased. Generally, unburned hydrogen in the exhaust fumes is as a result of incomplete combustion of hydrogen, or charge flowing through the exhaust valve during the valve overlap period. If hydrogen is injected after the exhaust valve shuts, the latter issue can be avoided.

## Chapter 5

# Comparison between Simulated and Experimental Diesel-Hydrogen Combustion

## Chapter 5

### Comparison between Simulated and Experimental Diesel-Hydrogen Combustion

#### 5.1 Introduction

In recent times, the effort to reduce harmful emissions produced by vehicles has increased due to increasing concern about public health and the impact on the environment. Governments worldwide have begun to become increasingly stringent on the levels of emissions that are acceptable in cities and heavily populated areas. Due to these legislations becoming harder to achieve, the importance of looking at alternate methods of reducing these harmful emissions is very high.

As discussed in the previous chapter, the possibility to reduce harmful emissions such as NO<sub>x</sub>, THC, and smoke emissions are being able to be achieved readily by using hydrogen gas as part of a dual-fuel operation with diesel fuel. Hydrogen can be stored on-board or even produced on-board as part of a gas reforming method which involves deriving hydrogen from within the EGR loop using diesel fuel [72]. Using hydrogen does bring some limitations however, where the storage and distribution infrastructure is difficult to achieve on a large scale. Testing also becomes difficult as there are certain risks involved when using hydrogen that researchers must be aware of. For this reason, computer simulated tests could provide a pathway to investigate hydrogen in ways that are potentially unachievable experimentally.

Simulated experiments are becoming increasingly popular in the current automotive emissions tests as it allows for a large amount of flexibility for manufacturers to carry out tests with. Recently, current emissions tests include very linear tests for obtaining data on emissions produced by engines, however from 2018 and beyond, new tests such as the real driving emissions (RDE) tests will become mandatory. These tests require vehicles to be

tested as closely as possible to actual driving conditions, taking into account factors such as routes, driver behaviour, elevation, air density, and various others to achieve a more accurate depiction of the emissions produced. Here is where simulations can become useful as it allows manufacturers to carry out these tests with maximum customisability of the above factors, before selecting the best conditions to test in the real world.

The outcomes of this chapter will create a wider understanding of the accuracy of simulated data and how closely it can be compared to experimental data. The emissions and operating conditions will be analysed and compared in this upcoming chapter.

## 5.2 Methodology

The experimental set-up for the hydrogen delivery system is explained in detail in chapter 4, and the results obtained during that experiment are going to be used to compare to the simulated data. Therefore this section will focus on the simulation set-up primarily.

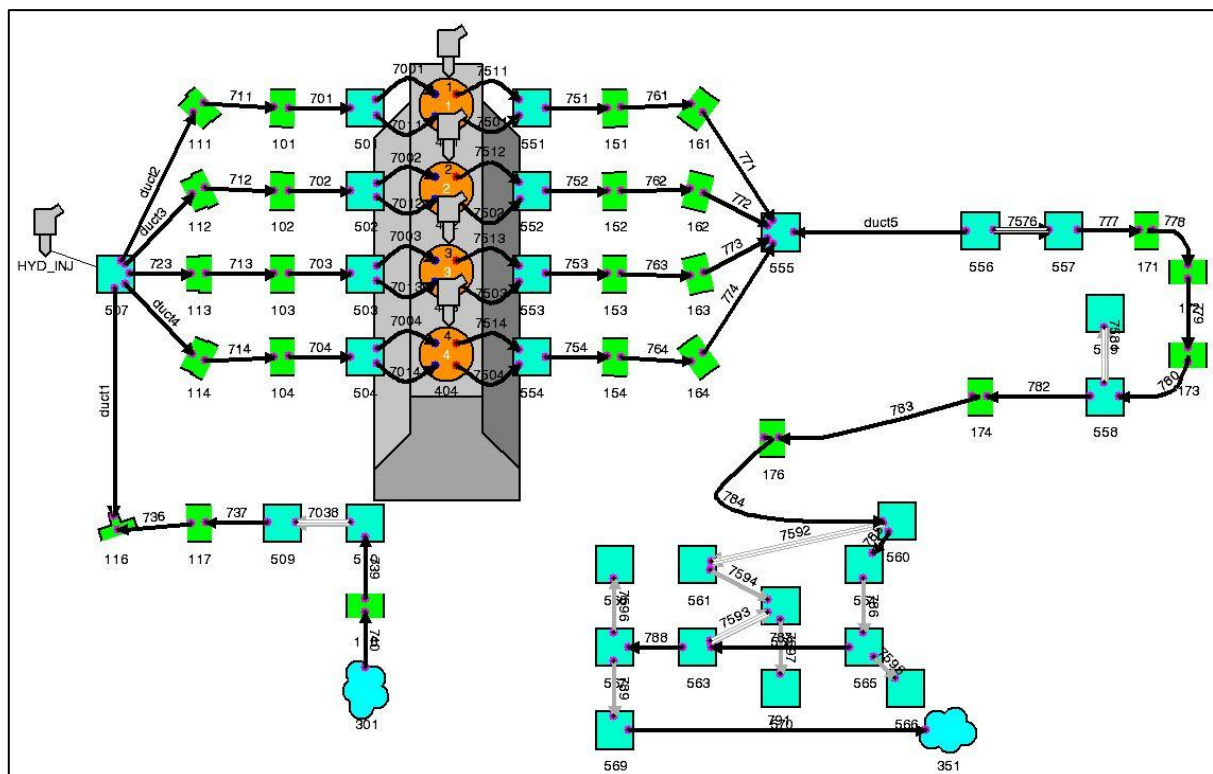


Figure 38: 1D engine model of multi-cylinder HSDI engine

Figure 27 presents a screenshot of the multi-cylinder engine model used for the simulations. The inlet and exhaust manifolds were measured and replicated in the model from the original experimental engine. The injectors were placed as closely as possible with respect to the hydrogen injector to replicate the positioning on the experimental engine. The piston geometry was replicated from the engine specifications as closely as possible, with the specially designed piston bowl modelled also. The model allowed for the measurement and alteration of various parameters such as injection rates, injection timings, cylinder pressures, emissions, and heat release rates to name a few.

The table of parameters that were altered for the simulated experiments is displayed in chapter 3, which mimics the test parameters of the experiments carried out on the test engine. These parameters were chosen to compare directly the difference in the simulated data and the experimental data. There was a total of 48 cases run for testing the emissions data presented. These cases covered the parameters set by the experimental tests. Should the convergence criteria be met before the end of the simulation, an extra cycle would be run by the current case before it had stopped.

The diesel fuel used for the simulation was using the diesel fuel file supplied by Ricardo Wave, which had similar properties to that of the diesel used for the test engine. This was to reduce the possibility for discrepancies due to fuel. It must be mentioned, that despite the efforts to maintain continuity with the diesel fuel properties, the experimental diesel fuel used had weather and time effects on it that the simulation could not replicate to the exact extent. Initially the simulation was run using single-fuel operation to obtain a benchmark and also to optimise the simulation as closely as possible to the experimental engine.

Ricardo software that was installed on the university PC did not contain a data file for a generic hydrogen gas fuel, therefore one needed to be modelled by selecting specific values and characteristics of the fuel that can then be used in the simulation model. The hydrogen

fuel properties that were used were obtained from chapter 3, specifically table 7. These values were selected as they closely represented the gas that was used during the experiments on the test engine. The specific heat profile of hydrogen had also been modelled in the file to provide a more realistic combustion characteristic for the gas [94]. The hydrogen was simulated to behave as if it had been produced on-board, as the experiments on the test engine did by replacing a percentage of the intake air with equal concentrations of hydrogen. Therefore, it was important to simulate hydrogen being pre-mixed as part of the intake charge, as it was when running the experiments on the test engine.

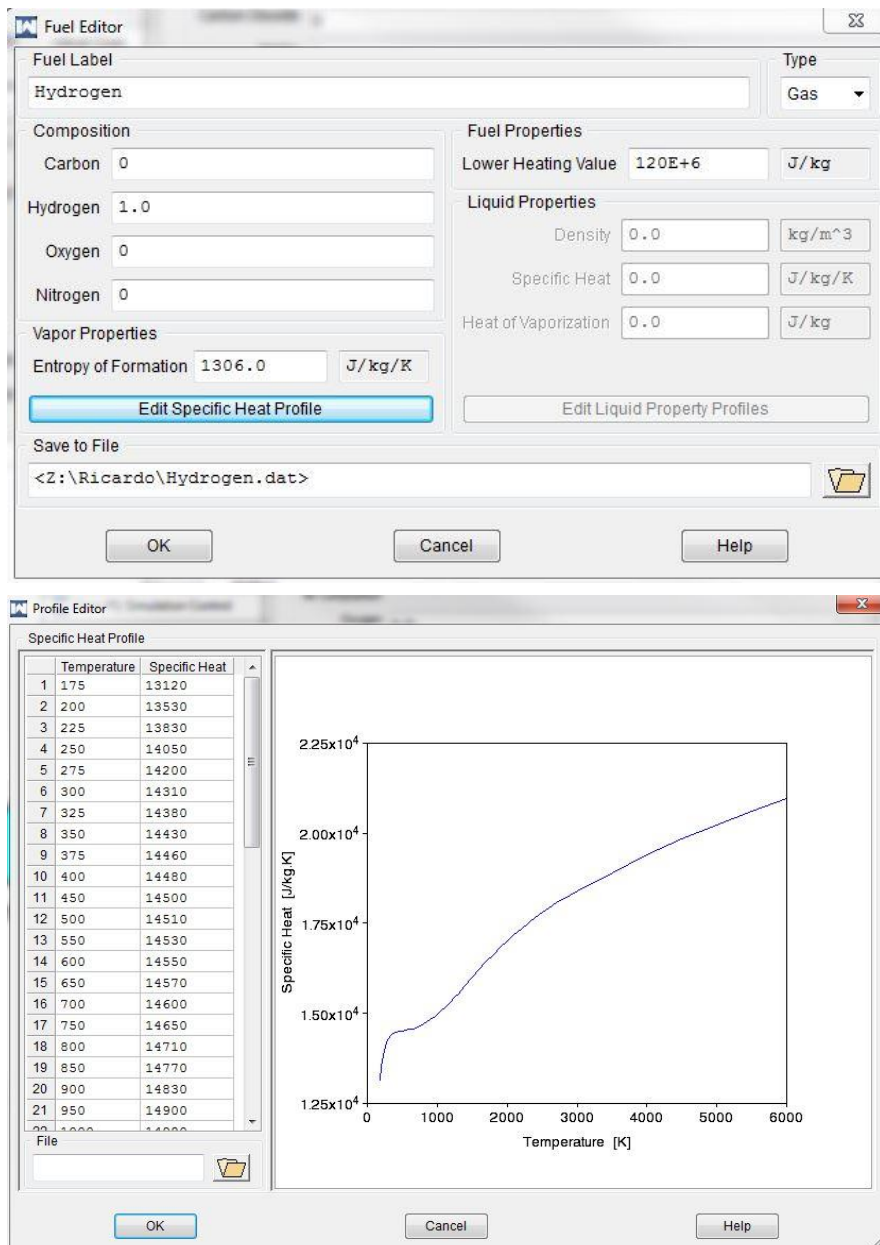


Figure 39: Properties of hydrogen fuel used for Ricardo WAVE [94][8]

The thermodynamic state of the cylinder was calculated using a two-zone model, which was made of burnt and unburnt zones. The unburnt zone contains the air, fuel vapour, and residual gases before combustion, whereas the burnt zone consists of the entirety of the mass that has been used by combustion. This thermodynamic state allows for the experimentation and analysis of gaseous emissions produced during dual-fuel combustion. Figure 39 displays the values used for the hydrogen gas model.

### **5.3 Results and Discussion**

As mentioned earlier in this chapter, the primary objective of simulating the experimental data was to gain a better understanding of the benefits of using simulation to test for emissions, which is why the emissions data for the experimental tests are what are primarily being focused on and compared with for the simulation. Specifically, the NO<sub>x</sub>, CO, and THC emissions that were gained from the test engine will be compared to see the level of accuracy of the simulated data due to the software's inability to measure smoke emissions directly from the simulation.

#### **5.3.1 Comparison of Pressure and Heat Release Rate between Experimental and Simulated data**

The in-cylinder pressure and the heat release rate is a useful tool to analyse the potential temperature changes in the cylinder as part of the combustion process. It was deduced in the previous chapter that the in-cylinder temperatures were one of the primary causes of NO<sub>x</sub> formation where higher temperatures usually led to higher quantities of NO<sub>x</sub> being formed. Therefore, the in-cylinder pressure and heat release rate can identify the points at which the temperatures are the highest under certain operating conditions.

For the comparison, the experimental data selected was based on the SOI 9 CAD BTDC and at 4% hydrogen concentration running at 1500 rpm, as this was the moment that was most ambiguous when analysing the NO<sub>x</sub> emissions.

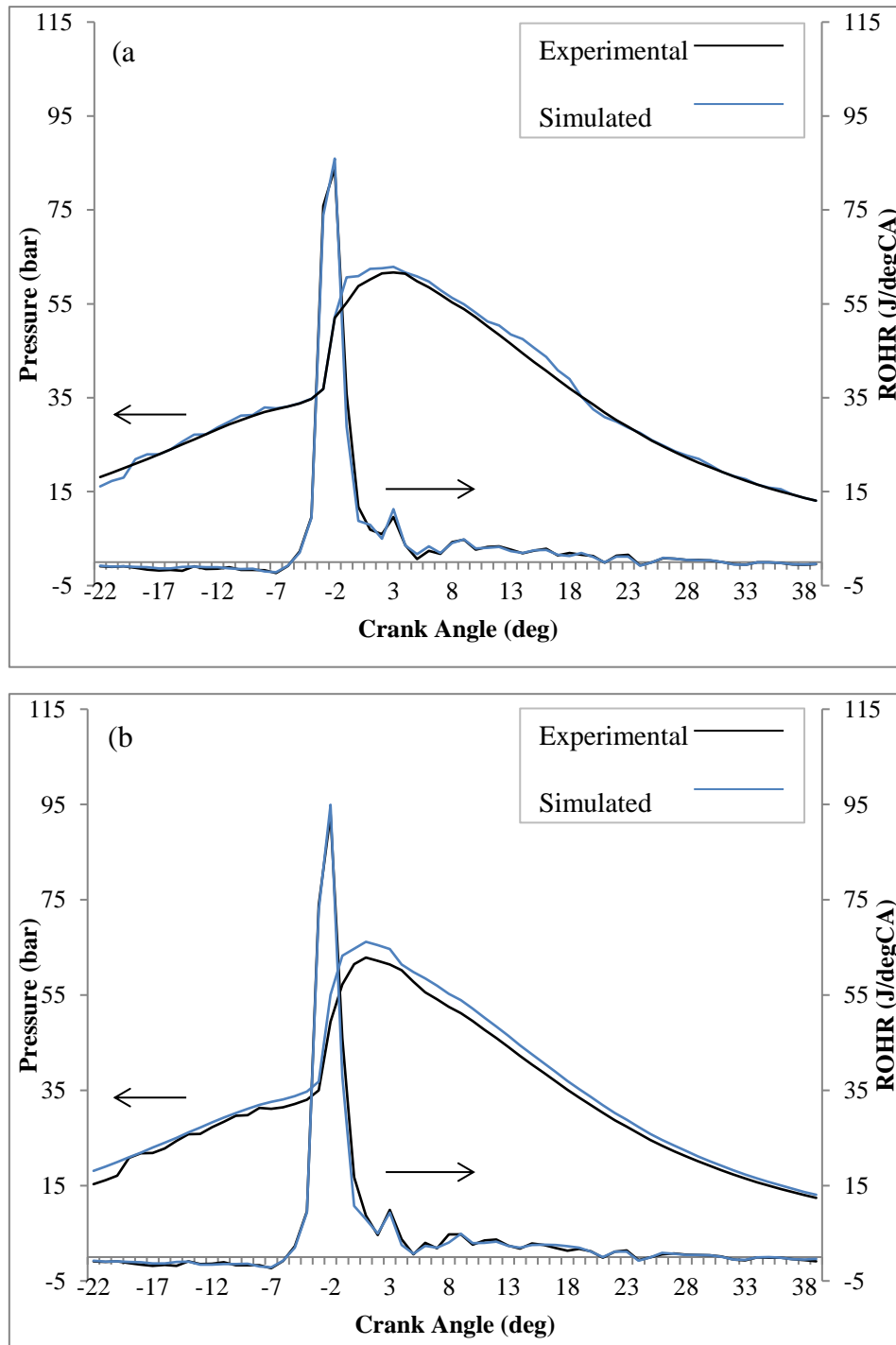
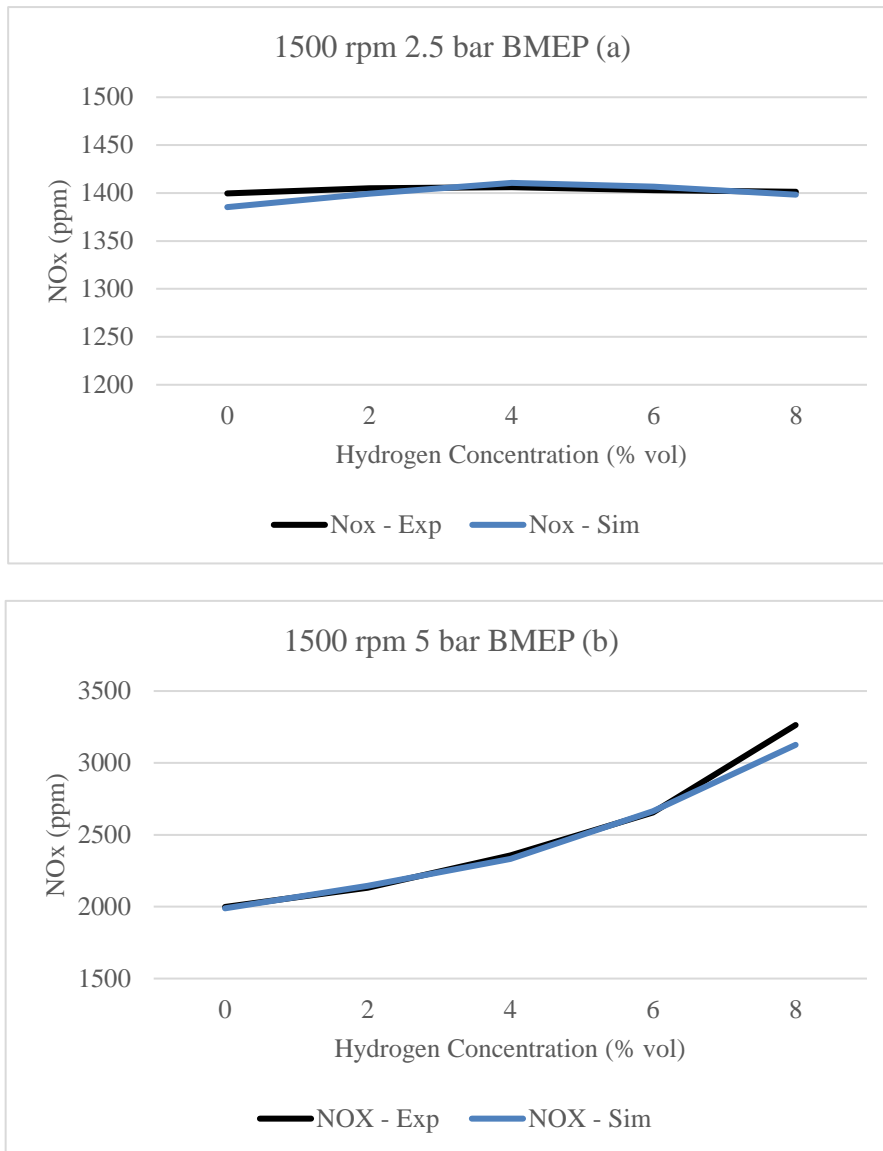


Figure 40: Comparison of pressure and heat release rate between simulated and experimental data at 1500 rpm, load (a) 2.5 bar and (b) 5 bar BMEP, 4% hydrogen concentration, SOI 9 CAD BTDC

When studying the pictures there are some obvious changes in the data and how accurate the simulations are in comparison to the experimental data. For example, in figure 40(a), it is clear that the simulated data is very closely matched with the experimental data. The greatest changes occurred during medium-load operation. This could be due to the ignition mechanics of the software which in some cases does not take into account environmental differences and fluctuations such as humidity and changing air temperature. In figure 40(b), the pressure was slightly lower than the experimental tests during the ignition stage. Again, this could be due to the combustion mechanics of the software. It could also have arisen from slight discrepancies in the hydrogen gas as the simulation again does not take into account the impact of the weather on the hydrogen gas where the experimental hydrogen was stored outside of the test cell. The heat release rate was much more stable throughout the simulation tests as can be seen in both figures. Ultimately, the difference in data values between the experimental and simulated data was ranging from 98-93%.

### **5.3.2 Comparison of NO<sub>x</sub> between Experimental and Simulated Data**

The importance of analysing NO<sub>x</sub> emissions cannot be overstated as many manufacturers are aiming to meet the ever-decreasing limits being set by governments and emissions regulators around the world. As discussed in the previous chapter, NO<sub>x</sub> is dependent on various factors, all of which can be analysed via simulation. This analysis can allow engine testers and manufacturers to fine-tune designs and operating conditions to achieve the lowest NO<sub>x</sub> emission at a much quicker rate than by using experimental methods. Below are the comparisons of the simulated and experimental data for the NO<sub>x</sub> emissions, where again the selected experimental data to compare to was based on the operating conditions which proved the most repeatable during the experiments. These conditions were at 1500-2500 rpm, 2.5-5 bar BMEP and SOI 9 CAD BTDC.



**Figure 41: Comparison of NOx between experimental and simulated data**

The immediate observation that can be made with figure 41 is that the accuracy is relatively close between the experimental and simulated data. Here the trends follow the expected trends seen in literature [50]. As the concentration of hydrogen increases, the quantity of NOx emissions increases at higher loads. At lower loads, the NOx does not appear to be affected, and in this case, displays a slight drop in emissions.

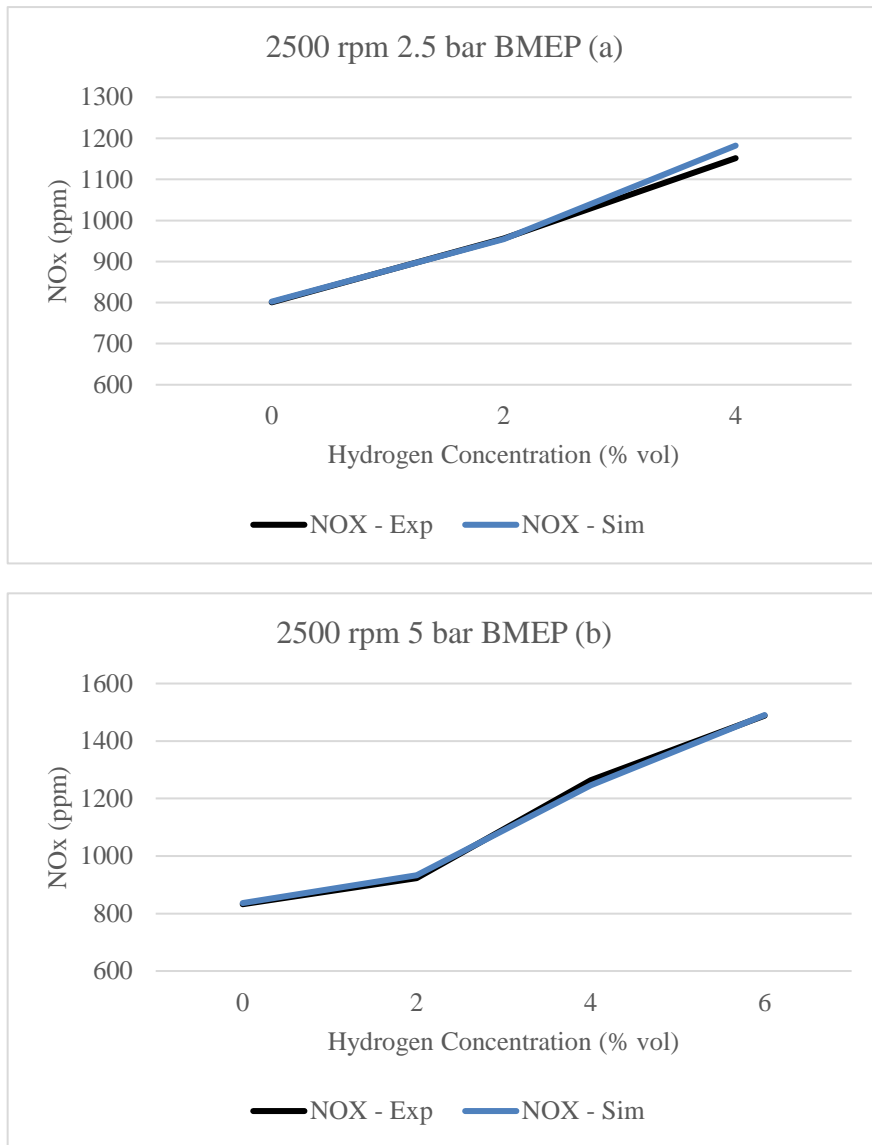


**Figure 42: Comparison of NOx and Smoke emissions between experimental and simulated data**

Looking at figure 42, again the level of accuracy between the simulated and experimental data is relatively high. For the NOx emissions, the general consensus is that the trend was maintained throughout the simulation tests. As with the in-cylinder pressure and the heat release rates, the accuracy was calculated to be roughly an average of 94%. The accuracy could be affected because of the lack of environmental input that is able to be simulated in the software, which could help bring the data closer to the experimental findings.

### 5.3.3 Comparison of CO Emissions between Experimental and Simulated Data

As was discovered in chapter 4, CI engines are known to produce lower CO emissions in comparison to SI engines because of their leaner operating conditions. This trend was found to be true also during simulation. The measurement and analysis of CO emissions is incredibly important because, like NO<sub>x</sub> emissions, CO emissions can be poisonous to the human health if inhaled directly into the lungs or under sustained exposure. Thus, the regulations revolving around CO emissions have become stricter in order to combat this.

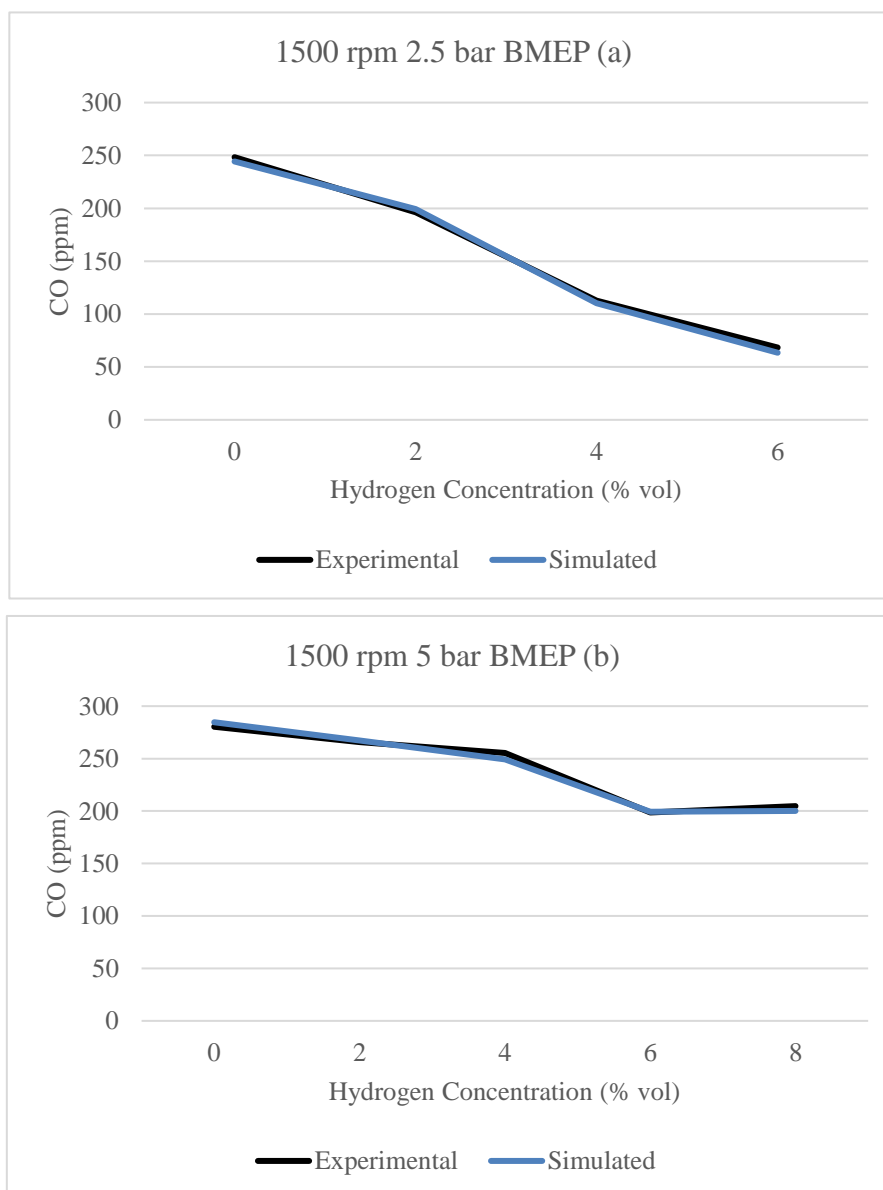


**Figure 43: Comparison of CO emissions between experimental and Simulated Data**

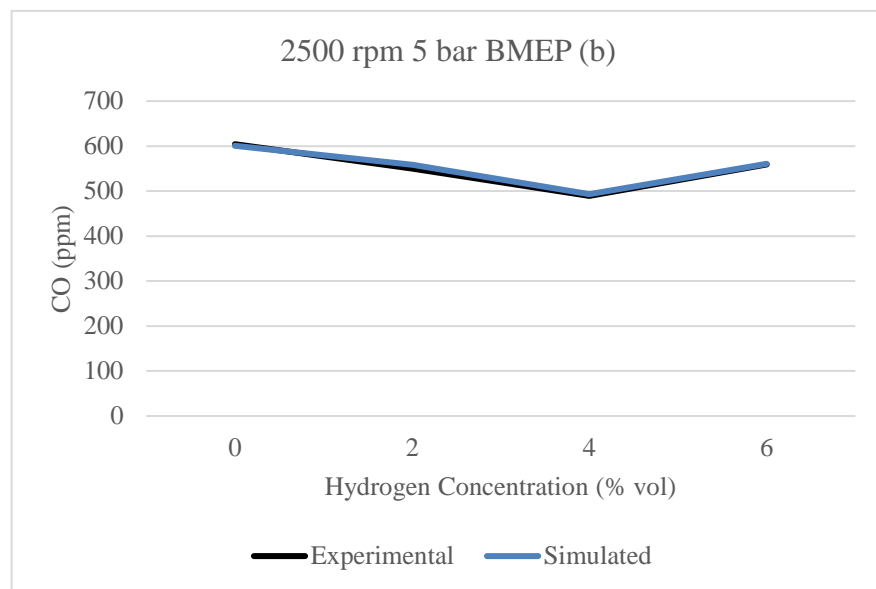
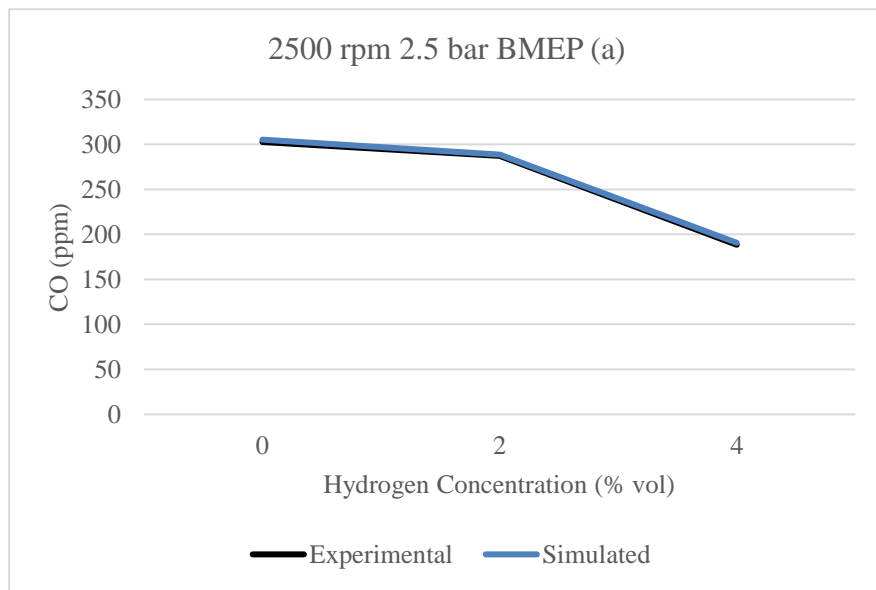


**Figure 44: Comparison of CO emissions between experimental and simulated data**

Figure 43 presents the data collected at low-speed and –load conditions, where the selection of experimental data was made consistent with the previous data (SOI 9 CAD BTDC). At low-speed low-load, the trend for the simulated data is very similar to that of the experimental data.

Figure 44 shows varying trends of CO emissions based on the hydrogen concentration admitted. The difference in trend could be attributed to the instability of combustion as a result of the lower oxygen concentration and diesel fuel when using higher concentrations of hydrogen.

With regards to the simulation accuracy, Figure 44 displays the same level of accuracy for the high-speed medium load runs. What can be deduced from running at these conditions testing for CO emissions is that the simulation software tends to follow the trends set from the experimentations and literature well and produces repeatable results with respect to the CO emissions. The accuracy of the simulated data was calculated to average roughly 95%.

#### 5.3.4 Comparison of THC Emissions between Experimental and Simulated Data

The study of THC emissions can allow manufacturers to gain a deeper understanding of the combustion mechanics and efficiency of the fuels and engines being developed. Poor combustion can lead to excessive THC emissions, appearing in varying formats such as NMHC and UHC which were discussed in chapter 4 that can be harmful to both the environment and human health. It was observed in chapter 4 that when using hydrogen during diesel combustion, the THC emissions appeared to fluctuate depending on the condition they operated at. The general trend was that under low-loads, the THC was reducing when hydrogen was admitted and at medium-loads the emissions increasing. This was found to be attributed to the increase in in-cylinder pressures. The optimum condition was found to be at high-speed medium-load conditions which produced the lowest THC emissions.

The simulated data selected was again based on the previous selections of using the same running conditions and being kept constant at SOI 9 CAD BTDC. The results for the THC emissions are displayed below.

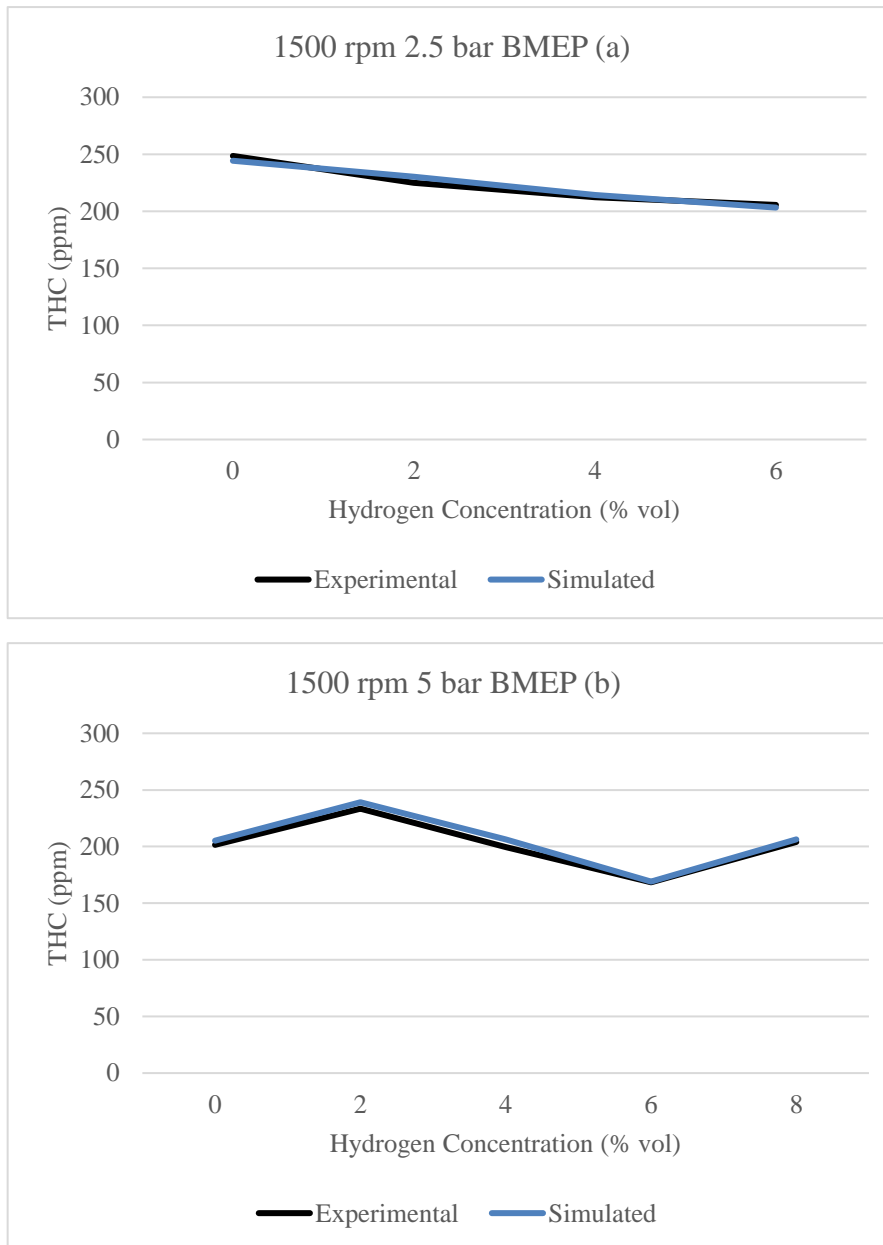


**Figure 45: Comparison of THC emissions between experimental and simulated**

For the low-speed operating conditions, the simulated data showed very similar trends and results to the experimental data. For the medium-load condition, there was a similar increase of THC emissions beyond 6% hydrogen concentration. There is a slight increase in THC emissions of the simulated data when compared with the experimental data between 2-6% concentration of hydrogen admission, however apart from that, the accuracy was relatively high in most cases.

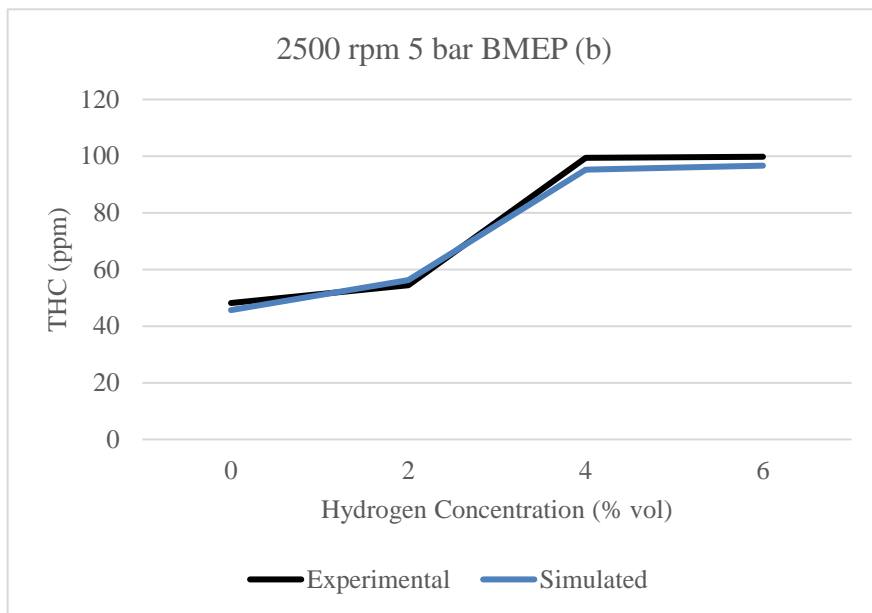
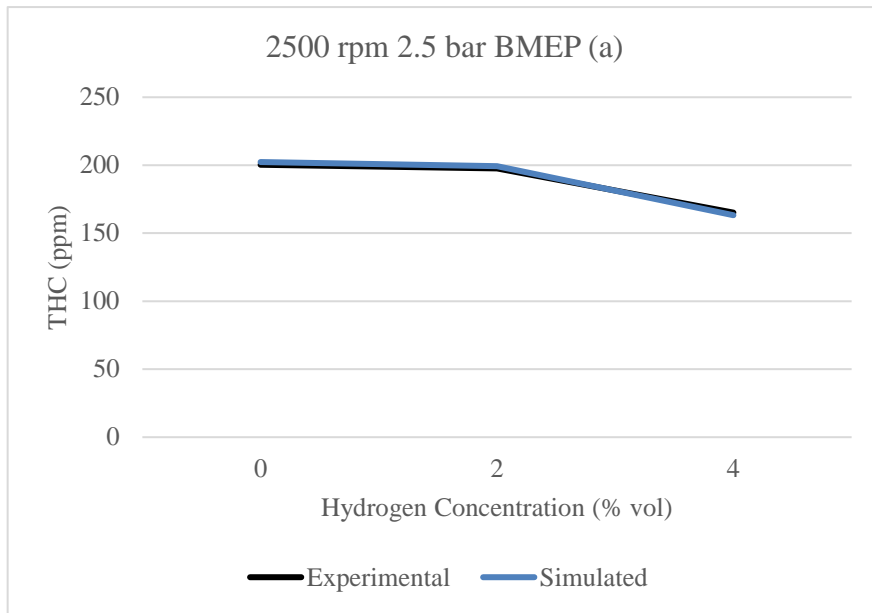


**Figure 46: Comparison of THC emissions between Experimental and Simulated data**

A similar trend is seen in figure 46 which displays the results for the high-speed runs at both low and medium loads. For figure 46(a), the trend is very similar with a high accuracy, which is promising. The accuracy is slightly less for the medium-load conditions whereby the THC emissions seemed to drop slightly more during the simulated runs in comparison to the experimental data. Overall, the calculated accuracy of the simulated THC emissions with respect to the experimental data is roughly 95.5%.

## 5.4 Summary

In this chapter the effects of hydrogen addition to an HSDI CI engine on the in-cylinder pressure and heat release rates, NO<sub>x</sub>, CO, and THC emissions were carried out using Ricardo Wave engine simulation software via 1-D simulation. These results were then compared to experimental data collected based on similar running conditions and operating parameters. The findings comparing the simulated and experimental data are summarised below:

- The overall majority of the conditions that were simulated with hydrogen admission displayed consistent trends based on experimental data and literature [50]. The accuracy was found to be affected during the simulations due to the fact that the effect of external weather and environmental conditions are unable to be simulated on the fuels and engine which meant that in some cases, the combustion mechanics did not mimic the experimental tests.
- The pressure and heat release rate simulations were consistent with the experimental data collected and showed similar trends. There were some irregularities which was assumed to be due to the inability to simulate environmental conditions on the fuels used. Here the accuracy was calculated to be around 98-93%, with the more accurate data being collected at the start of the combustion process.
- The NO<sub>x</sub> emissions were found to increase as the hydrogen concentration increased whilst reducing the smoke emissions during the simulations. This is in keeping with what was found during the experimental tests. The accuracy was calculated to be 94%.
- The CO emissions were reduced with the increasing admission of hydrogen concentration due to the carbon-hydrogen ratio being reduced. The simulations here were accurate as well displaying average accuracy figures of 95%.

- The THC emissions were generally decreasing as the hydrogen concentration increased. The low-load conditions appeared to produce this particular trend more regularly. The high-speed medium-load condition however produced the lowest THC emissions. The simulations displayed very similar results throughout and it was found that the simulations had an accuracy of around 95.5%.

## Chapter 6

# Studying the Effects of Hydrogen Addition on a Single-Cylinder Diesel Engine Using Ricardo Wave® Simulation Software

## Chapter 6

### Studying the Effects of Hydrogen Addition on a Single-Cylinder Diesel Engine Using Ricardo Wave® Simulation Software

#### 6.1 Introduction

Current legislations and market trends have slowly been directed towards the use of smaller, cleaner, and more efficient engines for passenger vehicles. With the increase in awareness of public health and environmental impact, the need for cleaner and more efficient engines has become more of a necessity as opposed to a choice that is made by manufacturers. One economically efficient way of achieving the stricter emissions targets set by governments is by producing smaller engines. Currently, the market share growth for down-sized engines over the last 6 years is roughly 6.5%, with a further 6.8% growth from 2019 and onwards [95]. Down-sized engines are becoming more popular due to the flexibility of operating as mild or full hybrid vehicles, which allow manufacturers to meet the legislations set in an easier fashion.

Despite the popularity of down-sized engines, the use of smaller CI engines in a wider light-duty use has not been extensively explored. One of the more prominent reasons is the cost of maintenance for CI engines, which is inherently higher than SI engines due to the higher pressures and temperatures that they reach during combustion. Another reason is, which was explored in chapter 2, they produce relatively higher NO<sub>x</sub> emissions as standard than SI engines which makes them unpopular for light-duty use.

The reliance on CI engines for heavy-duty and stationary applications has led to extensive research efforts focusing on experimenting with single-cylinder diesel engines with varying combustion and fuelling strategies, where a variety of results have been posted. Welch et al [96], experimented with a single-cylinder diesel engine using hydrogen as a substitute fuel as

part of a single-fuel combustion mode. They displayed that when using hydrogen as a fuel, they obtained an up to 40% increase in brake power when compared with standard diesel combustion. They did also report that the combustion efficiency of the hydrogen-fuelled engine was 90% of the equivalent diesel-fuelled diesel engine but found that NO<sub>x</sub> emissions were slightly lower during hydrogen combustion than with diesel.

Pedrozo et al [97] experimented on a single-cylinder DI CI engine using ethanol as an ethanol-diesel dual-fuel combustion mode to analyse the effects on the harmful emissions produced. They reported that when using ethanol-diesel they were able to reduce the NO<sub>x</sub> emissions substantially along with the reduction in the well-to-wheels CO<sub>2</sub> emissions also. They also displayed a reduction in soot emissions.

Bajraktari et al [98] experimented on a single-cylinder Yanmar CI engine using a dual-fuel combustion mode with diesel and propane gas. They reported a significant drop in the smoke emissions produced when operating under dual-fuel mode; however, they reported that there was an increase under higher loads of NO<sub>x</sub> and CO<sub>2</sub> emissions.

It is clear that there is definite scope with experimenting with smaller diesel engines, as the reliance of diesel outside of the down-sized gasoline and hybrid powertrains still remains relatively high. To truly expand the understanding of small diesel engines, testing the engines via simulation may provide the greatest flexibility in terms of analysis. For this reason, a model was designed and tested using Ricardo Wave® software to analyse the harmful emissions that can be produced in order to prolong the use of small diesel engines in the light-duty market segment. Initially, this model was to be tested experimentally to have a basis with which to compare the simulation results, but due to time constraints, the simulations were carried out as a stand-alone test on smaller, down-sized diesel engines.

## 6.2 Methodology

A 1-D engine model was created on Ricardo WaveBuild® Ver. 2016.1 simulation software to analyse the effects of hydrogen addition on a single-cylinder engine in relation to the quantity

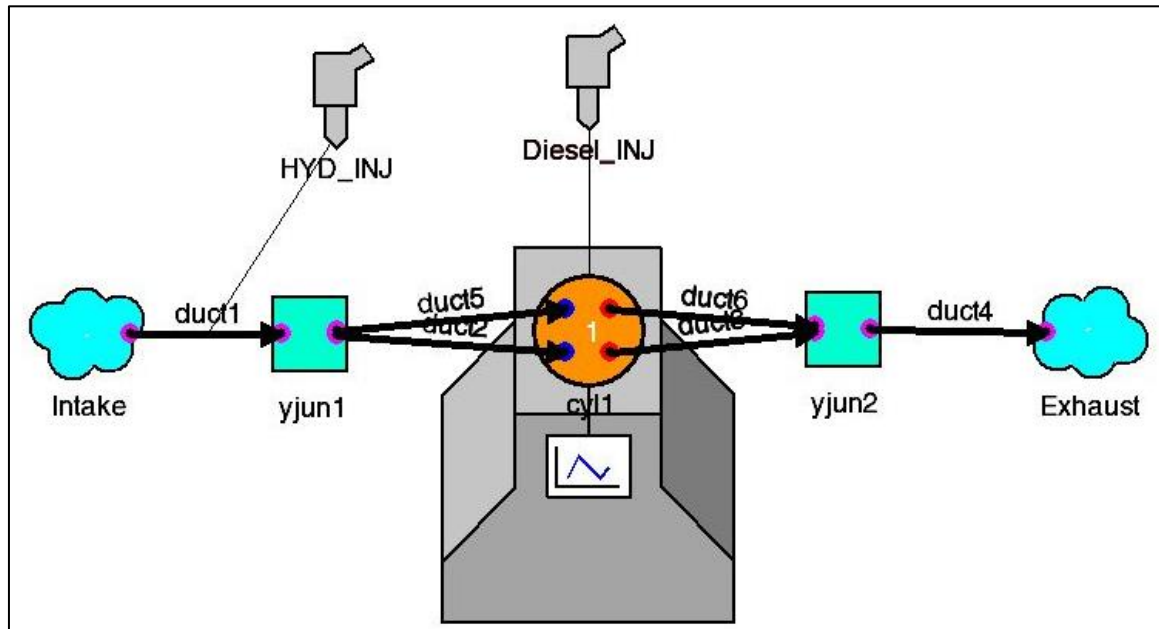


Figure 47: Screenshot of single-cylinder engine model

of hydrogen admitted into the intake. The software allows for intricate analysis of the thermodynamic reactions that occur during combustion, along with emissions measurement and analysis of engine performance.

Figure 35 shows a screenshot of the single-cylinder engine model that was modelled to analyse the effects of hydrogen addition on small CI engines. The geometry of the engine is based on the Yanmar L70N single-cylinder four-stroke diesel engine, with slight adjustments that were needed to make the engine compatible and optimised for the purpose of the experiments. Specifically, two extra valves were added to the existing model to incorporate a better flow of the intake charge and subsequent exhaust charge. Otherwise, the geometry and build are largely similar to the specifications of the Yanmar engine. Table 11 shows the specifications of the Yanmar engine used, which were provided by the manufacturer.

<b>Specification</b>	<b>Value</b>
<b>Bore</b>	78 mm
<b>Stroke</b>	67 mm
<b>Displacement</b>	0.320 litres
<b>Cylinders</b>	1
<b>Cooling System</b>	Air
<b>Dimensions Length; Width; Height</b>	378; 422; 453 mm
<b>Maximum Output</b>	6.7hp @ 3600 rpm

**Table 11: Yanmar L70N specifications**

The diesel fuel was direct injected into the cylinder at different timings and the specifications of the diesel used were taken from the software database. The hydrogen data was not available in the software which meant it had to be manually inputted using external reference points. This data was the same data created and tested with in chapter 5.

The engine operating conditions were set by the user and were simulated to run for 48 cycles. The main parameters that were altered during the simulations were the load, engine speed, and injection timing. The simulation would run an extra cycle beyond the user set cycles should the convergence criteria be met before the end of the simulation, which was as the previous tests had been carried out in chapter 5.

A more detailed thermal network was used for the engine conduction sub-model which allowed for more intricate appreciation of the various engine components that are used during combustion. The intake and exhaust gas side surface temperatures were set to the default software values of 350 and 500 K respectively. The coolant temperature was set to a default value of 380 K, with the corresponding heat transfer coefficient taken from an example model of a multi-cylinder diesel engine within the simulation.

For the combustion mechanics, the process was defined based on the empirical functions which were found within the 1-D simulation code. These were similar to those obtained by Watson et al [99]. A combustion simulation was carried out initially before the admission of hydrogen to optimise the engine. This single-fuel combustion was based on the multi-component Wiebe combustion model. For the dual-fuel operation, a multi-component multi-fuel Wiebe combustion sub-model was used.

Similar to chapter 5, a two-zone cylinder thermodynamic state model was used. This allowed for the measurement of NO<sub>x</sub>, CO, and THC. These emissions were what were focused on primarily due to the importance of reducing them in current EU legislations.

### **6.3 Results and Discussions**

The results obtained from the simulations are presented in this section, with an emphasis placed specifically on the harmful emissions such as NO<sub>x</sub>, CO, and THC due to the importance in the current emissions tests and legislations in the EU. The data gained from the single-cylinder engine during dual-fuel operation with diesel-hydrogen combustion will be compared in some cases with the multi-cylinder diesel-hydrogen dual-fuel combustion to gain a deeper understanding of the difference of single- and multi-cylinder combustion. Additionally, due to the novelty of the engine itself, in that it has been designed and modified slightly with no real experimental counterpart, the data will be compared to similar single-engine experiments in literature to gauge the accuracy and reliability of the data. The simulations were carried out at low and high engine speeds of 1500 rpm and 2500 rpm respectively and at loads of 2.5 bar and 5 bar BMEP, simulating low and medium load driving conditions. The hydrogen concentration was swept from 2-8% of the intake charge and the SOI of diesel fuel was altered in a range of 3-12 CAD BTDC.

### 6.3.1 Effects of Diesel-Hydrogen Combustion on NOx

In previous chapters, it was established that NOx tends to be negatively affected when adding hydrogen to the intake. This trend is primarily due to the increased in-cylinder pressures and temperatures that are generated as a result of the diesel-hydrogen combustion. However, at specific conditions, the NOx increase is not as aggressive, and it is possible to lower the NOx emissions, whilst still increasing the concentration of hydrogen. Figure 48 displays the effects of hydrogen addition on a single-cylinder diesel engine.

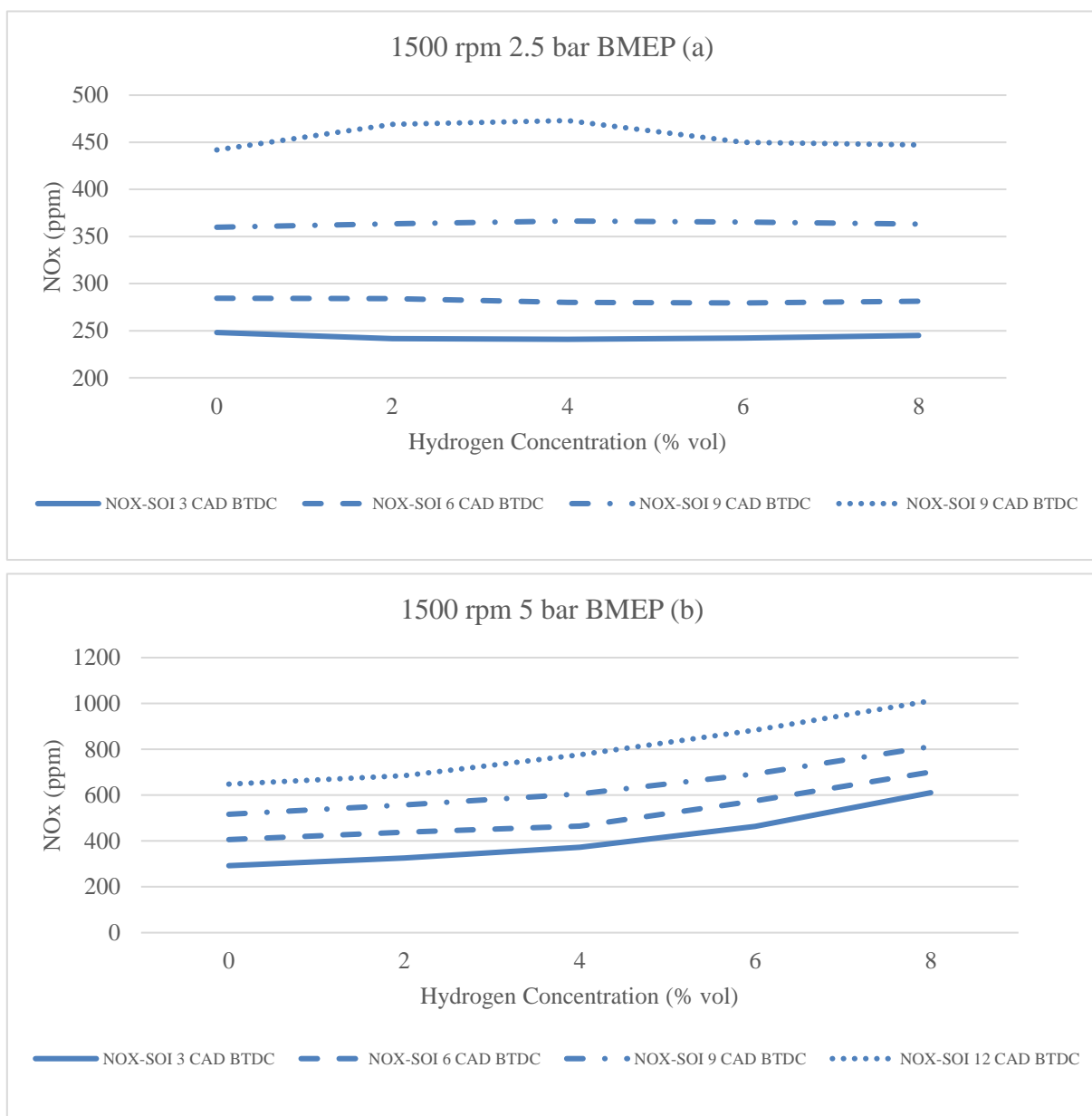


Figure 48: Effects of diesel-hydrogen Combustion on NOx emissions

At low speeds and loads, the NO<sub>x</sub> increase is not as prominent, in that the NO<sub>x</sub> emissions do not increase dramatically. As the diesel injection timing increases, the NO<sub>x</sub> emissions increase also, specifically at SOI 12 CAD BTDC. This could be due to the increased time that the intake charge has spent in the cylinder before combustion leading to slightly higher temperatures and thus eventually leading to increased NO<sub>x</sub> emissions.

Figure 48(b), displays a more prominent increase in NO<sub>x</sub> emissions. Also, it is clear that at higher loads, the NO<sub>x</sub> emissions generated are much higher, due to the increased operating pressure and temperature. Welch et al [96] displayed NO<sub>x</sub> emissions of roughly 850 ppm at SOI 6 CAD BTDC and 900 ppm at SOI 9 CAD BTDC whilst using hydrogen as a single-fuel combustion mode in a single cylinder engine. Therefore, the NO<sub>x</sub> emissions achieved from the simulation shows promise as it implies that even with the injection of diesel fuel the quantity of NO<sub>x</sub> produced has not been affected greatly.

Figure 49, represents the NO<sub>x</sub> emissions produced at high speeds. At the low-conditions, the formation of NO<sub>x</sub> is keeping within the trend displayed in earlier results in that as the hydrogen concentration increases, the quantity of NO<sub>x</sub> increases. It is also interesting to see that the reduced residence time of operating at higher speeds still has the desired effect by lowering the base amount of NO<sub>x</sub> emissions, as it did in the experimental tests.

Figure 49(b), displays a very aggressive increase in the NO<sub>x</sub> emissions when increasing the hydrogen concentration. The higher loads and speeds lead to an increase in the in-cylinder pressures and thus temperatures, which as discussed earlier, is fundamental in NO<sub>x</sub> formation. Although, the higher speeds do not result in higher net NO<sub>x</sub> emissions, when compared to figure 48(b), due to the reduced residence times.

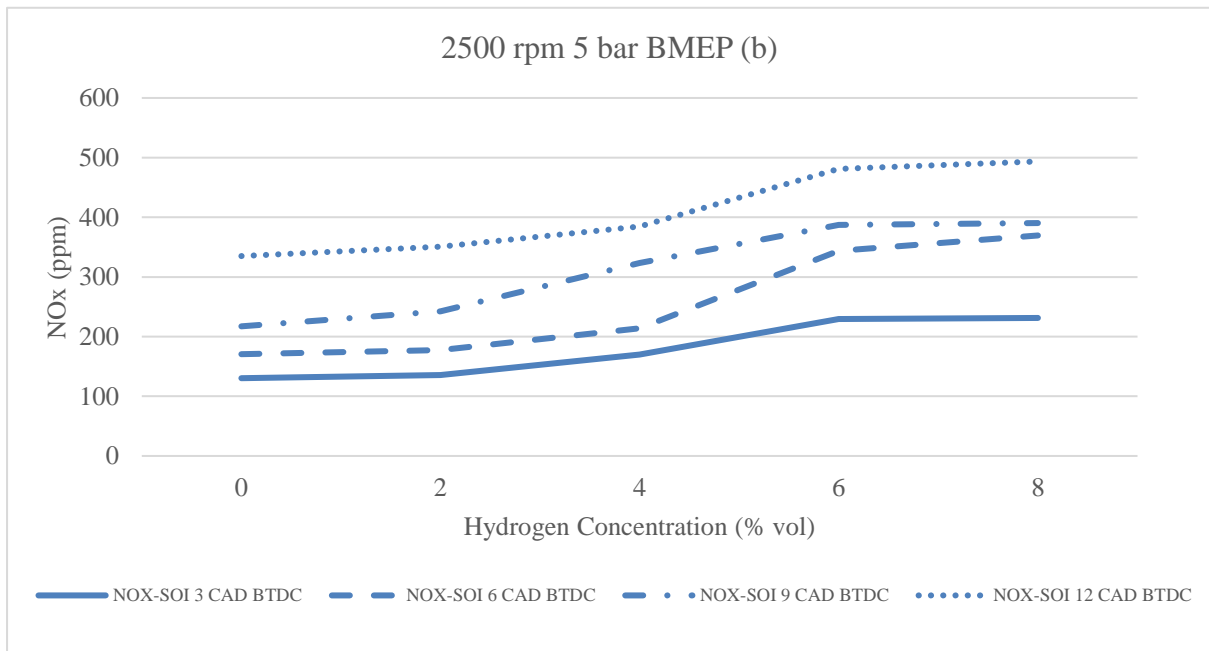
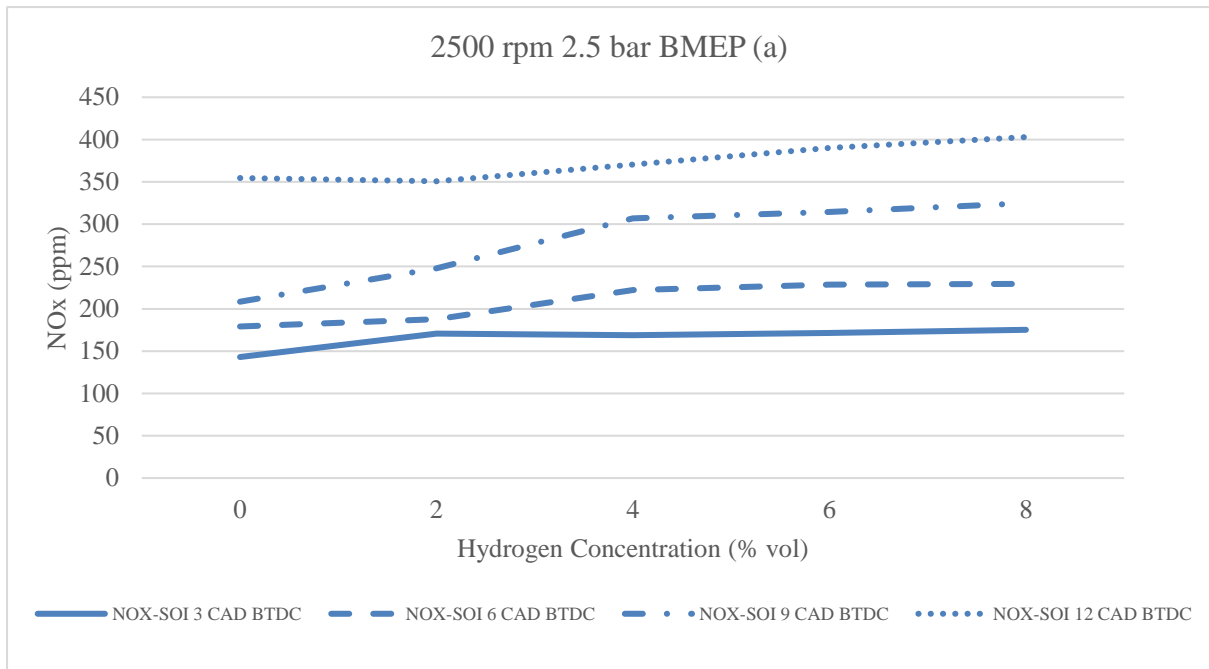


Figure 49: Effects of diesel-hydrogen on NOx emissions

### 6.3.2 Effect of Diesel-Hydrogen combustion on CO emissions

CO emissions are widely known to be harmful and any effort to reduce them is attempted specifically with passenger vehicles. Due to the nature of diesel combustion, CI engines

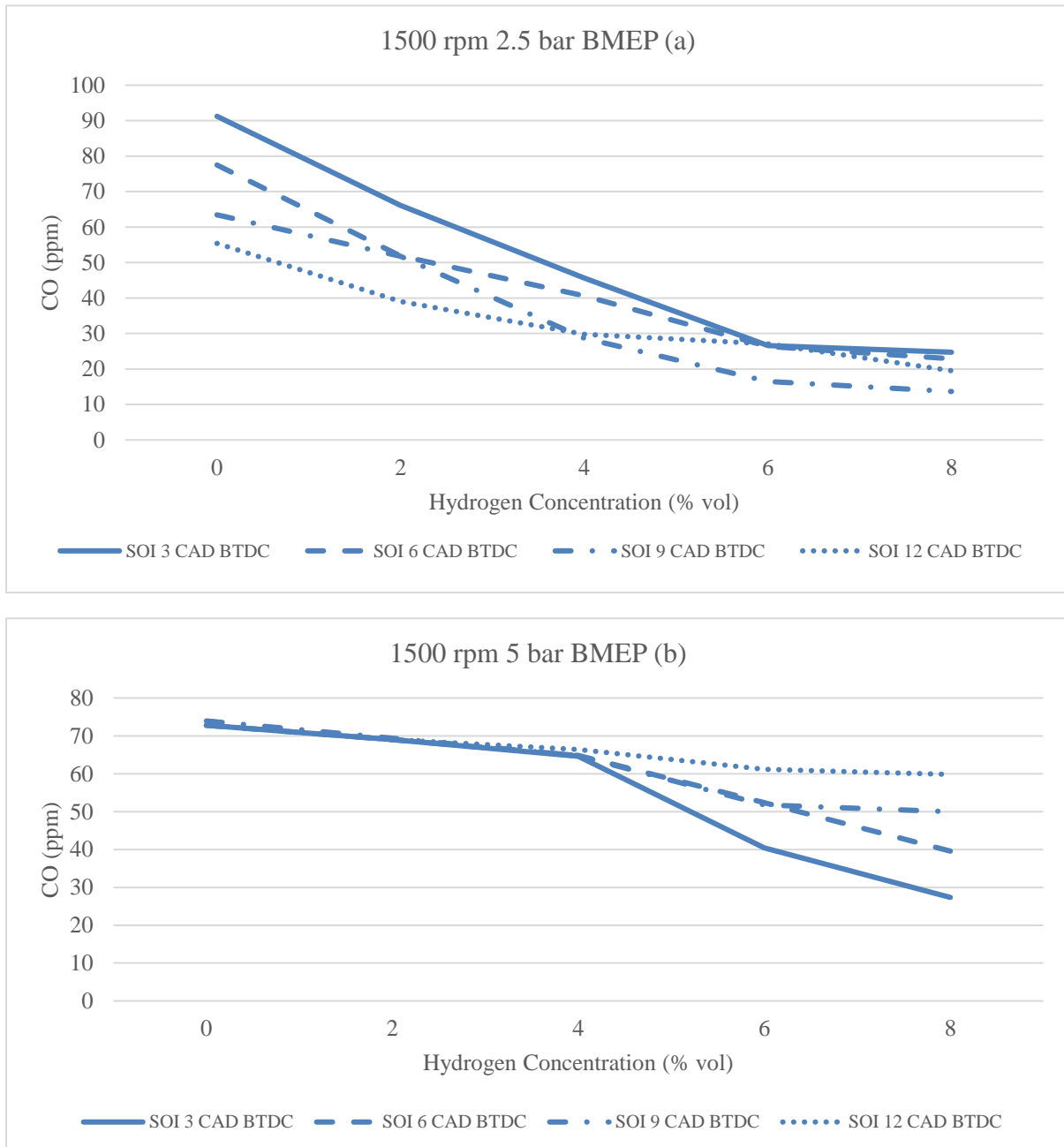
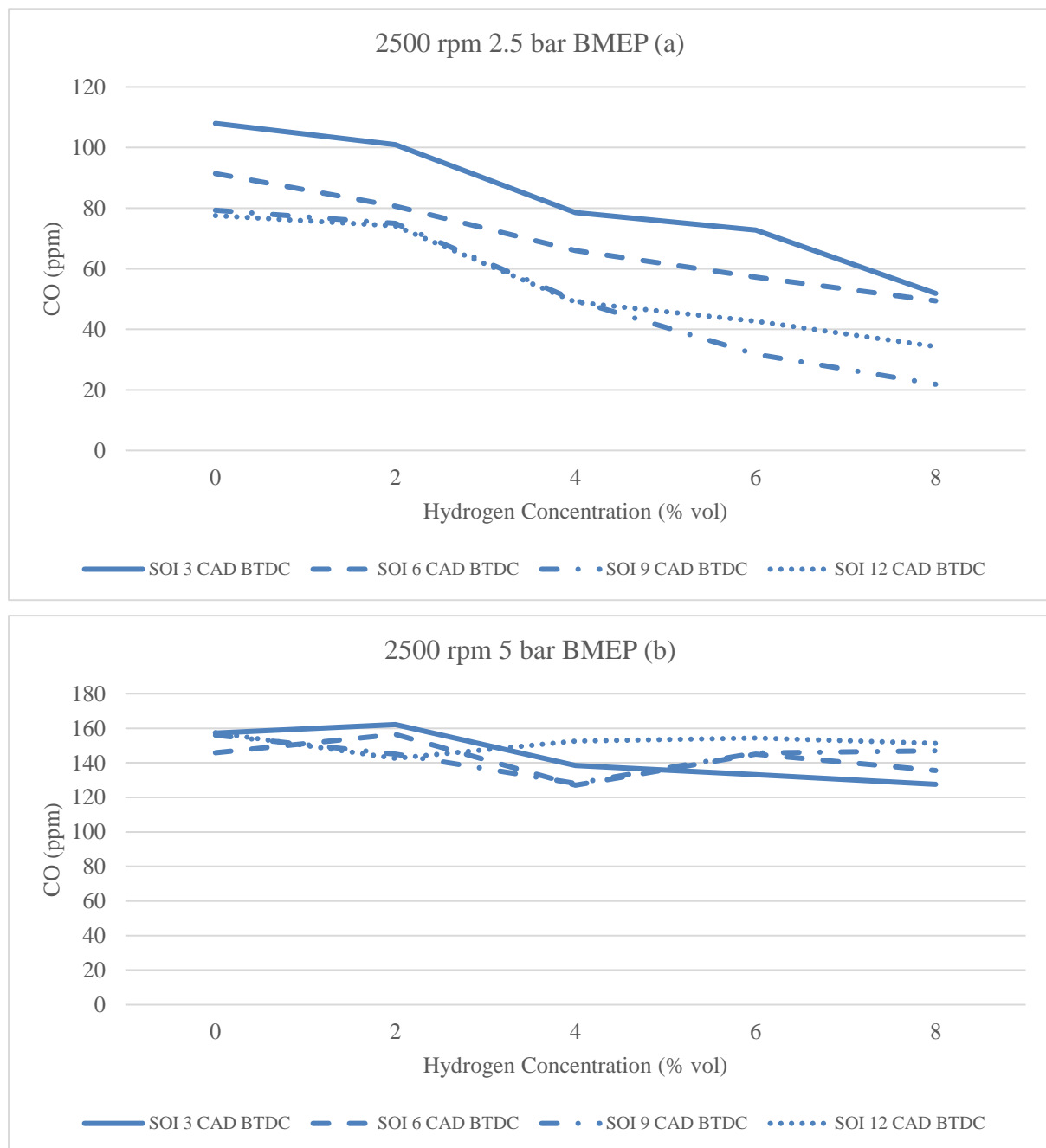


Figure 50: Effect of diesel-hydrogen combustion on CO emissions

usually exhibit low CO emissions, a trend that was visible in the previous chapters. In this case, there is no major convergence from this as the single-cylinder simulation displays, generally similar patterns.

Figure 50 displays the CO emissions produced during the low-speed operation modes. The single-cylinder simulation shows promising levels of CO emissions which reduced as the hydrogen concentration increased. This reduction could likely be attributed to the reduction in carbon-based products post-combustion. The most notable points to mention would be when the SOI exceeded 6 CAD BTDC and at hydrogen concentration levels of 6% and above, where the reduction in CO is not as dramatic as the other operating conditions. This



**Figure 51: Effects of diesel-hydrogen combustion on CO emissions**

may be due to temperature changes, where it has been recorded that lower combustion temperatures contribute to lower CO emissions [100].

In figure 51, the CO emissions originally started off higher in relation to the low-speed runs seen in figure 50. As discussed earlier, the higher temperatures achieved at these conditions could be the primary cause of this elevation. However, with hydrogen admission, the quantity of CO dropped and thus remained within the trend set in previous cases. At low loads, the CO emission reduction was much more substantial, whereas at high loads, the reduction was not. This occurred as a result of the reduction in oxygen when operating in a much richer condition under medium loads [101].

### **6.3.3 Effect of Diesel-Hydrogen Combustion on THC Emissions**

Measuring the THC emissions is not only beneficial to prevent over-exposure to the public and the environment, but also to analyse the efficiency of the combustion process, where the poorer and less efficient the combustion is, the more THC emissions are produced. In previous chapters, it was discovered that the correlation between the THC emissions and the hydrogen concentration was somewhat irregular in that certain conditions could either increase or decrease the THC emissions.

Despite the inconsistency of the trends, there was a clear pattern noticed during the multi-cylinder tests where at lower loads, the THC emissions reduced. For the simulated single-cylinder cases, it is seen that this trend seems to follow a similar pattern. Figure 52 displays the data obtained at low speeds and the trend here is seen clearly in figure 52(a), which is at low-speed low-load. The later injection timing appears to be the only discrepancy as the THC emissions increase as the hydrogen concentration increases beyond 4%.

Figure 52(b), shows a more sporadic change in THC emissions as the concentration of hydrogen increases. Again, beyond 4% concentration, the overall trend points towards an

increase in THC emissions, despite what some reports suggest whereby the admission of hydrogen is found to not have a detrimental effect on THC emissions [102, 27].

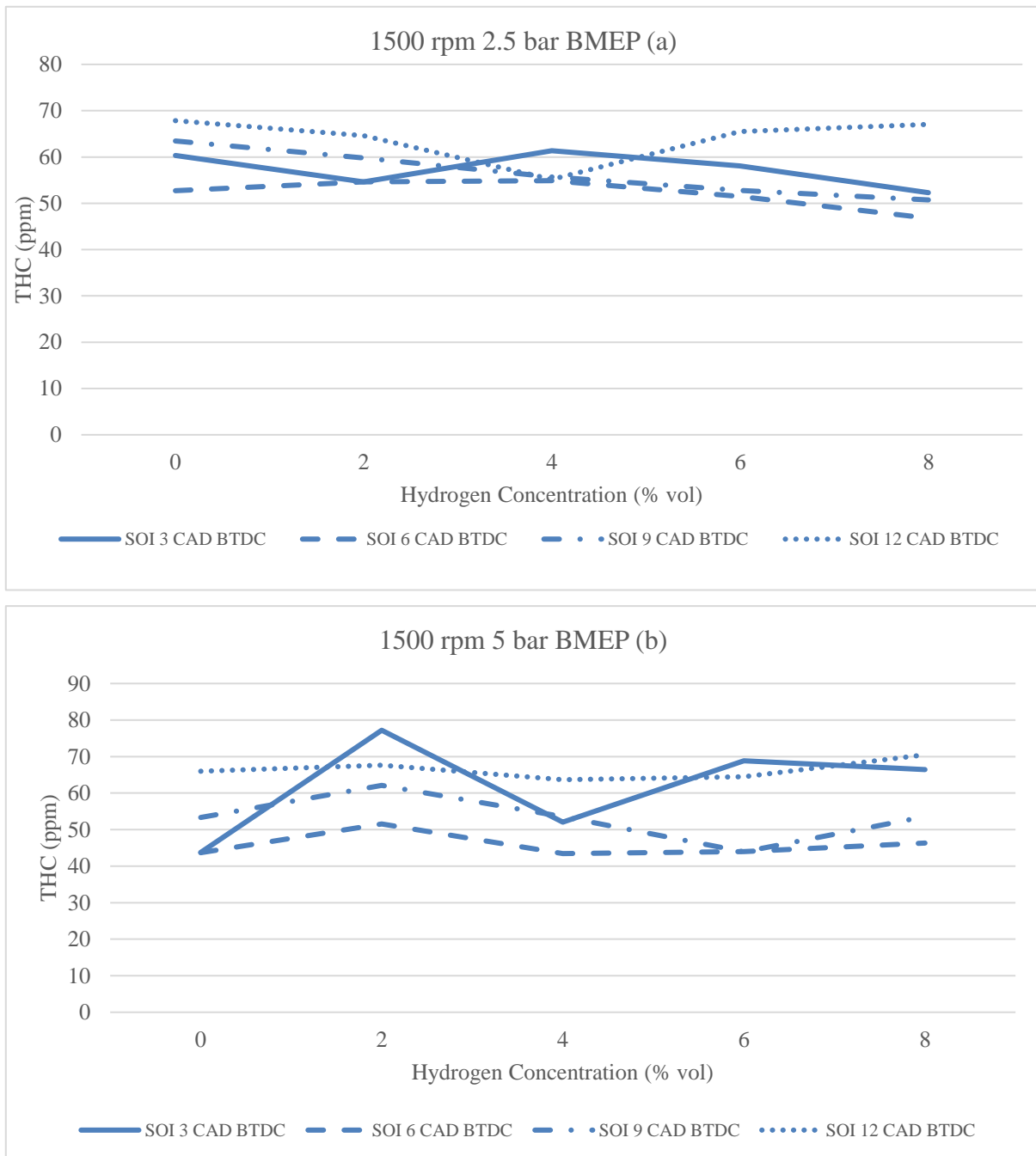


**Figure 52: Effect of diesel-hydrogen combustion on THC emissions**

Figure 53 follows the trend seen in figure 52 in that advancing the injection timing, the THC emissions at when higher hydrogen concentrations were used increased. This was found to be as a result of deeper penetration of the spray tip resulting in spray wall interference. The more interesting point to note is figure 52(a) where beyond 4% hydrogen concentration, the THC

emissions appear to be increasing. This could be as a result of the spray wall interference which was mentioned earlier.

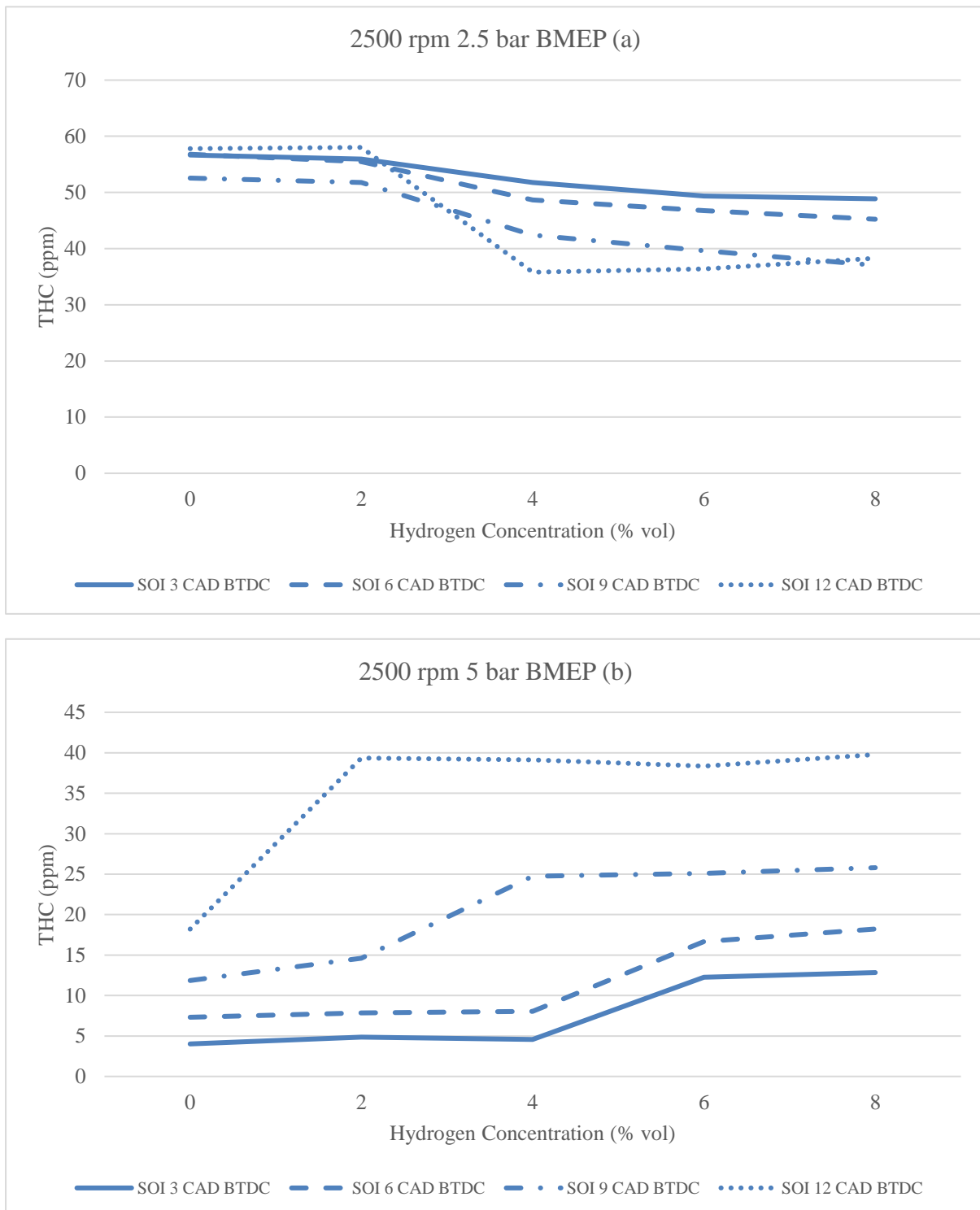


**Figure 53: Effects of Diesel-Hydrogen combustion on THC emissions**

## 6.4 Summary

A single-cylinder CI engine was modelled and simulated on Ricardo Wave® using a dual-fuel diesel-hydrogen combustion model which simulated hydrogen being admitted into the intake port in 2% increments from 2-8% of the intake charge at varying loads, speeds, and injection timings. The harmful emissions produced, most notably the NO<sub>x</sub>, CO, and THC emissions were measured with the objective of attempting to analyse smaller diesel engines for use in light-duty applications. The findings of these simulations are summarised below:

- Enrichment of the intake air with hydrogen led to an increase in NO<sub>x</sub> emissions at most of the operating conditions simulated at. The smoke emissions however were reduced as the concentration of hydrogen increased.
- At low speeds and medium loads, the increase of the NO<sub>x</sub> emissions was found to be relatively large, whereby NO<sub>x</sub> would increase substantially beyond 6 % hydrogen concentration.
- The single-cylinder produced comparable values of NO<sub>x</sub> emissions when compared to other experimental work and literature using similar equipment.
- CO emissions were low to begin with, as they are in most CI engines due to the lean combustion, were reduced further with hydrogen admission. At higher loads and beyond SOI 6 CAD BTDC and 6% hydrogen concentration, the reduction of CO emissions was not as substantial, in comparison to the other operating conditions. This could be because of the higher temperatures at higher loads.

- The THC emissions showed slight inconsistencies with the admission of hydrogen. Depending on the operating condition, the THC was found to be increasing. This was more the case when operating at higher loads. This was due to the spray tip penetrating deeper into the intake charge resulting in spray wall interference. At low loads, the THC emissions were relatively low and followed trends set in previous experimental data and literature.

# Chapter 7

## Conclusions and Recommendations for Future Work

## Chapter 7

### Conclusions and Recommendations for Future Work

#### 7.1 Conclusions

This chapter will summarise the key findings of the diesel-hydrogen dual-fuel combustion in an HSDI multi-cylinder and single-cylinder diesel engine using both experimental and simulated data.

##### 7.1.1 Effects of Combined Diesel-Hydrogen Combustion on Combustion Properties

This chapter investigated the effects of combined diesel-hydrogen combustion on a Ford Puma 2.0L HSDI engine, where the hydrogen was admitted via the intake manifold in 2% increments from 0-8% of the total volume of intake air. The engine's combustion characteristics and emissions were analysed.

It was found that the smoke emissions were reduced, whilst the NO<sub>x</sub> emissions increased when replacing a percentage of the intake charge with hydrogen. This was found to be as a result of the lower carbon content in the cylinder and the increase in combustion temperatures achieved when using hydrogen respectively. At low speed and low loads, the NO<sub>x</sub> emissions were largely unaffected. At higher engine speeds however, the NO<sub>x</sub> emissions were lower as a result of the reduced residence times.

By advancing the diesel injection timing, the THC emissions were found to have increased as a result of the lower charge density. This reduction in charge density lead to interference in the spray wall. The trends seemed to vary with varying hydrogen enrichment and operating conditions despite hydrogen combustion not producing THC emissions.

CO emissions were reduced substantially during certain conditions as a result of the reduction in the carbon content of the combustible charge within the cylinder. There were some

increases in CO emissions which could be due to some diesel misfires leading to combustion instability as a result of the lack of oxygen and diesel fuel when part substituted with hydrogen.

The combustion efficiency of hydrogen was also analysed and was found to be extremely efficient at all hydrogen concentrations and operating conditions, which increased as the speed, load, and hydrogen concentration increased.

Ultimately, the results displayed in this chapter show that with the part substitution of hydrogen with the intake charge, lower NO<sub>x</sub>, THC, CO, and smoke emissions can be achieved reliably whilst exhibiting a very efficient combustion of hydrogen.

### **7.1.2 Comparison between Simulated and Experimental Diesel-Hydrogen Combustion**

Chapter 5 looked at the use of Ricardo WAVE to compare the effects of combined diesel-hydrogen combustion between engine simulation software and experimental data. The experimental data used was that of the previous chapter. Ricardo WAVE was used to replicate the same Ford Puma 2.0L HSDI engine with the same characteristics and operating conditions as the experimental engine. The simulations also used the same testing procedures to maintain continuity between the two tests. The emissions and combustion performance of the engine was compared using the data collected at SOI 9 CAD.

When looking at the pressure and heat release rate, it was observed that there was a 93-98% accuracy rating. The lack of weather and environment simulation ability within the software may have had an effect on the fluctuation in accuracy levels. Despite this, the simulations behaved similarly to that of the experimental data collected.

The NO<sub>x</sub> emissions followed the same trends as those observed from the experimental data, showing promising levels of accuracy at around 94%. The trends showed that when

increasing the hydrogen concentration, the NO<sub>x</sub> emissions increased as a result of the higher combustion temperatures achieved. At low speeds and loads however, the NO<sub>x</sub> remained unchanged. At higher speeds, NO<sub>x</sub> emissions were found to be reduced in comparison to lower speeds due to the reduction in residence times.

The CO emissions also displayed similar trends to that of the experimental data with high levels of accuracy. Here, as the hydrogen concentration increased, the CO emissions decreased as a result of the lower oxygen concentration and diesel fuel, which is as expected. There were some fluctuations with the trends as it was also observed that the CO increased slightly at certain hydrogen concentrations which could be as a result of the slightly less stable combustion due to hydrogen admission. The accuracy achieved was found to be around 95%. THC emissions were analysed and were found to behave similarly to the experimental data. The accuracy again was relatively high at around 95.5%.

Ultimately, the simulation was very accurate; however, the changes that occurred could be the result of various factors. The first already being mentioned above with the lack of weather simulation on the bottled gas. Another is the fact that the hydrogen specification was entered manually and so will not behave exactly like the bottled hydrogen used for the experiments. Lastly, the experimental engine operates within a test cell which experiences certain environmental conditions that the simulation does not yet have the capability to fully model.

The key benefits that could arise because of this research are that it will allow greater confidence to be placed in simulation work and with advancing technology, the quality of simulation can improve dramatically to accommodate various parameters giving researchers valuable tools to conduct engine research and development.

### **7.1.3 Comparing Effects of Hydrogen Addition on a Single-Cylinder Diesel Engine between Simulated and Experimental Data**

The main purpose behind chapter 6 was to model and optimise a single-cylinder diesel engine running with a dual-fuel diesel-hydrogen combustion using Ricardo Wave® for investigating the uses of single-cylinder diesel engines in light-duty applications and how they can become more readily useable in smaller passenger vehicles or even, smaller stationery applications such as power generation. A comparison using an experimental engine was initially planned to supplement the findings of this chapter but unfortunately due to time constraints only the simulation work was carried out. The focus was on the harmful emissions produced and how they can be reduced.

The NO<sub>x</sub> emissions were found to have been increased when injecting hydrogen into the intake. At higher speeds, the lower residence time aided in preventing the formation of excessive NO<sub>x</sub> emissions. At low speeds and medium loads, the NO<sub>x</sub> increase was slightly more dramatic.

The CO emissions were low to begin with and were reduced further when admitting hydrogen as a result of the reduction in the carbon content in the combustion chamber. They still displayed some fluctuations as a result of the unstable nature of diesel-hydrogen combustion displayed in previous chapters.

The THC emissions were slightly less predictable, with some fluctuations in the quantity produced. At medium loads, the THC emissions increased as a result of the spray wall impingement with the less dense hydrogen-air mixture.

The single-cylinder model reacted well to the slight modifications made and was producing comparable results with other experimental work and literature. Overall, the research displayed positive results with regards to reducing the harmful emissions produced from diesel combustion. The findings of this chapter could pave the way for more research to be

carried out confidently on smaller diesel engines, and could allow for the possibility of using smaller diesel engines with cleaner combustion technology on a more wide-spread scale.

## **7.2 Recommendations for Future Work**

From the research carried out here, it is concluded that there is scope for future work regarding diesel-hydrogen combustion experimentally and simulated. They are as follows:

- The experiments can be performed on a turbocharged or other type of forced induction to evaluate the impact that forced induction has on the combustion process of diesel-hydrogen along with the emissions and engine performance.
- EGR can be employed as a larger part of the experiment, looking at the possible benefits the technique could bring to the combustion of diesel-hydrogen. As it was mentioned in previous chapters, the hydrogen could be produced on-board via exhaust gas reforming; therefore investigating a method of implementing this could provide an interesting insight.
- An investigation into the particulate matter size and distribution as a result of the diesel-hydrogen combustion.
- A potential topic could also be the impact of valve-timing on the combustion of diesel-hydrogen, and how the valves can affect the flow and movement of gases within the cylinder head. This coupled with the possible boosting techniques could allow for greater understanding of the flow mechanics of the charge within the cylinder.
- A 3-D simulation looking at the charge flow, and movement within the cylinder head could help shed more light on the combustion mechanics of diesel-hydrogen combustion.

- Investigate and optimise a diesel engine with dual-fuel via simulation to comply with current emissions tests which incorporate a more real-world driving dynamic to better represent the emissions produced from diesel-hydrogen combustion.
- Experimenting with other natural gases and fuels such as nitrogen, syngas, and ethanol as opposed to hydrogen to compare between diesel-hydrogen combustion and other methods as to which produces the least harmful emissions.

## References

- [1] Stone, R., Introduction to Internal Combustion Engines, Second Edition, MacMillan Press Ltd, ISBN 0-333-55084-6 Pbk, Basingstoke, Hampshire, 1992
- [2] (Smolinska J. EU economic report 2008 ACEA)
- [3] (Potter S. In: Hensher DA, Button KJ, editor. 'Transport energy and emissions: Urban public transport', chapter in 'Handbook of transport and the environment' Elsevier; 2003, ISBN 0-08-044103-3)
- [4] Ehsani M, Gao Y, Gay SE, Emadi A. Modern electric, hybrid electric, and fuel cell vehicles. Texas: CRC Press; 2005.
- [5] Chan CC, Chau KT. Modern electric vehicle technology. New York; Oxford University Press; 2001., the harmful pollutants produced are being scrutinised further still.
- [6] Bosch (2011). Automotive Handbook. 8th ed. Postfach, Plochingen: Robert Bosch Publishers. 403-418.
- [7] Beatrice, C., Belardini, P., Bertoli, C., Lisbona, M.G. and Sebastiano, G.M.R., 2002, Diesel Combustion Control in Common Rail Engines by New Injection Strategies, Int. J. Engine Res. Volume 3, No. 1, p23-36
- [8] Heywood JB. Internal combustion engine fundamentals. New York: McGraw-Hill;1988.
- [9] Zhao H., Peng Z., Ladommatos N., 2003, Understanding of controlled autoignition combustion in a four-stroke gasoline engine, Inst Mech Eng Part D J Automot Eng, 215:1297–310
- [10] Du X, Wu Y, Fu L, Wang S, Zhang S, Hao J. Intake fraction of PM<sub>2.5</sub> and NO<sub>x</sub> from vehicle emissions in Beijing based on personal exposure data. Atmos Environ 2012;57:233-43.
- [11] Payri F, Bermudez VR, Tormos B, Linares WG. Hydrocarbon emissions speciation in diesel and biodiesel exhausts. Atmos Environ 2009;43:1273-79.
- [12] Rohr AC, Wyzga RE. Attributing health effects to individual particulate matter constituents. Atmos Environ 2012;62:130-52.
- [13] Habib MA, Elshafei M, Dajani M. Influence of combustion parameters on NO<sub>x</sub> production in an industrial boiler. Comput Fluid 2008;37:12-23.

- [14] Twigg MV, Phillips PR. Cleaning the air we breathe - Controlling diesel particulate emissions from passenger cars. *Platinum Met Rev* 2009;5327-34.
- [15] Majewski A. Diesel particulate matter. 2002. Online Source: <http://www.dieselnet.com>. [Accessed 07 August 2018].
- [16] McEntee JC, Ogneva-Himmelberger Y. Diesel particulate matter, lung cancer, and asthma incidences along major traffic corridors in MA, USA: A GIS analysis. *Health Place* 2008;14:817–28.
- [17] Du CJ, Kittelson DB. Total cylinder sampling from a diesel engine: Part III – Particle measurements. SAE Paper; 1983. 830243.
- [18] Duggal V, Priede T, Khan I. A study of pollutant formation within the combustion space of a diesel engine. SAE Paper; 1978. 780227.
- [19] Chang YJ, Kobayashi H, Kaminoto T. A photographic study of soot formation and combustion in diesel flame with a rapid compression machine. *Proceedings of Comodia* 1985:149-57.
- [20] Raub JA, Mathieu-Nolf M, Hampson NB, Thom SR. Carbon monoxide poisoning - public health perspective. *Toxicology* 2000;145:1-14.
- [21] Kaur S, Nieuwenhuijsen MJ, Colville RN. Fine particulate matter and carbon monoxide exposure concentrations in urban street transport microenvironment. *Atmos Environ* 2007;41:4781-810.
- [22] Mendez S, Kashdan JT, Bruneaux G, Thirouard B, Vangraefschep F. Formation of unburned hydrocarbons in low temperature diesel combustion. SAE Paper; 2009. 2009-01 2729.
- [23] Greeves G, Khan IM, Wang CHT, Fenne I. Origins of hydrocarbon emissions from diesel engines. SAE Paper; 1977. 770259.
- [24] AA. (2017). Euro Emission Standards. Available: <https://www.theaa.com/driving-advice/fuels-environment/euro-emissions-standards>. Last accessed 9th August 2019.
- [25] Li CG, Mao F, Swartzmiller SB, Wallin SA, Ziebarth RR. Properties and performance of diesel particulate filters of an advanced ceramic material. SAE paper; 2004. 2004-01-0955.
- [26] Hemmings S, Megaritis A. Periodically regenerating diesel particulate filter with a hydrogen/carbon monoxide mixture addition. *Int J Hydrogen Energy* 2012;37:3573-84.

- [27] Christodoulou F. Hydrogen, nitrogen and syngas enriched diesel combustion. PhD Thesis, Brunel University, London 2014
- [28] Brogan MS, Clark AD, Brisley RJ. Recent progress in NOx trap technology. SAE paper; 1998. 980933.
- [29] Majewski WA. Dieselnets. 2007. Online Source: [www.dieselnets.com](http://www.dieselnets.com). [Accessed 08 2018].
- [30] Musculus MP, Miles PC, Pickett LM. Conceptual models for partially premixed low temperature diesel combustion. *Prog Energ Combust* 2013;39:246-83.
- [31] Dec JE. A Conceptual Model of DI Diesel Combustion Based on Laser-Sheet Imaging. SAE paper; 1997. 970873.
- [32] Flynn PF, Durrett RP, Hunter GL, Zur Loye AO, Akinyemi OC, Dec JE, Westbrook CK. Diesel combustion: An integrated view combining laser diagnostics, chemical kinetics, and empirical validation. SAE paper; 1999. 1999-01-0509.
- [33] Li Z, Song C, Song J, Lv G, Dong S, Zhao A. Evolution of the nanostructure, fractal dimension and size of in-cylinder soot during diesel combustion process. *Combust Flame* 2011;158:1624-30.
- [34] Zhang Q, Yao M, Zheng Z, Liu H, Xu J. Experimental study of n-butanol addition on performance and emissions with diesel low temperature combustion. *Energy* 2011;47:515-21.
- [35] Ghorbanpour M, Rasekhi R. A parametric investigation of HCCI combustion to reduce emissions and improve efficiency using a CFD model approach. *Fuel* 2013;106:15765.
- [36] Parks JE, Prikhodko V, Storey JME, Barone TL, Lewis SA, Kass MD, Huff SP. Emissions from premixed charge compression ignition (PCCI) combustion and affect on emission control devices, *Catal Today* 2010;151:278-84.
- [37] Benajes J, Molina S, García A, Belarte E, Vanvolsem M. An investigation on RCCI combustion in a heavy duty diesel engine using in-cylinder blending of diesel and gasoline fuels. *Appl Therm Eng* 2014;63:66-76.
- [38] Feng H, Zheng Z, Yao M, Cheng G, Wang M, Wang X. Effects of exhaust gas recirculation on low temperature combustion using wide distillation range diesel. *Energy* 2013;51:291-6.

- [39] Han X, Zheng M, Wang J. Fuel suitability for low temperature combustion in compression ignition engines. *Fuel* 2013;109:336-49.
- [40] Boot MD, Luijten CCM, Somers LMT, Eguz U, van Erp DDTM, Albrecht A, Baert RSG. Uncooled EGR as a means of limiting wall-wetting under early direct injection conditions. SAE paper; 2009. 2009-01-0665.
- [41] Beatrice C, Del Giacomo N, Guido C. Benefits and drawbacks of compression ratio reduction in PCCI combustion application in an advanced LD diesel engine. SAE paper; 2009. 2009-01-1447.
- [42] Splitter D, Wissink M, DelVescovo D, Reitz R. RCCI engine operation towards 60% thermal efficiency. SAE paper; 2013. 2013-01-0279.
- [43] Hanson R, Kokjohn S, Splitter D, Reitz R. Fuel effects on reactivity controlled compression ignition (RCCI) combustion at low load. SAE paper; 2011. 2011-01-0361.
- [44] Curran S, Hanson R, Wagner R, Reitz R. Efficiency and emissions mapping of RCCI in a light-duty diesel engine. SAE paper; 2013. 2013-01-0289.
- [45] Antunes JMG. The use of hydrogen as a fuel for compression ignition engines. PhD thesis, Newcastle University, United Kingdom 2010.
- [46] Saravanan N, Nagarajan G, Dhanasekaran C, Kalaiselvan KM. Experimental investigation of hydrogen port fuel injection in DI diesel engine. *Int J Hydrogen Energy* 2007;32:4071-80.
- [47] Shirk MG, McGuire TP, Neal GL, Haworth DC. Investigation of a hydrogen-assisted combustion system for a light-duty diesel vehicle. *Int J Hydrogen Energy* 2008;33:7237-44.
- [48] McWilliam L, Megaritis T, Zhao H. Experimental investigation of the effects of combined hydrogen and diesel combustion on the emissions of a HSDI diesel engine. SAE paper; 2008. 2008-01-1787.
- [49] Bose PK, Maji D. An experimental investigation on engine performance and emissions of a single cylinder diesel engine using hydrogen as inducted fuel and diesel as injected fuel with exhaust gas recirculation. *Int J Hydrogen Energy* 2009;34:4847-54.
- [50] Christodoulou F, Megaritis A. Experimental investigation of the effects of separate hydrogen and nitrogen addition on the emissions and combustion of a diesel engine. *Int J Hydrogen Energy* 2013;38:10126-40.

- [51] Köse H, Ciniviz M. An experimental investigation of effect on diesel engine performance and exhaust emissions of addition at dual fuel mode of hydrogen. *Fuel Process Technol* 2013;114:26-34.
- [52] Lata DB, Misra A, Medhekar S. Effect of hydrogen and LPG addition on the efficiency and emissions of a dual fuel diesel engine. *Int J Hydrogen Energy* 2012;37:6084-96.
- [53] Pullagura G, Kumar KR, Verma PC, Jaiswal A, Prakash R, Murugan S. Experimental investigation of hydrogen enrichment on performance and emission behaviour of compression ignition engine. *Int J Hydrogen Energy* 2012;37:1223-32.
- [54] Wichterlová B, Sazama P, Breen JP, Burch R, Hill CJ, Capek L, Sobalík Z. An in situ UV–vis and FTIR spectroscopy study of the effect of H<sub>2</sub> and CO during the selective catalytic reduction of nitrogen oxides over a silver alumina catalyst. *J Catal* 2005;235:195-200.
- [55] Bromberg L, Cohn DR, Wong V. Regeneration of diesel particulate filters with hydrogen rich gas. MIT Plasma Science and Fusion Centre 2005, PSFC/RR-05-2.
- [56] Tsolakis A, Megaritis A, Yap D, Abu-Jrai A. Combustion characteristics and exhaust gas emissions of a diesel engine supplied with reformed EGR. SAE paper; 2005. 2005-01-2087.
- [57] Sahoo BB, Sahoo N, Saha UK. Effect of H<sub>2</sub>:CO ratio in syngas on the performance of a dual fuel diesel engine operation. *Appl Therm Eng* 2012;49:139-46.
- [58] Bika AS, Franklin L, Kittelson D. Cycle efficiency and gaseous emissions from a diesel engine assisted with varying proportions of hydrogen and carbon monoxide (synthesis gas). SAE paper; 2011. 2011-01-1194.
- [59] Dong C, Zhou Q, Zhao Q, Zhang Y, Xu T, Hui S. Experimental study on the laminar flame speed of hydrogen/carbon monoxide/air mixtures. *Fuel* 2009;88:1858-63.
- [60] Zhao H. Advanced direct injection combustion engine technologies and development: Diesel engines (Volume 2). Cambridge: Woodhead Publishing Ltd and CRC Press; References 169, 2009.
- [61] Wikipedia. 2018. Online Source: <http://en.wikipedia.org/wiki/Autogas>. [Accessed 12 08 2018].
- [62] Sita Rama Raju AV, Musa SE, Ramesh A, Nagalingam B. Development and testing of a lean burn spark ignition engine operation on LPG. Proceedings of the XV national conference on I.C. engines and combustion, Chennai, 1997.

- [63] Fontaras G, Manfredi U, Martini G, Dilara P, Deregibus G. Experimental assessment of a diesel-LPG dual fuel supply system for retrofit application in city busses. SAE paper; 2012. 2012-01-1944.
- [64] Lata DB, Misra A, Medhekar S. Investigations on the combustion parameters of a dual fuel diesel engine with hydrogen and LPG as secondary fuels. *Int J Hydrogen Energy* 2011;36:13808-19.
- [65] Saleh HE. Effect of variation in LPG composition on emissions and performance in a dual fuel diesel engine. *Fuel* 2008;87:3031-39.
- [66] Abdelaal MM, Hegab AH. Combustion and emission characteristics of a natural gasfueled diesel engine with EGR. *Energ Convers Manage* 2012;64:301-12.
- [67] Namasivayam AM, Korakianitis T, Crookes RJ, Bob-Manuel KD, Olsen J. Biodiesel, emulsified biodiesel and dimethyl ether as pilot fuels for natural gas fuelled engines. *Appl Energ* 2010;87:769-78.
- [68] Board NB. Biodiesel org, National biodiesel board. 2018. Online Source: <http://www.biodiesel.org/what-is-biodiesel/biodiesel-basics>. [Accessed 12 08 2018].
- [69] Labecki L. Combustion and emission characteristics of biofuels in diesel engines. PhD thesis, Brunel University, United Kingdom 2010.
- [70] Lapuerta M, Armas O, Rodriguez-Fernandez and J. Effect of biodiesel fuels on diesel engine emissions. *Prog Energ Combust* 2008;34:198-223.
- [71] Atadashi IM, Aroua MK, Abdul Aziz A. High quality biodiesel and its diesel engine application: A review. *Renew Sust Energ Rev* 2010;14:1999–2008
- [72] Tsolakis A, Megaritis A, Wyszynski ML, Low temperature exhaust gas fuel reforming of diesel engine. *Fuel* 2004;83:1837-45.
- [73] Tsolakis A, Megaritis A. Exhaust gas fuel reforming for diesel engines - A way to reduce smoke and NOx emissions simultaneously. SAE Paper; 2004. 2004-01-1844.
- [74] Abu-Jrai A, Tsolakis A, Megaritis A. The influence of H<sub>2</sub> and CO on diesel engine combustion characteristics, exhaust gas emissions, and after treatment selective catalytic NOx reduction. *Int J Hydrogen Energy* 2007;32:3565-71.
- [75] Ajhar M, Follmann M, Matthias C, Melin T. Membranes producing nitrogen-enriched combustion air in diesel engines: Assessment via dimensionless numbers. *J Membrane Sci* 2008;323:105-12.

- [76] Poola RB, Longman DE, Anderson JL, Stork KC, Sekar R, Callaghan K, Nemser S. Membrane-Based Nitrogen-Enriched Air for NO<sub>x</sub> Reduction in Light-Duty Diesel Engines. SAE paper; 2000. 2000-01-0228.
- [77] Li T, Izumi H, Shudo T, Ogawa H, Okabe Y. Characterization of Low Temperature Diesel Combustion with Various Dilution Gases. SAE paper 2007. 2007-01-0126.
- [78] Ladommatos N, Balian R, Horrocks R, Cooper L. The effect of exhaust gas recirculation on combustion and NO<sub>x</sub> emissions in high-speed-direct-injection diesel engine. SAE paper; 1996. 960840.
- [79] Suresh Neethirajan, D.S. Jayas, Shashikant Sadistap. (2009). Carbon Dioxide (CO<sub>2</sub>) Sensors for the Agri-food Industry—A Review. Food and Bioprocess Technology. 2 (2), 115-121.
- [80] Cambustion. (2018). Fast FID Principles. Available: <https://www.cambustion.com/products/hfr500/fast-fid-principles>. Last accessed 14 August 2018.
- [81] DRGP DREAM DOT. (2014). Thermal Conductivity Detector. Available: <https://drgpinstitute.wordpress.com/2014/12/26/thermal-conductivity-detector/>. Last accessed 14 August 2018.
- [82] AVL List GmbH, AVL 415 variable sampling smoke meter operating manual. AVL; 1991.
- [83] Choudhuri AR, Gollahalli SR. Characteristics of hydrogen-hydrocarbon composite fuel turbulent jet flames. Int J Hydrogen Energy 2002;28:445-54.
- [84] Verhelst S, Verstraeten S, Sierens R. A comprehensive overview of hydrogen engine design features. J Auto Eng 2007;8:911-20.
- [85] Ceclre E, Depcik C, Guo J, Peltier E. Analysis of the effects of reformat (hydrogen/carbon monoxide) as an assistive fuel on the performance and emissions of used canola-oil biodiesel. Int J Hydrogen Energy 2012;37:3510-27.
- [86] Christodoulou F, Giannakakis P, Kalfas A. Performance benefits of a portable hybrid micro-gas-turbine power system for automotive applications. J Eng Gas Turb Power 2011;133:022301-8.
- [87] Lata DB, Misra A. Theoretical and experimental investigations on the performance of dual fuel diesel engine with hydrogen and LPG as secondary fuels. Int J Hydrogen Energy 2010;35:11918-31.

- [88] Singh R, Maji S. Dual fuelling of a twin-cylinder compression ignition engine with diesel and CNG. *J Eng Appl Sci* 2012;7:90-9.
- [89] Peirce D. Biodiesel and Oxides of Nitrogen: Investigations into their Relationship. PhD Thesis, Brunel University London, 2016
- [90] Tsolakis A, Hernandez JJ, Megaritis A, Crampton M. Dual fuel diesel operation using H<sub>2</sub>. Effect on particulate emissions. *Energ Fuel* 2005;19:418-25.
- [91] Derwent R, Simmonds P, O'Doherty S, Manning A, Collins W, Stevenson D. Global environmental impacts of the hydrogen. *Int J Nucl Hydrog Prod Appl* 2006;1:57-67.
- [92] Bond SW, Alvarez R, Vollmer MK, Steinbacher M, Weilenmann M, Reimann S. "Molecular hydrogen (H<sub>2</sub>) emissions from gasoline and diesel vehicles. *Sci Total Environ* 2010;408:3596-606.
- [93] Karim GA, Wierzba I, Boon S. Some considerations of the lean flammability limits of mixtures involving hydrogen. *Int J Hydrogen Energy* 1984;10:117-23.
- [94] Engineering ToolBox, (2005). Hydrogen - Specific Heat. [online] Available at: [https://www.engineeringtoolbox.com/hydrogen-d\\_976.html](https://www.engineeringtoolbox.com/hydrogen-d_976.html) [Accessed 30th July 2018].
- [95] Pavan Potluri. (2015). European Engine Outlook – Potential of the Gasoline Engine. Available: [https://ihsmarkit.com/pdf/IHS-European-Engine-Outlook-Potential-of-the-Gasoline-Engine\\_227832110913052332.pdf](https://ihsmarkit.com/pdf/IHS-European-Engine-Outlook-Potential-of-the-Gasoline-Engine_227832110913052332.pdf). Last accessed 31st August 2018.
- [96] A.B. Welch;J.S. Wallace. (1990). Performance Characteristics of a Hydrogen-Fueled Diesel Engine with Ignition Assist. SAE International.
- [97] Pedrozo V. An experimental study of ethanol-diesel dual-fuel combustion for high efficiency and clean heavy-duty engines. PhD Thesis, Brunel University London, 2017.
- [98] Bajraktari B. Dual-Fuel Conversion of an Existing Compression Ignition Engine to Propane-Diesel and an Investigation of Performance. MEng Thesis, Brunel University London, 2018.
- [99] Watson N, Pilley A, Marzouk M. A Combustion Correlation for Diesel Engine Simulation. SAE Technical Paper 1980. doi:10.4271/800029.
- [100] BRESSON. G, SOLERI. D. (2008). A Study of methods to lower HC and CO emissions in Diesel HCCI. SAE International. 01 (0034)

[101] N. Saravanan; G. Nagarajan. (2008). An Experimental Investigation on a Diesel Engine with Hydrogen Fuel Injection in Intake Manifold. SAE International Powertrains.

[102] S. Samuel, G. McCormick. (2010). Hydrogen Enriched Diesel Combustion. SAE International. 01 (2190)